ANTIMICROBIAL ACTIVITIES OF COMPOUNDS ISOLATED FROM *PYCNANTHUS ANGOLENSIS* (WELW.) WARB AND *BRYOPHYLLUM PINNATUM* (LAM) OKEN

Olawale H. Oladimeji[a]* and Ngozi O. Onu[a]

Keywords: *Pycnanthus angolensis; Bryophyllum pinnatum;* chromatography; bioactivity;

In the present study a semi-pure residue each from *Pycnanthus angolensis* (Welw.) Warb and *Bryophyllum pinnatum* (Lam) for the presence of biologically active compound(s) were investigated. This exercise led to two compounds whose identities have been established to be 1,6-dihydro-2-methyl-4-hydroxy-6-oxo-3-pyridine carboxylic acid ethyl ester (1,6-dihydro-2-methyl-4-hydroxy-6-oxo-3-nicotinic acid ethyl ester) (5-ethoxycarb, **NG5-a**) and 1-ethoxy-2-hydroxy-4-prophenylguaethol (vanitrope, **KF-1a**), respectively using MS and IR spectral techniques. **NG-5a** was proved to be bacteriostatic against *Escherichia coli* but recorded no activity against *Staphylococcus aureus* and *Candida albicans.* **KF-1a** recorded only minimal activity against *S. aureus* but demonstrated no activities against *E. coli* or *C. albicans.*

* Corresponding Authors
Tel: +2347038916740, +2348173486285
E-Mail: wale430@yahoo.co.uk,
olawaleoladmeji70@gmail.com,
hakeemoladmeji@uniuyo.edu.ng
[a] Department of Pharmaceutical & Medicinal Chemistry, Faculty of Pharmacy, University of Uyo, Uyo, Nigeria.

Introduction

The seeds of *P. angolensis* are rich in palmitic, linoleic and linolenic acids as useful precursors in phytochemical biogenesis.[1] Furthermore, myristoleic acid (potent anti-arthritic agent) and tocotrenoils (antioxidant and anti-inflammatory agents) have been obtained from the plant.[2] Also, four compounds namely, 3-ethoxy-3,7-dimethyl-1,6-octadiene (ethyl linalool), 1,2-benzenedicarboxylic acid diethyl ester (diethyl phthalate),[3] ethyl cinnamate and 9-oximino-2,7-diethoxy fluorene (2,7-diethoxy-9H-fluoren-9-one oxime)[4] have also been isolated from the ethyl acetate fraction of its leaves by column chromatography (CC) and preparative thin-layer chromatography (p-TLC) respectively.

The presence of cardiac glycosides, alkaloids, terpenes and tannins has also been indicated in *B. pinnatum*.[5] In addition, a steroid, 3-hydroxy-(3β,17β)-spiro(androst-5-ene-17,1′-cyclobutan)-2′-one has been isolated from the butanol fraction of this plant by preparative thin-layer chromatography (p-TLC).[3,6] In continuation of work on these plants, residues coded **NG-5** and **KF-1** obtained from previous studies were subjected to preparative thin-layer chromatography (p-TLC) with the aim of isolating more compound(s) from the plants and as well as evaluating the antimicrobial activities of compound(s) so obtained.

Experimental

Preparation of plates

Similar 20 x 20 cm glass plates were washed in detergent solution, rinsed with water and air-dried. Silica gel (Sigma-Aldrich, USA) was treated with $CaSO_4$ (Bond Chemicals, Nigeria) which served as a binding agent. The slurry obtained there from was vigorously shaken, thereby making it homogenous and free flowing. A thickness of 0.5 mm of the slurry was uniformly applied across the glass plates and allowed to set for 24 h. The coated plates were then activated in a laboratory oven (Gallenkamp, England) at 60 ^{0}C for at least 10 h prior to use.[4]

Isolation of NG-5a

In order to isolate **NG-5**, the residue (deep brown, 65 mg) was painstakingly dissolved in some methanol and applied across the coated silica plate using a micro Pasteur pipette (Simax, India) 1 cm above the bottom edge of the plate and then allowed to dry. Afterward, the plate was developed in toluene:$(CH_3)_2CO$:H_2O (40:80:4) inside a large chromatographic glass tank (Pyrex, USA). The obtained chromatogram showed two excellently resolved layers which were carefully scrapped, separately filtered with methanol and concentrated in vacuo on a rotary evaporator (R205D, shensung BS & T, China). The pure sub-fractions were monitored on commercial silica plates in toluene:$(CH_3)_2CO$:H_2O (10:20:1) and $(CH_3)_2CO$:EtOAc (35:65) using $FeCl_3/CH_3OH$, Dragendoff's and vanillin-H_2SO_4 as spray reagents. Further TLC evaluations indicated a spot in **NG-5a** (yellow compound, R_f (0.22), 21 mg). $C_9H_{11}NO_4$, MS (ES): *m/z* 197 (M^+, 43.17 %), 179 (M-H_2O^+, 4.39 %), 151 (M-OC_2H_5-H^+, 78.71 %), 139 (M-OC_2H_5-N+3^+, 9.21 %), 123 (M-OC_2H_5-CO-H^+, 88.49 %), 110 (M-OC_2H_5-N-CO^+, 8.69 %), 95 (M-OC_2H_5-CO-CH_3-OH+3^+, 51.26 %), 83 M-OC_2H_5-CO-CH_3-OH-9^+, 45.78 %), 69 (M-OC_2H_5-CO-CH_3-N-9^+, 62.02 %) and 42 M-OC_2H_5-COO-CH_3-N-OH-20^+ 100.00 %). FTIR: 717, 863 (alkyl substitution), 1076 (-C-O-C), 1621 (-C=C), 1715 (-C=O), 1732 (-C=O), 3456 (-NH) and 3567(-Ar-OH) cm^{-1}.

Isolation of KF-1a

The KF-1 residue (yellow, 47 mg) was dissolved in some methanol and applied across the coated silica plate using a micro Pasteur pipette (Simax, India) 1 cm above the bottom edge of the plate and then allowed to dry. Afterward, the plate was developed in toluene: $(CH_3)_2CO$:H_2O (40:80:4)

inside a large chromatographic glass tank (Pyrex, USA). The obtained chromatogram showed three layers which were carefully scrapped, separately filtered with methanol and concentrated in vacuo on a rotary evaporator (R205D, Shensung BS & T, China).

The pure sub-fractions were monitored on commercial silica plates in toluene:$(CH_3)_2CO$:H_2O (10:20:1) and $(CH_3)_2CO$:EtOAc (35:65) using $FeCl_3/CH_3OH$ and vanillin-H_2SO_4 as spray reagents. Further TLC evaluations indicated a spot in **KF-1a** (amorphous pale yellow solid, R_f(0.61), 0.18 mg).

KF-1a: $C_{11}H_{14}O_2$, MS (ES) *m/z* 178 $(M)^+$ (100.00 %), 161 $(M\text{-}OH)^+$ (5.16 %), 149 $(M\text{-}C_2H_5)^+$ (54.91 %), 131 $(M\text{-}OC_2H_5\text{-}2H)^+$ (38.87 %), 121 $(M\text{-}OC_2H_5\text{-}OH+5)^+$ (7.33 %), 103 $(M\text{-}C_6H_5+2)^+$ (30.29 %), 91 $(M\text{-}OC_2H_5\text{-}CH_3\text{-}OH\text{-}10)^+$ (20.81 %), 77 $(M\text{-}C_6H_5\text{-}OH\ \text{-}7)^+$ (27.89 %), 66 $(M\text{-}C_6H_5\text{-}OH\text{-}CH_3\text{-}3)^+$ (12.82 %) and 55 $(M\text{-}C_6H_5\text{-}OH\text{-}CH_3\text{-}C_2H_5)^+$ (21.80 %). FTIR: 767, 823 (alkyl substitution), 1056 (-C-O-C), 1618 (Ar-C=C), 1642 (exocyclic -C=C) and 3312 (Ar-OH) cm^{-1}.

Structural elucidation

The mass spectra of the compounds were obtained on Kratos MS 80 (Germany) while the infra-red analyses were done on Shimadzu FTIR 8400S (Japan).

Antimicrobial screening

The microorganisms used in this study were limited to three *viz*: *Staphylococcus aureus* (ATCC 21824) (Gram positive, *Escherichia coli* (ATCC 23523) (Gram negative) and *Candida albicans* (NCYC 106) (fungus) were clinically isolated from specimens of diarrheal stool, abscesses, necrotizing fascitis, urine and wounds obtained from the Medical Laboratory, University of Uyo Health Centre, Uyo. The clinical isolates were collected in sterile bottles, identified and typed by conventional biochemical tests.[7,8] These clinical microbes were then refrigerated at -5 ^{0}C. prior to use.

The media and plates were sterilized in an autoclave at 121 °C for 15 min. The hole-in-plate agar diffusion method was used observing standard procedure with Nutrient Agar-CM003, Mueller-Hinton-CM037 (Biotech Limited, Ipswich, England) and Sabouraud Dextrose Agar (Biomark, India) for the bacteria and fungus respectively. The inoculum of each micro-organism was introduced into each petri-dish (Pyrex, England). Cylindrical plugs were removed from the agar plates by means of a sterile cork borer (Simax, India) to produce wells with a diameter of approximately 6 mm. The wells were equidistant from each other and the edge of the plate (Washington, 1995, N.C.C.L.S, 2003).[9,10]

Concentrations of 20 mg mL^{-1} of crude extracts of *P. angolensis* (CE_p) and *B. pinnatum* (CE), 10 mg mL^{-1} of ethyl acetate fraction (ET) and butanol fraction (BT), 2 mg mL^{-1} of **NG-5a** and **KF-1a** were introduced into the wells. Also, different concentrations of 10 µg mL^{-1} ^{s}treptomycin (Orange Drugs, Nigeria), 1 mg mL^{-1} of nystatin (Gemini Drugs, Nigeria) and deionized water were introduced into separate wells as positive and negative controls respectively.[11]

The experiments were carried out in triplicates. The plates were labeled on the underside and left at room temperature for 2 h to allow for diffusion. The plates were then incubated at 37± 2 ^{0}C for 24 to 48 h. Zones of inhibition were measured in mm with the aid of a ruler.

Results and discussion

3-Pyridine carboxylic acid (3-nicotinic acid) and its derivatives are well-known compounds and can easily be identified by their MS and IR spectra. **NG-5a** was isolated and identified as an ethyl ester derivative of 3-nicotinic acid.

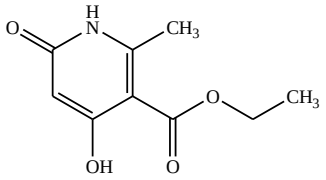

Figure 1. 1,6-Dihydro-2-methyl-4-hydroxy-6-oxo-3-pyridine carboxylic acid, ethyl ester (1,6-dihydro-2-methyl-4-hydroxy-6-oxo-3-nicotinic acid, ethyl ester, **NG-5a**).

It is pertinent to note that this could be due to partial esterification of 3-pyridine carboxylic acid in ethanol during extraction**.** In addition, **NG-5a** tested positive for the ferric chloride and Dragendoff's reagents indicating the presence of a hydroxyl group and an alkaloidal nucleus respectively.

Due to the nature of its matrix, many fragmented ions could be seen in the mass spectrum of the compound. Those that are easily identifiable include $(M)^+$ at *m/z* 197 (43.17 %) while the peak at 179 (4.39 %) indicates the loss of water from the matrix. However, the fragments at 151(79.71 %) and 139 (9.21 %) represent the removal of ethoxy and ethoxy and nitrogen units respectively from the molecule. Furthermore, ions at 123 (88.49 %), 110 (28.69 %), 95(51.26 %)and 83 (45.78 %) correspond to the excisions of ethoxy and carbonyl, ethoxy, carbonyl and nitrogen and ethoxy, carbonyl, methyl and hydroxy groups respectively from **NG-5a.** The most abundant ion (base peak) at 42 (100 %) shows the removal of ethoxy, carboxylate, methyl, nitrogen and hydroxyl units from the molecular matrix.

The IR spectrum of the compound shows characteristic stretching bands at 717, 863, 1070, 1621, 1715, 1732, 3450 and 3567 cm^{-1} indicating alkyl substitutions, ether linkage, endocyclic -C=C, carbonyl, -NH and aromatic hydroxyl absorptions respectively.

The chemical structure of **KF**-1**a** was established by a combination of spectroscopic techniques as highlighted above. These data were matched with those in the library data of organic compounds and were found to be consistent with those in literature. Consequently, **KF**-1**a** (Figure 2) has been identified to be 1-ethoxy-2-hydroxy-4-prophenyl guaethol (vanitrope).

Table 1. Antimicrobial screening of crude extract, ethyl acetate fraction, **NG-5a** and **KF-1a** at different concentrations on test microbes in water.

Test microbe	CE_p/CE 20 mg mL^{-1}	ET/BT 10 mg mL^{-1}	NG-5a 2 mg mL^{-1}	KF-1a 2 mg mL^{-1}	deionized water	SP 10 µg mL^{-1}	NY 1mg mL^{-1}
S. aureus	6	6	6.5	7.5	6	27	6
E. coli	6	6	11.5	6	6	28	6
C. albicans	6	6	6	6	6	6	25

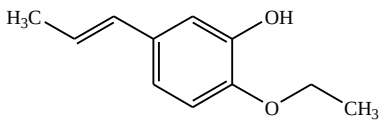

Figure 2. 1-Ethoxy-2-hydroxy-4-prophenyl guaethol (**KF-1a**).

Due to the nature of the matrix, many fragmented peaks appeared in the MS of the compound. Those that are easily identifiable include $(M)^+$ which shows as the most abundant ion (base peak) at *m/z* 178 (100.00 %) while fragments at 161 (5.16 %) and 149 (54.41 %) represent the loss of hydroxy and ethyl groups from the molecule, respectively. Furthermore, the ions at 103 (30.29 %), 77 (27.89 %) 66 (12.82 %) and 55 (21.80 %) indicate the disintegration of the molecular matrix by the excisions of phenyl and some smaller units such as methyl and hydroxy from $(M]^+$. However, peaks at 131 (38.87 %) and 121 (7.33%) reveal the removal of ethoxy groups from the compound.

The IR spectrum of **KF-1a** shows absorptions at767, 823, 1056, 1618, 1642 and 3312 cm^{-1} indicating diagnostic alkyl substitutions, an ether linkage (-C-O-C), aromatic -C=C, exocyclic -C=C and aromatic -OH functional groups respectively. It should be noted that **KF-1a** was isolated with a sweet fragrance characteristic of oils, spices, perfumes and food additives.[16]

Antimicrobial tests

The spectrum of microbes employed in these tests was narrow, encompassing one each of gram-positive (*S. aureus*) and gram negative (*E. coli*) bacterial strains and a fungus (*C. albicans*). The results presented in Table 1 show that the crude extracts and fractions were inactive against *S. aureus, E. coli* and *C. albicans.* However, **NG-5a** was appreciably bacteriostatic against *E. coli.* It but recorded no activities against *S. aureus* and *C. albicans.*, **KF-1a** was minimally active against *S. aureus* but recorded no activities against *E. coli* or *C. albicans.* The activity given by **NG-5a** against *E. coli* has importance because of the resistance of this microorganism against known antimicrobial agents. This resistance is believed due to the presence of a three-layered envelope which does not allow permeation of external agents. The compounds demonstrated no antifungal activity against *C. albicans.*

Conclusion

The isolation of these compounds is being reported for the first time from the plants. Hence, **NG-5a** and **KF-1a** are expected to serve as chemotaxonomic markers for both plants. Furthermore, the results of the antimicrobial screening lend some justification to the uses of these plants especially in the treatment /management of some bacterial infections. However, the compounds will be screened against other bacterial and fungal strains in the future with the aim of obtaining better activities.

Conflict of Interest

The authors declare no conflict of interest

Acknowledgments

The authors acknowledge the assistance of the National Research Institute for Chemical Technology (NARICT) Zaria, Nigeria in obtaining the spectra of the compounds. The contribution of E. Akpan, Principal Technologist, Pharmaceutical Microbiology Unit, Faculty of Pharmacy, University of Uyo, Uyo, Nigeria is equally appreciated.

References

[1]Olaoye, A. J., *Physico-chemical analysis of Pycnanthus angolensis seed oil*, Shaneson C. I. Limited, **2017**, 177-188.

[2]Gustafson, K., Qing-Li, W., Asante-Dartey, J., Simon, J. L., Pycnanthus angolensis: Bioactive compounds and medicinal applications, *ACS Symp. Ser.*, **2013**, *1127*, 63-78. DOI: 10.1021/bk-2013-1127.ch005

[3]Oladimeji, H. O., Attih, E. E., Onu, O. N., Ethyl linalool and diethyl phthalate from Pycnanthus angolensis (Welw.) Warb., *Eur. Chem. Bull.*, **2017**, 6, 76-78. DOI: http://dx.doi.org/10.17628/ecb.2017.6.76-78

[4]Oladimeji, H. O., Onu, O. N., Isolation of ethyl cinnamate and a subtituted fluorene from Pycnanthus angolensis (Welw.) Warb., *Eur. Chem. Bull.*, **2017**, *6*, 421-423. DOI: http://dx.doi.org/10.17628/ecb.2017.6.421-423

[5]Kamboj, A., Saluja, A. K., *Bryophyllum pinnatum (Lam.) Kurz.*: Phytochemical and pharmacological profile: A review, *Pharmacogn. Rev.*, **2009**, *3*, 364-374. http://www.phcogrev.com/text.asp?2009/3/6/364/59536

[6]Oladimeji, H. O., Eberefiak, K. E., Isolation and antimicrobial analysis of a steroidal terpene from the butanol fraction of Byrophyllum pinnatum (Lam.) Oken, *Eur. Chem. Bull.*, **2017**, *6*, 292-294. DOI: http://dx.doi.org/10.17628/ecb.2017.6.292-294

[7]Gibson, L., Khoury, J., Storage and survival of bacteria by ultra-freeze, *Lett. Applied Microbiol.*, **1986**, *3*, 127-129. https://doi.org/10.1111/j.1472-765X.1986.tb01565.x

[8]Murray, P., Baron, E., Pfaller, M., Tenover, F., Yolken, R., in *Manual of clinical microbiology*, American Society of Microbiology Press, Washington, D.C., **1995**, 213-220.

[9]Washington, J., in *Manual of clinical microbiology*, American Society of Microbiology Press, Washington, D.C., **1995**, 971-973.

[10]*Performance standard for antimicrobial susceptibility test*, 8th Ed., National Committee for Clinical Laboratory Standards, Villanova (PA), **2003**, 130.

[11]Oladimeji, H. O., Johnson, E. C., Glucolipid from the ethyl acetate fraction of Acalypha wilkesiana var. lace-acalypha (Muell & Arg), *J. Pharm. Biol. Res.*, **2015**, *12*, 48-53**.** http://dx.doi.org/10.4314/jpb.v12i1.7

Received: 20.08.2018.
Accepted: 03.09.2018.

SYNTHESIS, STRUCTURAL AND BIOLOGICAL STUDIES OF Co(II), Ni(II), Cu(II) AND Zn(II) COMPLEXES OF 4-[(3-ETHOXY-4-HYDROXYBENZYLIDENE)AMINO]-3-MERCAPTO-6-METHYL-5-OXO-1,2,4-TRIAZINE

Kiran Singh,[a]* Prerna Turk[a] and Anita Dhanda[b]

Keywords: Metal complexes; Schiff base; 4-[(3-ethoxy-4-hydroxybenzylidene)amino]-3-mercapto-6-methyl-5-oxo-1,2,4-triazine.

Co(II), Ni(II), Cu(II) and Zn(II) complexes with the bidentate ligand 4-[(3-ethoxy-4-hydroxybenzylidene)amino]-3-mercapto-6-methyl-5-oxo-1,2,4-triazine have been synthesized. The Schiff base and its metal complexes have been characterized by various physicochemical techniques like IR, ^{1}H-NMR, ESR, electronic and fluorescence spectroscopy and cyclic voltammetry. Elemental analysis, conductivity measurements and thermal analysis of synthesized compounds were also carried out. All the complexes were colored and non-electrolytic in nature. In vitro biological activities of the ligand and complexes have been checked against some pathogenic gram positive, gram negative bacteria and different fungi and then compared with some standard drugs as control.

* Corresponding Authors
[a] Department of Chemistry, Kurukshetra University Kurukshetra, 136119, India
[b] Department of Microbiology, Kurukshetra University Kurukshetra, 136119, India

Introduction

Schiff bases are generally formed by the condensation of an amine and an active carbonyl group containing compound.[1-3] During the recent years, there have been many investigations of Schiff bases possessing nitrogen-containing heterocyclic compounds.[4] Amino-group containing heterocyclic compounds consisting of two or more potential donor centers play an important role in the study of competitive reactivity of a bidentate ligand system.[5] The development of new drugs based on 1,2,4-triazines further enhances the interest in synthesis of these compounds. It has been well established that the triazine derivatives are potent antibacterial, antioxidant, antifungal, anti-tuberculosis and anti-inflammatory agents.[6-13] In addition, their applications as herbicides, fungicides and insecticides are also well known.[14-15] Metal ion complexes with Schiff bases are synthesized and their biological activities have been checked.[16] These complexes can be used in various catalytic reactions and as models for biological systems. It has been well reported that some drugs possess higher activity when administered as metal complexes than as the free ligand. Increase of biological activity has been reported by the incorporation of transition metals in Schiff bases. Importance of Schiff base metal complexes has spurred the search for new metal-based drugs using different biologically activemetals.[17-18]

Triazine derivatives with additional N or S donor atoms exhibit strong chelating ability and provide potential binding sites for complexation with various metal ions. Certain cobalt, copper metal complexes are significant antiviral agents.[19-22]

Here we report the synthesis and characterization of Co(II), Ni(II), Cu(II) and Zn(II) metal complexes of a newly synthesized ligand obtained from the condensation of 3-ethoxy-4-hydroxybenzaldehyde with 4-amino-3-mercapto-6-methyl-5-oxo-1,2,4-triazine.

Experimental

All the chemicals and solvents used were of analytical grade. IR spectra of Schiff base and its metal complexes were recorded in KBr pellets/Nujol mulls on a MB-3000 ABB spectrometer. ^{1}H-NMR spectra of Schiff base and its Zn(II) complexes were recorded on bruker ACF 300 spectrometer at 300 MHz in DMSO-d_6 using TMS as a reference compound. Electronic spectra of metal complexes were recorded on T90 (PG instruments Ltd.) UV/VIS spectrophotometer in DMF solvent, in the region of 200-900 nm. Fluorescence spectra of ligand and metal complexes were recorded on SHIMADZU RF-5301 PC spectrofluorometer. Ivium Stat Electrochemical Analyzer was used for cyclic voltammetry measurement of Cu(II) complexes. Magnetic moment measurements were carried out on Vibrating Sample Magnetometer at the Institute Instrumentation Centre, IIT Roorkee.

Thermogravimetric analysis was carried out on the Perkin Elmer (Pyris Diamond) instrument at a heating rate of 10 °C min^{-1} by using alumina powder as reference. ESR spectra of copper complexes were recorded under the magnetic field 0.3 T at frequency 9.1 GHz by using Varian E-112 ESR spectrometer at SAIF, IIT Bombay. Elemental analyses (C, H, N) of compounds were carried out by using a Perkin-Elmer 2400 Elemental analyzer. Gravimetric methods were used to determine the metal contents in synthesized metal complexes i.e. cobalt was estimated as cobalt pyridine thiocyanate, nickel as nickel dimethylglyoximate, copper as cuprous thiocyanate and zinc as zinc ammonium phosphate.[23]

Synthesis of ligand

First, 4-amino-3-mercapto-6-methyl-5-oxo-1,2,4-triazine (AMMOT) was synthesized by a reported procedure.[24] Its ethanolic solution (1.50 g, 9.49 mmol) was mixed with an ethanolic solution of 3-ethoxy-4-hydroxybenzaldehyde (1.578 g, 9.49 mmol) and the reaction mixture was refluxed for 7 h. The progress of reaction was checked by TLC. The precipitated ligand, 4-[(3-ethoxy-4-hydroxybenzylidene)-amino]-3-mercapto-6-methyl-5-oxo-1,2,4-triazine (HL), was filtered, washed with ethanol, recrystallized from ethanol and then dried at room temperature, m.p. 182˚-184 ˚C (Figure 1).

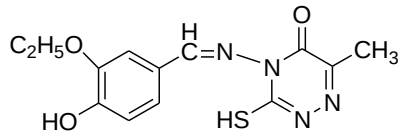

Figure 1. Schiff Base: 4-[(3-ethoxy-4-hydroxybenzylidene)-amino]-3-mercapto-6-methyl-5-oxo-1,2,4-triazine.

Synthesis of metal complexes

Synthesis of 1:1 metal complexes

The metal complexes were prepared by the reaction of the ligand (0.4 g, 1.30 mmol) with the respective acetates of Co (0.326 g, 1.30 mmol), Ni (0.325 g, 1.30 mmol), Cu (0.261 g, 1.30 mmol) and Zn (0.286 g, 1.30 mmol) in ethanolic solution. The solid products formed were filtered, washed with warm water, alcohol and acetone and then dried in desiccator.

Synthesis of 1:2 metal complexes

Hot ethanolic solutions of ligand (0.8 g, 2.61 mmol) were mixed with hot ethanolic solutions of acetates of Co (0.326 g, 1.30 mmol), Ni (0.325 g, 1.30 mmol), Cu (0.261 g, 1.30 mmol), Zn (0.286 g, 1.30 mmol). The products formed were filtered off, washed with warm water, alcohol and finally with acetone and then dried in desiccator.

Pharmacology

The newly synthesized ligand and its metal complexes have been screened in vitro for their antimicrobial activity against two Gram-positive (*Staphylococcus aureus* MTCC 96 and *Bacillus subtilis* MTCC 121), two Gram-negative (*Escherichia coli* MTCC 1652 and *Pseudomonas aeruginosa* MTCC 741) and two fungi (*Candida albicans* MTCC 227 and *Saccharomyces cerevisiae* MTCC 170) by agar well diffusion method as reported in previous papers from our laboratory.[25] All the bacterial cultures were procured from Microbial Type Culture Collection (MTCC), IMTECH, Chandigarh. Ciprofloxacin and amphotericin B were used as standard antibacterial and antifungal drugs respectively.

The agar well diffusion method was used to check the antibacterial activity of synthesized compounds.[26] All the microbial cultures were adjusted to 0.5 McFarland Standard, which is visually comparable to a microbial suspension of approximately 1.5×10^8 cfu mL^{-1}. 20 mL of Mueller Hinton agar medium was poured into each Petri dish and dishes were swabbed with 100 µL inoculum of the test microorganisms and kept for 20 minutes for adsorption. Using sterile cork borer of 8 mm diameter, wells were bored into the seeded agar plates and these were loaded with a 100 µL volume with concentration of 4.0 mg mL^{-1} of each compound reconstituted in DMSO. All the plates were incubated at 36 ˚C for 24 h. Antibacterial activity of each compound was analyzed by measuring the zone of growth inhibition against the test organisms with zone reader (Hi Antibiotic zone scale). This procedure was performed in three replicate plates for each organism.

Minimum inhibitory concentration (MIC) is the lowest concentration of an antimicrobial compound that will inhibit the visible growth of a microorganism after overnight incubation. MIC of the various compounds against bacterial strains was tested through a modified agar well-diffusion method.

Results and discussion

Schiff base and its metal complexes are colored and non-hygroscopic in nature. Though Schiff base is soluble in common organic solvents such as ethanol and methanol, its metal complexes are insoluble in common organic solvents but soluble in DMF and DMSO. The molar conductance of all the complexes was measured in DMF using 10^{-3} M solutions at room temperature. The molar conductance values (36.89 – 43.29 S cm^2 mol^{-1}) indicate that all the complexes are non-electrolytic in nature. The purity of the ligand and its metal complexes was checked by TLC. Analytical data of all compounds are given in Table 1.

IR spectra

The comparative IR frequencies of ligand and its metal complexes were recorded in the region 400-4000 cm^{-1}. The important IR frequencies of Schiff base and metal complexes are summarized in Table 2. In the free ligand, a characteristic band observed at 1697 cm^{-1} due to azomethine ν(-CH=N) group,[27,28] which is shifted to lower frequency (20-30 cm^{-1}) in spectra of the metal complexes, indicating a coordination through the nitrogen of azomethine group. A weak band observed at 2893 cm^{-1} due to ν (SH) group in the ligand, has disappeared in the metal complexes, which indicates the deprotonation of thiol group. In metal complexes, a broad band appeared in the region 3232-3742 cm^{-1} due to ν (OH/H_2O), which is assigned to phenolic OH and water molecules associated with the complexes. A characteristic band was observed at 1582 cm^{-1} in Schiff base and its metal complexes due to ν(C=O) stretch, its unaltered position indicates the non-participation of keto group in chelation. In 1:1 metal complexes, band was observed at 1744 cm^{-1} due to acetate group.[25] The coordination of ligand to the metal through the azomethine nitrogen atom and sulfur atom is further supported by (M-N) and (M-S) bands in the range 482-488 cm^{-1} and 323-342 cm^{-1} respectively.[29,30]

Table 1. Analytical data of the synthesized compounds.

Compounds	Color	Mp. °C, dec*	Yield, %	Elemental analysis, calculated (found), %			
				C	H	N	M
Schiff Base, HL $C_{13}H_{14}N_4O_3S$	Light yellow	182	84 %	50.98 (50.32)	4.57 (4.18)	18.30 (18.09)	
$Co(L)(OAc).3H_2O$	Dark Green	200	81 %	37.74 (37.64)	4.61 (4.56)	11.74 (11.44)	12.35 (11.93)
$Co(L)_2.2H_2O$	Dark Green	202	80 %	44.26 (43.91)	4.25 (4.13)	15.88 (15.80)	8.36 (7.81)
$Ni(L)(OAc).3H_2O$	Yellowish Green	224	77 %	37.76 (36.39)	4.61 (4.18)	11.75 (11.69)	12.31 (11.87)
$Ni(L)_2.2H_2O$	Yellowish Green	210	78 %	44.27 (44.13)	4.26 (4.11)	15.89 (15.43)	8.32 (8.12)
$Cu(L)(OAc).H_2O$	Brown	214	84 %	37.38 (37.10)	3.74 (3.15)	11.63 (11.56)	13.18 (12.35)
$Cu(L)_2$	Brown	196	82 %	46.32 (45.74)	3.86 (3.08)	16.63 (15.97)	9.42 (9.06)
$Zn(L)(OAc).3H_2O$	Light Yellow	240	80 %	37.24 (37.02)	4.55 (4.26)	11.59 (11.08)	13.52 (12.89)
$Zn(L)_2.2H_2O$	Light Yellow	260	82 %	43.86 (43.23)	4.22 (3.19)	15.74 (14.82)	9.19 (8.23)

d* = decomposed

Table 2. Important IR frequencies (cm^{-1}) of the Schiff base and its metal complexes.

Compound	ν(N=CH)	ν(C-S)	ν(S-H)	ν($OCOCH_3$)	ν(H_2O/OH)	ν(M-S)	ν(M-N)
HL	1697	-	2893	-	-	-	-
$Co(L)(OAc).3H_2O$	1674	741	-	1744	3232	340	485
$Co(L)_2.2H_2O$	1674	779	-	-	3240	341	485
$Ni(L)(OAc).3H_2O$	1671	779	-	1745	3232	342	486
$Ni(L)_2.2H_2O$	1674	779	-	-	3240	341	485
$Cu(L)(OAc).H_2O$	1674	779	-	1744	3395	325	488
$Cu(L)_2$	1682	779	-	-	3742	323	488
$Zn(L)(OAc).3H_2O$	1674	771	-	1744	3456	342	482
$Zn(L)_2.2H_2O$	1651	771	-	-	3742	342	485

^{1}H-NMR spectra

The ^{1}H-NMR spectral data of Schiff base and Zn(II) complexes are displayed in Table 3.

Table 3. ^{1}H NMR spectral data of Schiff base and its Zn(II) complexes.

Compounds	δ (ppm)
Schiff Base	7.46 (s, 1H, Ar-H), 7.31 (d, 1H, Ar-H), 6.96 (d, 1H, Ar-H), 4.11 (q, 2H, -OC**H$_2$**-CH_3), 1.39 (t, 3H, -OCH_2C**H$_3$**) 2.27 (s, 3H, triazine-CH_3), 8.39 (s, 1H, -N=CH-), 13.64 (s, 1H, -SH), 4.08 (m, 1H, -OH)
$Zn(L)(OAc).3H_2O$	7.44 (s, 1H, Ar-H), 7.27 (d, 1H, Ar-H), 6.93 (d, 1H, Ar-H), 2.27 (s, 3H, triazine-CH_3), 4.07 (q, 2H, -OC**H$_2$**-CH_3), 8.36 (s, 1H, -N=CH-), 1.34 (t, 3H, -OCH_2C**H$_3$**), 4.08 (m, 1H, -OH)
Zn(L)2.2H2O	7.43 (s, 2H, Ar-H), 7.25 (d, 2H, Ar-H), 6.93 (d, 2H, Ar-H), 2.27 (s, 6H, triazine-CH3), 4.09 (q, 4H, -OCH2-CH3), 8.36 (s, 2H, -N=CH-), 1.34 (t, 6H, -OCH2CH3), 4.08 (m, 1H, -OH)

^{1}H-NMR spectra of Schiff base and its metal complexes were recorded in DMSO-d_6. In Schiff base, a peak appears at δ = 8.39 ppm due to azomethine proton, which is deshielded in the spectra of Zn(II) complexes, indicating the complexation through azomethine nitrogen atom.

The signal for the SH proton appearing at δ=13.64 ppm in the spectrum of the free ligand has disappeared in the spectra of Zn(II) complexes, further supporting the complexation through S atom of the thiol group.[29,30] The peak appearing at δ = 2.27 ppm due to CH_3 group present in triazine ring did not change in the spectra of metal complexes.

Electronic spectra and magnetic moment measurements

The electronic spectral and magnetic moment data are given in Table 4. In order to understand the nature of the M-L bond, the electronic spectral data of the complexes were calculated in DMF. $Co(L)(OAc).3H_2O$ and $Co(L)_2.2H_2O$ complexes of HL exhibit two absorption bands, which fall in the region 10230-10900 cm^{-1} and 19615-20271 cm^{-1}, attributed to $^4T_{1g}(F) \rightarrow {}^4T_{2g}(F)$ (υ_1) and $^4T_{1g}(F) \rightarrow {}^4T_{1g}(P)$ (υ_3) transitions,[31] respectively. υ_2 was not observed but it could be calculated by using the relation $\upsilon_2 = \upsilon_1 + 10\ D_q$. By using band-fitting equation,[32] the ligand field parameters (D_q, B, β, β%) were also calculated.

Table 4. Electronic spectral data and ligand field parameters of metal complexes.

Compounds	Transitions (cm^{-1})			D_q (cm^{-1})	B(cm^{-1})	ν_2/ν_1	β	β %
	υ_1	υ_2	υ_3					
Co(L)(OAc).3H_2 O	10230	21615[a]	19615	1138.56	702.70	2.11	0.724	27.6
Co(L)$_2$.2H_2 O	10900	22989[a]	20271	1208.98	704.05	2.109	0.725	27.5
Ni(L)(OAc).3H_2O	10523	16530	23813	1052.3	584.93	1.57	0.562	43.8
Ni(L)$_2$.2H_2O	10618	17681	24940	1061.8	717.80	1.665	0.689	31.1
Cu(L)(OAc).H_2O	18681			-	-	-	-	-
Cu(L)$_2$	19952			-	-	-	-	-

The calculated values of crystal field splitting energy (D_q) are 1138.56 and 1208.98 cm^{-1} for 1:1 and 1:2 Co(II) complexes, respectively. These values lie within the range reported for octahedral complexes. The value of Racah parameter (B) was less than free ion value (971 cm^{-1}), indicating the orbital overlap and delocalization of *d*-electron on the ligand. The nephelauxetic ratio (β) was found to be less than 1, which indicated the partial covalent nature of metal ligand bonds.

The magnetic moment data of Co(II) complexes indicate the presence of three unpaired electrons. The magnetic moment values were found in the range of 4.5-5.0 BM, which is in the expected range (4.3-5.2 BM) of octahedral complexes.[33]

Ni(L)(OAc).3H_2O and Ni(L)$_2$.2H_2O complexes exhibit three absorption bands in the region 10523-10618 cm^{-1} (υ_1), 16530-17681 cm^{-1} (υ_2) and 23813-24940 cm^{-1} (υ_3), attributed to $^3A_{2g}(F) \rightarrow {}^3T_{2g}(F)$ (υ_1), $^3A_{2g}(F) \rightarrow {}^3T_{1g}(F)$ (υ_2) and $^3A_{2g}(F) \rightarrow {}^3T_{1g}(P)$ (υ_3) transitions, respectively. The ligand field parameters (D_q, B, β, β%) were also calculated for Ni(II) complexes. These parameters indicate octahedral arrangement around the Ni(II) complexes[34] and suggest the partial covalent nature of the metal ligand bond. The calculated values of crystal field splitting energy (D_q) are 1052.3 cm^{-1} and 1061.8 cm^{-1} for 1:1 and 1:2 Ni(II) complexes respectively. The observed magnetic moment values were found in the range of 3.3-3.4 BM, which is in the range of reported octahedral compounds.[35]

For 1:1 and 1:2 Cu (II) complexes, a band observed in the region of 18681-19952 cm^{-1}, assigned to $^2B_{1g} \rightarrow {}^2A_{1g}$, indicating the square planar geometry of the copper complexes.[36] Further confirmation was achieved by magnetic moment measurements 1.9-2.0 BM, which is well within expected range of square planar geometry of Cu(II) complexes.

ESR spectral studies

ESR spectra for 1:1 and 1:2 Cu(II) complexes i.e., Cu(L)(OAc).H_2O and Cu(L)$_2$ were recorded at room temperature on the X-Band at 9.1 GHz under the magnetic field set 0.3 T. The observed g values for Cu(L)(OAc).H_2O ($g_{\|}$=2.197, $g_{\perp}$=2.129, g_{av} =2.152) and Cu(L)$_2$ ($g_{\|}$ =2.197, $g_{\perp}$=2.126, g_{av}=2.150) corresponds to square planar geometry of both the complexes. The trend $g_{\|} > g_{\perp} > 2.0023$ was observed for Cu(II) complexes, indicates that the unpaired electron is localized in the $d_{x^2-y^2}$ orbital of the Cu(II) ion and corresponds to square planar geometry around Cu(II) ions.[37]

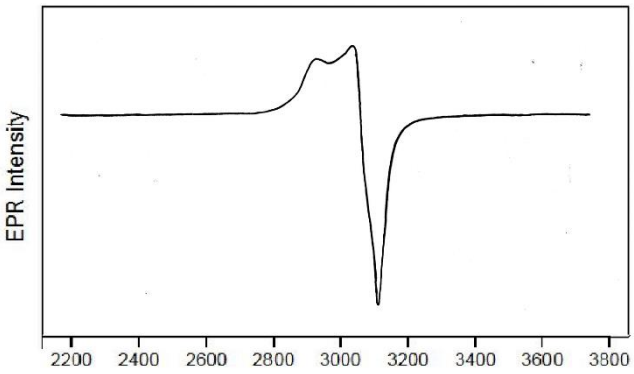

Figure 2. ESR spectrum of Cu(L)(OAc).H_2O.

The $g_{\|} < 2.3$ value confirms the covalent character of the metal ligand bond. According to Hathaway and Billing[38] if axial symmetry parameter i.e. $G > 4$, the exchange interaction is negligible, but if $G < 4$, a considerable exchange interaction in the solid complexes would be found. The 1:1 and 1:2 Cu(II) complexes gave the G value in the range of 1.537-1.574 indicating exchange interaction in solid complexes. ESR spectrum of Cu(L)(OAc).H_2O is shown in Figure 2.

Fluorescence spectral studies

The fluorescence spectra of the ligand and its Co(II), Ni(II), Cu(II) and Zn(II) complexes (10^{-3} M) were recorded in DMF solution at room temperature with excitation wavelength at 265 nm.

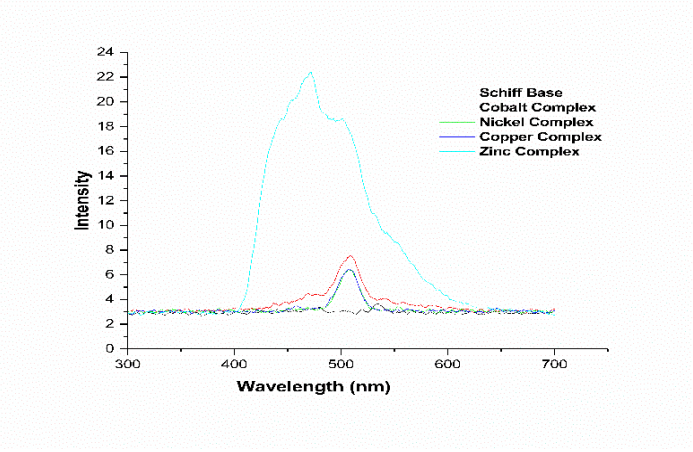

Figure 3. Fluorescence spectra of the Schiff base and its metal complexes.

Table 5. In vitro antimicrobial activity of synthesized chemical compounds and standard drugs.

S. No.	Compounds	Diameter of growth of inhibition zone (mm)[a]					
		Gram positive bacteria		Gram negative bacteria		Fungi	
		B. subtilis	*S. aureus*	*E. coli*	*P. aeruginosa*	*C. albicans*	*S. cerevisiae*
1	Schiff Base (HL)	18	-	-	-	-	-
2	$Co(L)(OAc).3H_2O$	16	21	16	16	15	16
3	$Co(L)_2.2H_2O$	15	-	-	23	7	16
4	$Ni(L)(OAc).3H_2O$	11	13	9	-	-	18
5	$Ni(L)_2.2H_2O$	12	18	7	-	6	18
6	$Cu(L)(OAc).H_2O$	8	-	8	18	-	16
7	$Cu(L)_2$	7	-	8	15	6	15
8	$Zn(L)(OAc).3H_2O$	22	25	20	20	21	20
9	$Zn(L)_2.2H_2O$	21	32	19	13	21	20
10	Ciprofloxacin	24.0	26.6	25.0	22	-	-
11	Amphotericin-B	-	-	-	-	16.6	19.3

(-) No activity; [a] Values, not including diameter of the well (8mm), are means of three replicates.

Table 6. MIC ($\mu g\ ml^{-1}$) of synthesized chemical compounds and standard drugs.

S. No.	Compounds	Gram positive bacteria		Gram negative bacteria		Fungi	
		B. subtilis	*S. aureus*	*E. coli*	*P. aeruginosa*	*C. albicans*	*S. cerevisiae*
1	Schiff Base	25	-	-	-	-	-
2	$Co(L)(OAc).3H_2O$	25	25	25	50	50	-
3	$Co(L)_2.2H_2O$	50	-	-	12.5	-	50
4	$Ni(L)(OAc).3H_2O$	50	50	-	-	-	-
5	$Ni(L)_2.2H_2O$	50	25	-	-	-	50
6	$Cu(L)(OAc).H_2O$	-	-	-	50	-	-
7	$Cu(L)_2$	-	-	-	50	-	-
8	$Zn(L)(OAc).3H_2O$	12.5	12.5	25	12.5	12.5	50
9	$Zn(L)_2.2H_2O$	25	6.25	50	50	12.5	50
10	Ciprofloxacin	6.25	6.25	6.25	12.5	-	-
11	Amphotericin-B	-	-	-	-	12.5	12.5

The data obtained indicate about the changes in fluorescence property of Schiff base, when it binds with metal ions. All the metal complexes show increased fluorescence intensity with strong emission at 510 nm for Co(II), 508 nm for Ni(II), 507 nm for Cu(II) and 472 nm for Zn(II) complexes. The enhanced fluorescence intensity of metal complexes in comparison to ligand may be due to the formation of coordination bonds between metal ions and ligand which increases the rigidity of the complex thereby reducing the loss of energy through vibrational motion.[39,40] The decrease in emission maxima was in the order of Zn(II) > Co(II) > Ni(II) > Cu(II) > Schiff base (Figure 3).

Antimicrobial activity

Schiff base and its metal complexes were checked for their in vitro antimicrobial activity by agar well diffusion method against two gram positive bacteria (*B. subtilis* and *S. aureus*), two gram negative bacteria (*E. coli* and *P. aeruginosa*) and two fungi (*C. albicans* and *S. cerevisiae*).

Schiff base (HL) and its metal complexes possessed variable biological activity against *B. subtilis, S. aureus, E. coli, P. aeruginosa, C. albicans* and *S. cerevisiae* (Table 5). Zones of inhibition were observed in the range 7-32 mm, 7-23 mm and 6-21 mm against gram positive bacteria, gram negative bacteria and fungi, respectively (Figure 4). On the basis of growth of inhibition zone, compound $Zn(L)(OAc).3H_2O$ and $Zn(L)_2.2H_2O$ were found to be most effective against *B. subtilis* and *S. aureus* with inhibition zone 22 mm, 25 mm and 21 mm, 32 mm, respectively, Compounds $Zn(L)(OAc).3H_2O$, $Zn(L)_2.2H_2O$ show good activity against *E. coli* with inhibition zone 20 mm and 19 mm respectively. $Zn(L)(OAc).3H_2O$ and $Co(L)_2.2H_2O$ exhibit good activity against *P. aeruginosa* with inhibition zone 20 mm and 23 mm and $Zn(L)_2.2H_2O$ was found to be most effective against *C. albicans* with inhibition zone found 21 mm.

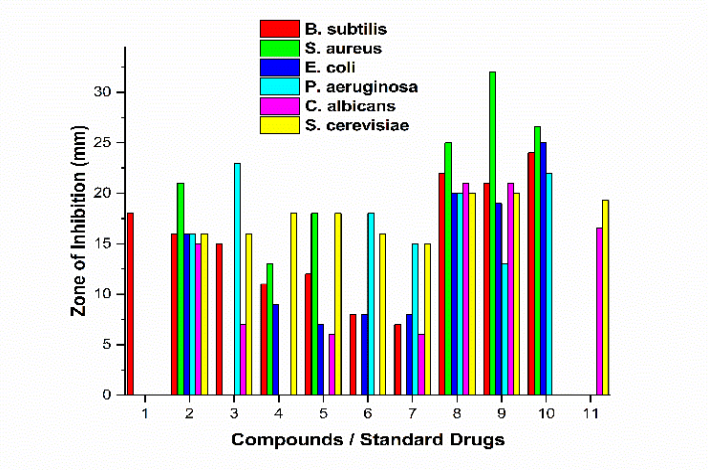

Figure 4. Comparison of Zone of inhibition of compounds with standard drugs.

$Zn(L)_2.2H_2O$, $Ni(L)(OAc).3H_2O$ and $Ni(L)_2.2H_2O$ were found to be effective against *S. cerevisiae* with inhibition zone 20 mm, 18 mm & 18 mm respectively.

The MIC of the tested compounds have been observed from 6.25-50 µg mL^{-1} against gram positive and gram negative bacteria and (12.5-50) µg mL^{-1} in case of fungi (Table 6). Among these compounds, $Zn(L)_2.2H_2O$ shows best antibacterial activity against *S. aureus* and shows lowest MIC value 6.25 µg mL^{-1}. Compounds $Zn(L)(OAc).3H_2O$ and $Zn(L)_2.2H_2O$ show good activity against *E. coli, C. albicans* and *P. aeruginosa, S. cerevisiae* respectively with lowest MIC values 12.5 µg mL^{-1}. MIC values of the metal complexes indicate moderate activity against the microbial strains as compared to standard drugs, Ciprofloxacin and amphotericin B.

Thermal analysis

To determine the thermal stability and chemical composition of 1:1 Co(II), Ni(II), Cu(II) and Zn(II) complexes, thermogravimetric analysis has been carried out over a temperature range of 50-600 ˚C by using alumina as a reference compound. The percentage mass loss of the complexes with temperature is shown in the Figure 5.

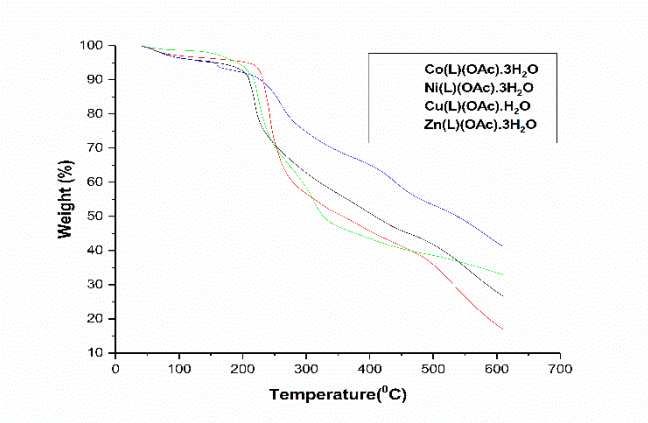

Figure 5. TG curves of synthesized metal complexes.

Table 7. Calculated activation energies (kJ mol^{-1}) for different stages in degradation of metal complexes.[a]

Compounds	E_2* (R^2)	E_3 *(R^2)
$Co(L)(OAc).3H_2O$	50.26 (0.9892)	100.38 (0.9384)
$Ni(L)(OAc).3H_2O$	73.65 (0.9972)	126.0 (0.9132)
$Cu(L)(OAc).H_2O$	60.54 (0.9794)	43.00 (0.9895)
$Zn(L)(OAc).3H_2O$	28.754 (0.9901)	26.168 (0.9941)

[a]Heating rate was 10 °C min^{-1}. *R^2 stands for regression coefficient and 2,3 represents second and third stages of degradation.

The Co(II) complex decomposes in the three stages. The TG curve of $Co(L)OAc.3H_2O$ indicates first weight loss of 8.26 % (calcd. 11.32 %) in the temperature range 40-205 °C attributed to loss of three coordinated water molecules. The next step represents a mass loss of 40.87 % (calcd. 43.82 %) from 205-400 °C corresponding to the loss of organic moiety. The final step resulted in the decomposition of triazine ring with mass loss of 30.42 % (calcd. 32.50 %) from 400°C to 610 °C.[41]

The TG curve of $Ni(L)(OAc).3H_2O$ exhibits first weight loss of 9.64 % (calcd. 11.32 %) at 40-230˚C, attributed to the loss of three coordinated water molecules. The subsequent steps correspond to the decomposition of organic moiety with weight loss of 42.66 % (calcd. 43.84 %) within the temperature range 230-380 ˚C and triazine ring with weight loss of 30.73 % (calcd. 32.51 %) from 380-610 ˚C. The TG curve of $Cu(L)(OAc).H_2O$ shows three decomposition steps within the temperature range 40-160˚C, 160-310˚C and 310-600˚C corresponding to loss of one water molecule, organic moiety and triazine ring respectively[42] whereas the complex $Zn(L)OAc.3H_2O$ shows three decomposition steps in the temperature range 40-210˚C, 210-400˚C and 400-595˚C respectively. Activation energies for different stages in degradation of metal complexes are shown in Table 7. The TG curves are further supported by the DTA curves Figure 6.

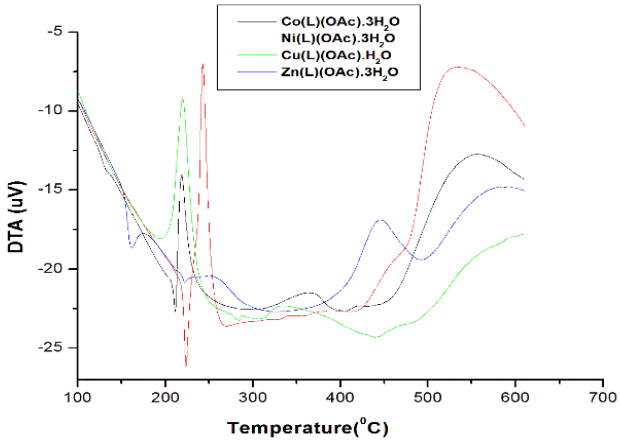

Figure 6. DTA curves of synthesized metal complexes.

Determination of degradation activation energy

For a second order reaction, Coats and Redfern[43] provided an approximation. This is an integral form of the rate equation. The simplified form of the equation is

$$\ln\left[\frac{g(\alpha)}{T^2}\right] = \ln\left[\frac{AR}{E\beta}\right] - \frac{E}{RT} \qquad (1)$$

where,

T=temperature,

A =pre-exponential term (min^{-1}),

R =gas constant,

E =energy of activation,

B =heating rate (˚C min^{-1}),

α =degree of conversion and

$g(\alpha)$=degradation mechanism but $g(\alpha) = (1/1-\alpha) - 1$

For second order mechanism E can be calculated from the slope of the graph between $ln[[g(x)/T^2]$ and 1/T. Table (7) presents the activation energy values for second and third decomposition stages obtained using Coats – Redfern method and corresponding regression coefficients (R^2).

Table 8. Selected calculated bond angles (˚) and bond lengths (Å) for ligand and its 1:1 and 1:2 copper metal complexes.

Compounds	Atoms	Bond Angles (˚)	Atoms	Bond Lengths (Å)
Schiff Base	N(5)-N(14)-C(15)	120	C(4)-S(12)	1.815
	C(4)-S(12)-H(13)	109.5	N(14)-C(15)	1.26
	N(5)-C(6)-O(7)	123.43	C(15)-C(17)	1.503
	C(15)-C(17)-C(22)	119.9	C(6)-O(7)	1.208
Cu(L)(OAc).H_2O	C(4)-S(13)-Cu(21)	109.5	N(12)-Cu(21)	2.491
	H(19)-O(18)-Cu(21)	109.5	O(14)-Cu(21)	1.81
	N(5)-N(12)-C(22)	120	O(18)-Cu(21)	1.81
	N(12)-Cu(21)-O(14)	109.5	S(13)-Cu(21)	1.247
$Cu(L)_2$	N(5)-N(12)-Cu(30)	97.882	C(4)-S(16)	1.856
	N(5)-C(4)-S(16)	109.5	S(16)-Cu(30)	1.644
	C(4)-S(16)-Cu(30)	109.5	N(18)-N(29)	1.352
	S(16)-Cu(30)-S(28)	128.169	N(12)-Cu(30)	2.502

Based on activation energy values (E2) and (E3) as deduced using second order model, following stability order is suggested:

$$Ni(II) > Cu(II) > Co(II) > Zn(II) \quad (E_2)$$

$$Ni(II) > Co(II) > Cu(II) > Zn(II) \quad (E_3)$$

Electrochemical behavior

Electrochemical properties of 1:1 Cu(II) complex (10^{-3}M) in DMF was investigated with the help of cyclic voltammetry in potential ranging from -2.0 to +1.0 V in DMF solution with a scan rate of 0.1 V/s, containing tetrabutylammonium perchlorate as the supporting electrolyte. Cyclic voltammogram (CV) is shown in Figure 8.

The complex Cu(L)(OAc).H_2O exhibits two reduction peaks at E_{pc} = 0.5 V and E_{pc} = -0.12 V for Cu(II) to Cu(I) and Cu(I) to Cu(0) and corresponding two oxidation peaks at E_{pa} = -0.82 V and E_{pa} = +0.26 V for Cu(0) to Cu(I) and Cu(I) to Cu(II) complexes. ΔE for these processes is very high, which is consistent with the quasi reversible process. The ratio of cathodic to anodic peak current (I_c/I_a = 0.214) was found to be less than one.[44]

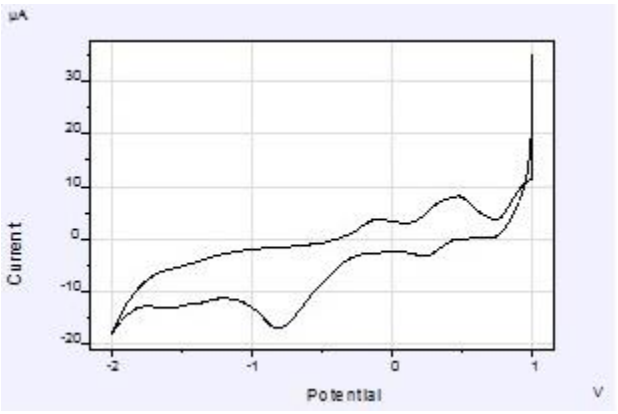

Figure 7. Cyclic Voltammogram of Cu(L)(OAc).H_2O.

Structural determination by computational method.

The optimized geometries of Schiff base and its some 1:1 and 1:2 metal complexes are shown in Figure 8. Bond length and bond angles of some complexes are depicted in Table 8 respectively.

(A)

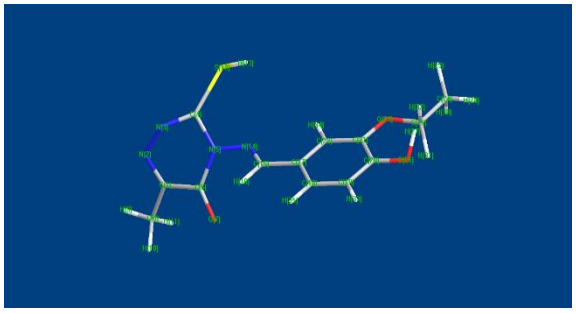

(B)

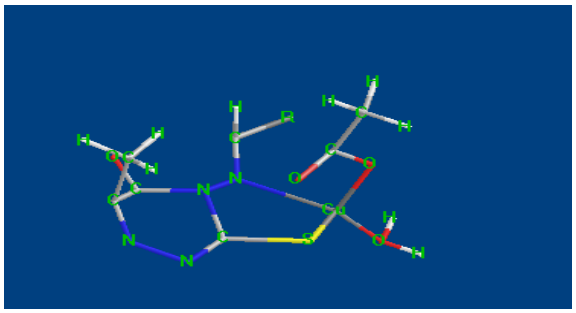

(C)

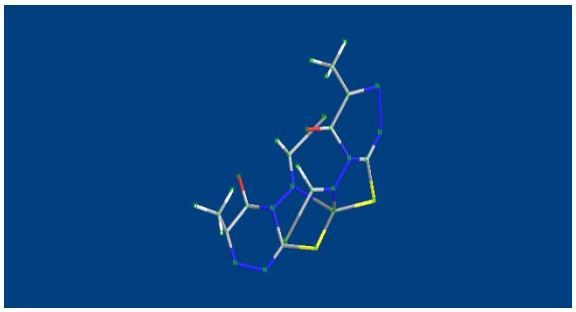

(D)

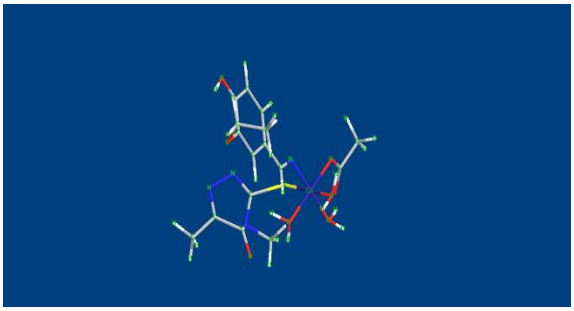

(E)

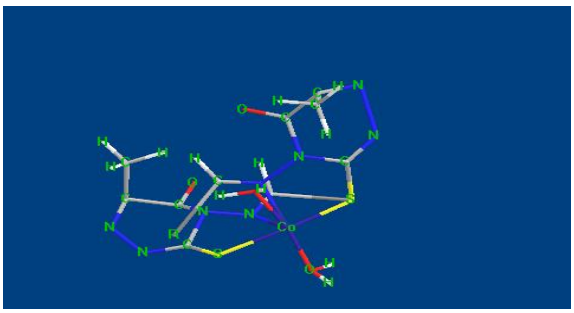

Figure 8. 3D structures of Schiff base (A),Cu(L)(OAc).H_2O (B), $Cu(L)_2$ (C), Co(L)(OAc).$3H_2O$ (D) and $Co(L)_2.2H_2O$ (E)

Conclusion

The synthesized 4-[(3-ethoxy-4-hydroxybenzylidene)-amino]-3-mercapto-6-methyl-5-oxo-1,2,4-triazine (HL) Figure 1. Schiff base is a bidentate ligand, coordinates through azomethine nitrogen and sulphur to the different metal ions. Synthesized compounds were characterized with the help of IR, NMR, ESR, electronic, Fluorescence spectroscopy, cyclic voltammetry, magnetic and thermal studies.

The results of the investigations suggest octahedral geometry for the Co(II), Ni(II) and Zn(II) complexes and square planar geometry around the Cu(II) metal ion. On the basis of above studies, Schiff base is versatile ligand which can coordinate with different metal ions and also biologically active. Metal complexes exhibit enhanced antimicrobial and antifungal activities against various microbial strains as compared to parent ligand and also possess comparable activities with standard drugs.

Acknowledgements

One of the authors (Prerna) expresses sincere gratitude to HSCST (Haryana State Council for Science and Technology, Panchkula) for providing financial support & Department of Chemistry, Kurukshetra University, Kurukshetra for providing the necessary facilities. We would also like to thank SAIF, IIT Bombay for ESR analysis, IIC IIT Roorkee for VSM analysis, SAIF PU Chandigarh for FT-IR and elemental analysis.

References

[1]Khouba, Z., Benabdallah, T., Maschke, U., Spectrophotometric study of liquid crystal containing pentadentate Schiff base type systems, *Phys. Procedia*, **2009**, *2*, 1305. DOI: doi.org/10.1016/j.phpro.2009.11.096

[2]Schiff, H., The syntheses and characterisation of Schiff bases, *Ann. Suppl*, **1864**, *3*, 343.

[3]Zhang, L. X., Liu, Y., Cia, L.-H., Hu, Y.-J., Yin, J., Hu, P.-Z., Inhibitory study of some novel Schiff base derivatives on staphylococcuss aures by microcalorimetry, *Thermochim. Acta*, **2006**, *440*, 51. DOI: doi.org/10.1016/j.tca.2005.10.012.

[4]Pandey, S. K., Singh, A., Singh, A., Antimicrobial studies of some novel quinazolinones fused with [1,2,4]-triazine and [1,2,4,5]-tetrazine rings, *Eur. J. Med. Chem.*,**2009**, *44*, 1188. DOI: doi.org/10.1016/j.ejmech.2008.05.033.

[5]Klayman, D. L., Scovill, J. P., Bartosevich, J. F., Bruce, J., *J. Med. Chem.*, **1983**, *26*, 35. DOI: 0022-2623/83/1826-0039$01.50/0

[6]Culakova, H., Dzugasova, V., Gbelska, Y., Subik, J., Antibacterial activity of CTBT (7-chlorotetrazolo[5,1-c]benzo[1,2,4]-triazine) generating reactive oxygen species, *Microbiol. Res.*, **2013**, *168*, 147. https://doi.org/10.1016/j.micres.2012.10.003

[7]Singh, K., Kumar, Y., Puri, P., Sharma, C., Aneja, K.R., Synthesis, spectroscopic, thermal and antimicrobial studies of Co(II), Ni(II), Cu(II) and Zn(II) complexes with Schiff base derived from 4-amino-3-mercapto-6-methyl-5-oxo-1,2,4-triazine, *Med. Chem. Res.*, **2012**, *21*(8),1708-1716. DOI: https://doi.org/10.1007/s00044-011-9683-4

[8]Abdel-Rahman, R., Role of uncondensed 1,2,4-triazine derivatives as biocidal plant protection agents--a review, *Die Pharmazie*, **2001**, *56*, 195.

[9]Aboul-Fadl, T., Mohammed, F. A.-H., Hassan, E. A.-S., Synthesis, antitubercular activity and pharmacokinetic studies of some schiff bases derived from 1- alkylisatin and isonicotinic acid hydrazide, *Arch. Pharm. Res.*, **2003**, *26*, 778. DOI: https://doi.org/10.1007/BF02980020

[10]Sathe, B. S., Jaychandran, E., Jagtap, V., Sreenivasa, G., In vitro anti-inflammatory activity of 2-amino-3-(substituted benzylidine-carbohydrazide)-4, 5, 6, 7-tetrahydrobenzothio-phenes, *Int. J. Pharm. Res. Dev.*, **2011**, *3*, 164.

[11]Sondhi, S. M., Singh, N., Kumar, A., Lozach, O., Meijer, L., Synthesis, anti-inflammatory, analgesic and kinase (CDK-1, CDK-5 and GSK-3) inhibition activity evaluation of benzimidazole/benzoxazole derivatives and some Schiff's bases, *Bioorg. Med. Chem.*, **2006**, *14*, 3758. DOI: https://doi.org/10.1016/j.bmc.2006.01.054

[12]Pandey, A., Dewangan, D., Verma, S., Mishra, A., Dubey, R. D., Synthesis of Schiff bases of 2-amino-5-aryl-1,3,4-thiadiazole and its analgesic, antiinflammatory, antibacterial and antitubercular Activity, *Int. J. Chem. Tech. Res.*, **2011**, *3*, 178.

[13]Chandramouli, C., Shivanand, M., Nayanbhai, T., Bheemachari, B., Udupi, R., Synthesis and biological screening of certain new triazole schiff bases and their derivatives bearing substituted benzothiazole moiety, *J. Chem. Pharm. Res.*, **2012**, *4*, 1151.

[14]Kearney, P. C., Kaufman, D. D., *Herbicides: Chemistry, degradation and mode of action*, Marcel Dekker, Inc., **1975**.

[15]Singh, K., Barwa, M. S., Tyagi, P., Synthesis, characterization and biological studies of Co(II), Ni(II), Cu(II) and Zn(II) complexes with bidentate Schiff bases derived by heterocyclic ketone, *Eur. J. Med. Chem.*, **2006**, *41*, 147. DOI: https://doi.org/10.1016/j.ejmech.2005.06.006

[16]Losada, J., Del Peso, I., Beyer, L., Electrochemical and spectroelectrochemical properties of copper(II) Schiff-base complexes, *Inorg. Chim. Acta*,**2001**, *321*, 107. DOI: https://doi.org/10.1016/S0020-1693(01)00511-4

[17]Santos, M. L. P., Bagatin, I. A., Pereira, E. M., Ferreira, A. M. D. C., Redox behaviour and reactivity of some di-Schiff base copper(II) complexes towards reduced oxygen species, *J. Chem. Soc., Dalton Trans.*, **2001**, 838. DOI:10.1039/B004985I.

[18]Cozzi, P. G., Metal–Salen Schiff base complexes in catalysis: practical aspects, *Chem. Soc. Rev.*, **2004**, *33*, 410. **DOI:**10.1039/B307853C

[19]Yoshikawa, Y., Yasui, H., Zinc Complexes Developed as Metallopharmaceutics for Treating Diabetes Mellitus based on the Bio-Medicinal Inorganic Chemistry, *Curr. Top. Med. Chem.*, **2012**, *12*, 210. DOI: https://doi.org/10.2174/156802612799078874

[20]Chandra, S., EPR, magnetic and spectral studies of copper(II) and nickel(II) complexes of schiff base macrocyclic ligand derived from thiosemicarbazide and glyoxal, *J. Indian Chem. Soc.*, **2004**, *81*, 203. DOI: https://doi.org/10.1016/S1386-1425(03)00220-8

[21]Mohindru, A., Fisher, J. M., Rabinovitz, M., Bathocuproine sulphonate: a tissue culture-compatible indicator of copper-mediated toxicity, *Nature*, **1983**, *303*, 64. DOI: https://doi.org/10.1038/303064a0

[22]Pandeya, S., Yogeeswari, P., Sriram, D., De Clercq, E., Pannecouque, C., Witvrouw, M., Synthesis and Screening for Anti-HIV Activity of Some N-Mannich Bases of Isatin Derivatives, *Chemotherapy*, **1999**, *45*, 192. DOI: https://doi.org/10.1159/000007182.

[23]Vogel, A. I.,, *A Text Book of Quantitative Chemical Analysis*, 5th edn. Addison Wesley Longman, London. **1999.**

[24]Dornow, A., Menzel, H., Marx, P., Syntheses of nitrogen-containing heterocycles, XXVII. * About 1.2.4-triazines, I view some new s triazolo [3.2- c] - as triazines, *Chem. Ber*, **1954**, *97*, 2173. DOI: https://doi.org/10.1002/cber.19640970811

[25]Singh, K., Thakur, R., Kumar, G., Synthesis, spectroscopic, thermal and antimicrobial studies of Co(II), Ni(II), Cu(II) and Zn(II) complexes with Schiff base derived from 4-amino-3-mercapto-6-methyl-5-oxo-1,2,4-triazine, *Eur. Chem. Bull.*, **2016**, *5*, 46. DOI: https://doi.org/10.1007/s00044-011-9683-4

[26]Okeke, M. I., Iroegbu, C. U., Eze, E., Okoli, A., Esimone, C., Evaluation of extracts of the root of Landolphia owerrience for antibacterial activity, *J. Ethnopharmacol.*, **2001**, *78*, 119. DOI: https://doi.org/10.1016/S0378-8741(01)00307-5

[27]Patil, S. A., Unki, S. N., Kulkarni, A. D., Naik, V. H., Badami, P. S., Co(II), Ni(II) and Cu(II) complexes with coumarin-8-yl Schiff-bases: Spectroscopic, in vitro antimicrobial, DNA cleavage and fluorescence, *Spectrochim. Acta A*, **2011**, *79*, 1128. DOI: https://doi.org/10.1016/j.saa.2011.04.032s.

[28]Singh, K., Barwa, M. S., Tyagi, P., Synthesis, characterization and biological studies of Co(II), Ni(II), Cu(II) and Zn(II) complexes with bidentate Schiff bases derived by heterocyclic ketone, *Eur. J. Med. Chem.*, **2006**, *41*, 147. DOI: https://doi.org/10.1016/j.ejmech.2005.06.006

[29]Singh, K., *J. Enzyme Inhib. Med. Chem.*, 2006, *21*, 557.

[30]Singh, K., Singh, D., Singh Barwa, M., Tyagi, P., Mirza, Y., Some bivalent metal complexes of Schiff bases containing N and S donor atoms, *J. Enzyme Inhib. Med. Chem.*, **2006**, *21*, 749. DOI: https://doi.org/10.1080/14756360600838648.

[31]Singh, K., Raparia, S., Surain, P., Co(II), Ni(II), Cu(II) and Zn(II) Complexes of 4-(4cyanobenzylideneamino)-3-mercapto-5-oxo-1,2,4-triazine: synthesis, characterization and biological studies, *Med. Chem. Res.*, **2015**, *24*, 2336. DOI: 10.1007/s00044-014-1298-0

[32]Reddy, V., Patil, N., Angadi, S., Synthesis, Characterization and Antimicrobial Activity of Cu(II), Co(II) and Ni(II) Complexes with O, N, and S Donor Ligands, *J. Chem.*, **2008**, *5*, 577. DOI: http://dx.doi.org/10.1155/2008/170631

[33]Patil, S. A., Unki, S. N., Kulkarni, A. D., Naik, V. H., Badami, P. S., Co(II), Ni(II) and Cu(II) complexes with coumarin-8-yl Schiff-bases: Spectroscopic, in vitro antimicrobial, DNA cleavage and fluorescence studies, *Spectrochim. Acta A*, **2011**, *79*, 1128. DOI: https://doi.org/10.1016/j.saa.2011.04.032

[34]Khalil, S., Dioxouranium(VI) Schiff Base Complexes as Ligands towards Cu(II) and Ni(II) Ions, *Chem. Papers-Slovak Acad. Sci.*, **2000**, *54*, 12.

[35]Bagihalli, G. B., Avaji, P. G., Patil, S. A., Badami, P. S., Synthesis, spectral characterization, in vitro antibacterial, antifungal and cytotoxic activities of Co(II), Ni(II) and Cu(II) complexes with 1,2,4-triazole Schiff bases, *Eur. J. Med. Chem.*, **2008**, *43*, 2639. DOI: baseshttps://doi.org/10.1016/j.ejmech.2008.02.013

[36]Balhausen, C. J., *Introduction to Ligand Fields, McGraw Hill*, New York, **1962**.

[37]Drago, R. S., *Physical Methods in Inorganic Chemistry*, Reinhold Publishing Corporation, New York, **1968**.

[38]Kalanithi, M., Kodimunthiri, D., Rajarajan, M., Tharmaraj, P., Synthesis, characterization and biological activity of some new VO(IV), Co(II), Ni(II), Cu(II) and Zn(II) complexes of chromone based NNO Schiff base derived from 2-aminothiazole, *Spectrochim. Acta A*, **2011**, *82*, 290. DOI: https://doi.org/10.1016/j.saa.2011.07.051

[39]Boghaei, D. M., Behzadian Asl, F., Synthesis, characterization and fluorescence spectra of mixed ligand Zn(II), Cd(II) and Hg(II) complexes with 1,10-phenanthroline-5,6-dione ligand, *J. Coord. Chem.*, **2007**, *60*, 1629. DOI: https://doi.org/10.1080/00958970601099183

[40]Maxim, C., Pasatoiu, T. D., Kravtsov, V. C., Shova, S., Muryn, C. A., Winpenny, R. E., Tuna, F., Andruh, M., Copper(II) and zinc(II) complexes with Schiff-base ligands derived from salicylaldehyde and 3-methoxysalicylaldehyde: Synthesis, crystal structures, magnetic and luminescence properties, *Inorg. Chim. Acta*, **2008**, *361*, 3903. DOI: https://doi.org/10.1016/j.ica.2008.03.013.

[41]Coats, A. W., Redfern, J., Kinetic Parameters from Thermogravimetric Data, *Nature*, **1964**, *201*, 68. DOI: https://doi.org/10.1038/201068a0

[42]Vargová, Z., Zeleòák, V. R., Císaøová, I., Györyová, K. N., Correlation of thermal and spectral properties of zinc(II) complexes of pyridinecarboxylic acids with their crystal structures, *Thermochim. Acta*, **2004**, *423*, 149. DOI: https://doi.org/10.1016/j.tca.2004.03.016

[43]Singh, K., Kumar, Y., Puri, P., Kumar, M., Sharma, C., Cobalt, nickel, copper and zinc complexes with 1,3-diphenyl-1H-pyrazole-4-carboxaldehyde Schiff bases: Antimicrobial, spectroscopic, thermal and fluorescence studies, *Eur. J. Med. Chem.*, **2012**, *52*, 313. DOI: https://doi.org/10.1016/j.ejmech.2012.02.053

[44]Kasumov, V. T., Köksal, F., Synthesis, ESR, UV–Visible and reactivity studies of new bis(N-dimethoxyaniline-3,5-tBu2-salicylaldiminato)copper(II) complexes, *Spectrochim. Acta A*, **2012**, *98*, 207. DOI: https://doi.org/10.1016/j.saa.2012.07.122.

Received: 03.05.2018
Accepted: 15.09.2018.

NOVEL SELECTIVE SPECTROPHOTOMETRIC METHOD FOR HYDROSULFIDE (HS^-) IONS ASSESSMENT USING VITAMIN B_{12} PRECURSOR, AQUACYANOCOBYRINIC ACID HEPTAMETHYL ESTER

Hadeel H. El-Shalakany[a], M. S. A. Hamza[a] and Ayman H. Kamel[a]*

Keywords: Aquacyanocobyrinic acid heptamethylester (aquacyanocobester), spectrophotometry, hydrosulfide determination.

A simple spectrophotometric method with good selectivity and high sensitivity towards sulfide ions has been introduced. The method is based on the replacement of the axial water molecule of the aquacyanocobyrinic acid heptamethyl ester (ACCbs) reagent after the reaction with HS^- ions, and forming stable complex. ACCbs reagent is characterized with three distinguishable absorption bands with absorption maxima at 353, 497 and 527 nm. After adding HS^-, a new absorption band at 582 nm has been obtained. The decrease of the absorption bands of the reaction product at 353, 497 and 527 nm and the enhancement of the band at 582 nm are quantitatively linear to HS^- concentration over the concentration range 0.02-1.543 µg mL^{-1} with lower limit of detection 0.019 µg mL^{-1}. No noticeable interferences are caused by most common ions. Suitability for the assessment of HS^- in complex matrices without prior treatment was shown after validation of the method according to the standards of quality assurance. The results compare fairly well with data obtained using the standard method.

* Corresponding Authors
Fax:
E-Mail: ahkamel76@sci.asu.edu.eg
[a] Chemistry Department, Faculty of Science, Ain Shams University, Cairo, Egypt

Introduction

Sulfides (H_2S, HS^-, and S^{2-}) have been found in anoxic environments including natural water, wastewater, crude petroleum, natural gas and volcanic gases.[1] Hydrogen sulfide is a colorless gas that can exist naturally in groundwater. It is corrosive and can leach metals from plumbing systems into the water. Corrosion of metals by hydrogen sulfide forms a black precipitate that can stain laundry and bathroom fixtures, darken silverware, and discolor copper and brass utensils. Water that is giving off a distinctive smell is most likely contaminated with hydrogen sulfide.[2] It is also can enter a groundwater through sulfur-reducing bacteria present in groundwater well. These bacteria use sulfur as an energy source to chemically change sulfates to hydrogen sulfide. They can also use sulfur from decaying plants and other organic matter in oxygen-deficient environments. They can occur in deep or shallow wells, and reside in plumbing systems.[3] In the human body, mercaptans are readily oxidized to their respective sulfides and, consequently, sulfide can be founded in animal halite. Animals showing signs of liver cirrhosis produce more sulfides in their bloodstream and halite. Thus, determination of sulfide could be used as a marker of liver diseases.[4] Environmental sulfide concentration has been usually found in concentrations of µmol L^{-1}. For example, the recognition threshold range which hydrogen sulfide odor can be detected by humans is 0.30-90 µmol L^{-1}.[5] Thus, the determination of sulfide is necessary in different human activities, but continues to present challenges due to the complexity of samples, and the necessity to determine low concentrations of sulfide. In addition to the above, sulfides can be also present in hydrogen sulfide pretreated fruits and vegetables. Therefore, rapid detection of hydrogen sulfide and its existing forms in aqueous media (total sulfides) has been gaining a great interest from researchers. In addition, to assure the quality control of manufactured products, a sensitive and selective method for sulfide determination is required.

Various analytical methods for hydrogen sulfide quantification and monitoring have been reported. These include simple titremitry.[6,7] However, this method is not useful for measurement of low concentrations, not selective and requires sample pre-treatment. Other techniques and methods have been developed including electrochemistry,[8-10] chromatography,[11-13] inductively coupled plasma-atomic emission spectroscopy,[14,15] fluorimetry,[16-18] and capillary electrophoresis.[19]

Many spectrophotometric methods have been reported in the literature for monitoring sulfide. Some of these methods are based on the inhibitory effect of sulfide ion on the reactions of peroxidase/pyrogallol and H_2O_2 system,[20] reducing effect on Fe^{3+}/phenthroline complex,[21] 2,6-dichlorophenolindophenol (DCPI),[22] N,N-dimethyl-*p*-phenylenediamine/Fe^{3+},[23,24] production of phenothiazine dyes,[25] nitroprusside,[26]1, 2-naphthoquinone-4-sulfonate,[27] and phenylseleno-nitrobenzoxadiazole derivative.[28]

In this work, a novel spectrophotometric method is introduced for sulfide assessment. The method is based on the selective axial coordination of sulfide ion to the central cobalt atom in aquacyanocobyrinic acid heptamethyl ester (ACCbs) to cause significant changes in the spectrum of ACCbs reagent. The method offers a very high selectivity, sensitivity and accuracy for assessment of sulfide ions as compared with many of those previously reported methods. Application for determining sulfide in domestic wastewater and ground water samples gives precise results that agree fairly well with those obtained by the official method.

Experimental

Apparatus

All absorbance measurements were carried out using Shimadzu UV-vis spectrophotometer (Model UV-1601) with 1.0 cm light path length matched quartz cells. For all pH measurements, Orion digital pH/mV meter (Model SA 720) and an Orion combined glass pH electrode (Model 80-02) were used.

Reagents

All Chemicals and reagents used were of analytical grade and deionized water was used throughout. Sodium sulfide, $Na_2S.9H_2O$, was purchased from Sigma-Aldrich. Phosphoric acid 85%, acetic acid (glacial) and boric acid were obtained from Fluka. Aquacyanocobester (ACCbs) was prepared as described previously.[29,30] In brief, vitamin B_{12} was dissolved in methanol solution containing 1 mol L^{-1} H_2SO_4 and was refluxed under nitrogen atmosphere for 4 days. The reaction mixture was then diluted with deionized water, neutralized with $NaHCO_3$ and treated with solid NaCN to produce dicyanocobester (DCCbs; violet color). The product is then extracted firstly with CCl_4 followed by CH_2Cl_2. The solid is then collected after solvent removal. The purity of DCCbs was checked with HPLC using 4.6 mm x 256 mm column filled with TSK-Gel silica-60 stationary phase, dichloromethane (97.3 %) as a mobile phase and a 1 mL min^{-1} elution rate. Aquacyanocobester (ACCbs) was prepared by adding CH_3COOH to methanolic solution of DCCbs and adjusting the pH at 3. Formation of ACCbs was detected by the appearance of a characteristic absorption band at 353 nm. Universal buffer solutions were prepared by mixing 0.04 mol L^{-1} phosphoric, acetic and boric acids as reported[31] followed by pH adjustment with 0.2 mol L^{-1} NaOH.

Calibration curve and analytical procedure

A 2.5 mL of ACCbs (3.5 x 10^{-5} mol L^{-1}) working reagent solution, buffered with 0.04 mol L^{-1} universal buffer of pH 9, was transferred into 1.0 cm path light length spectrophotometer quartz cell (4 mL total capacity) then titrated with small aliquots of HS^- solution to obtain series of solutions containing 0.02-1.55 µg mL^{-1} of HS^- ion and the absorbance was measured after 1 min at 353, 497, 527 and 582 nm, against a blank containing universal buffer adjusted to the same pH. The calibration plots between the absorbance changes at each wavelength against the sulfide concentration were constructed. All spectrophotometric measurements were in triplicate.

Determination of sulfide in wastewater samples

Domestic sewage water samples were collected and were filtered through Whatman filter paper no. 41 prior to analysis. A 2.5 mL portion of ACCbs reagent buffered with 0.04 mol L^{-1} of universal buffer (pH 9) was introduced in a 1.00 cm light path length cuvette and placed in the thermo-stated cell block of the spectrophotometer. A100 µL of the test sample was introduced to the cuvette, shaken and the absorbances at 353, 497, 528 and 582 nm were recorded. Sulfide concentration was calculated from the calibration graph.

Wastewater samples were collected from sugarcane refinery factory, power plant and petrochemical industry, and filtered prior to analysis. A known volume, 1 mL of the effluent was introduced to a 10 mL volumetric flask and diluted to the mark with buffer at pH 9. For Power plant and petrochemical industry samples, 0.5 mL of the sample was diluted to 1 L with buffer at pH 9.

Results and Discussion

Characteristics of the absorption spectra

As previously reported,[32] aqueous solution of ACCbs exhibits three distinct absorption bands with absorption maxima at 353, 497 and 527 nm. After the addition of HS^-, a new absorption band at 582 nm and three isobestic points at 365, 440 and 554 nm have been also obtained as shown in figure 1. In alkaline solutions (pH 9), the reaction of ACCbs with hydrogen sulfide is not straightforward. HS^- can act as both ligands and reducing agents in which coordination (thermodynamic factor) and reduction (kinetic factor) can occur.[33] It reacts with ACCbs in three consecutive and rapid steps at pH 9.0. The first is the formation of $(HS)(CN)Cbs^{(III)}$ complex between aquocyanocobester and hydrogen sulfide ion. The second step is a short-lived intermediate via inner-sphere electron transfer with to form reduced cobester $[(H)S]Cbs^{(II)}$or even super reduced cobester (+1 oxidation state). The third is the addition of a second HS^- ion to the already reduced cobester. Kinetics and mechanism of the reaction of hydrogen sulfide with cobalamin in aqueous solution have been previously described.[34]The equilibrium established between HS^- ion and ACCbs can be simplified and represented as shown in figure 2.

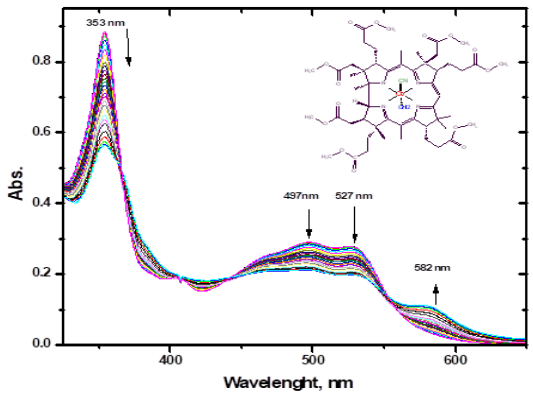

Figure 1. Absorption spectra of $[ACCbs]^+$ reagent (3.5 x 10^{-5} mol L^{-1}) of pH 9 with different concentrations of HS^- ion (0.02-5.5 µg mL^{-1}).

Optimum reaction conditions

The effect of pH on the stability of HS/ACCbs system was investigated by measuring the decrease of the absorbances at 353, 497 and 527 nm and the increase of the absorbance at 582 nm for a series of solutions containing 0.5 µg mL^{-1} HS^- ion and 2.6 x 10^{-5} mol L^{-1} $[ACCbs]^+$.

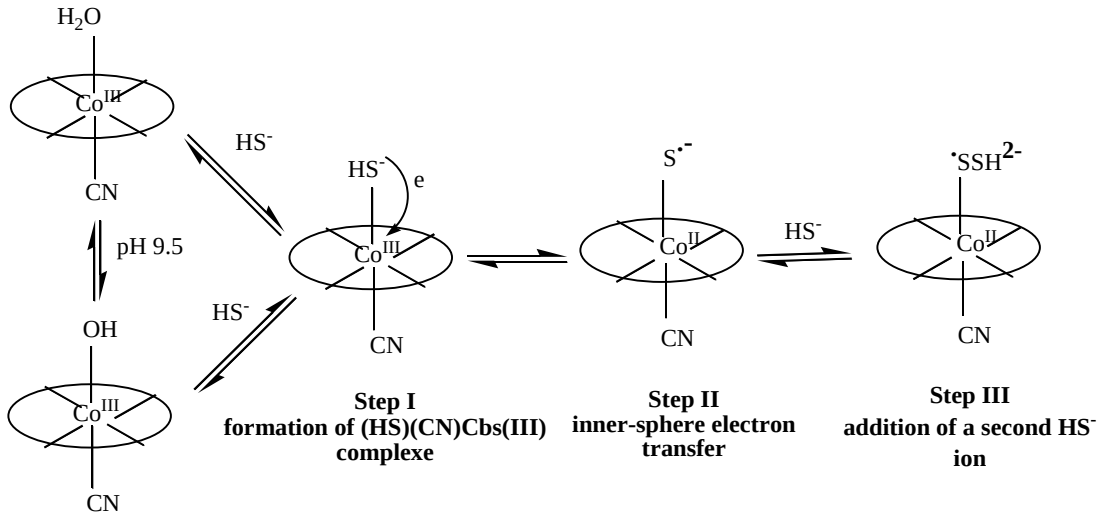

Figure 2. Schematic representation of the interaction of hydrosulphide ion with ACCbs.

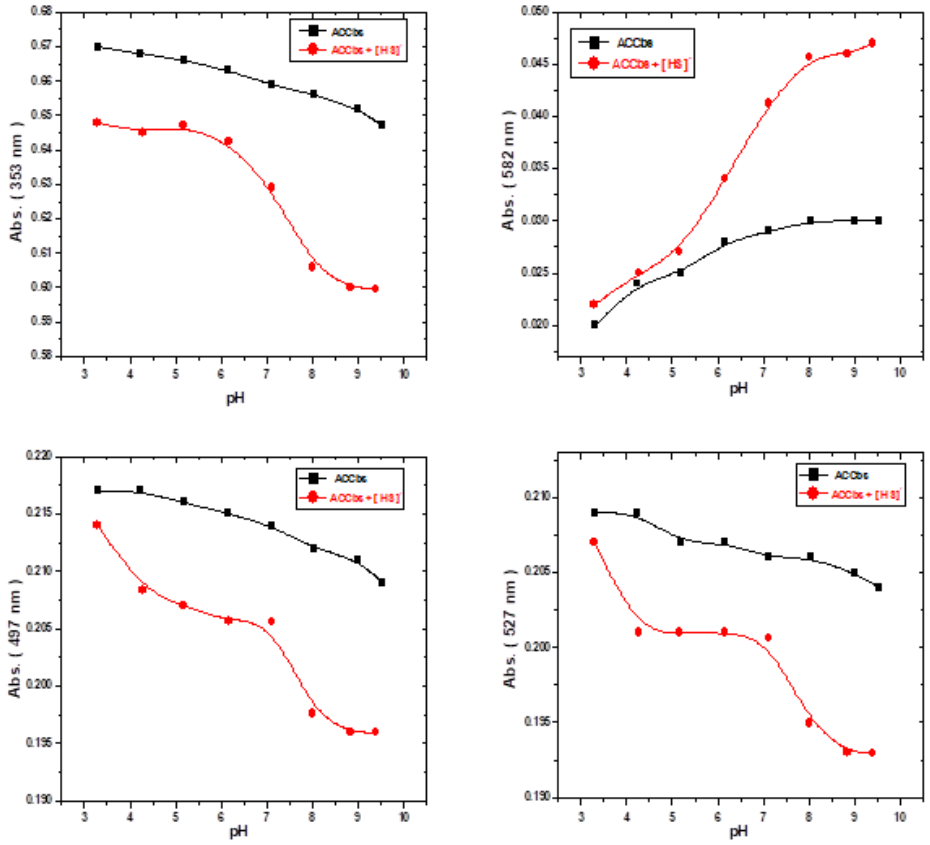

Figure 3. Effect of pH on the absorbance of (2.6 x 10^{-5}mol L^{-1}) $[ACCbs]^+$ reagent in absence and presence of 0.5µg mL^{-1} hydrosulphide ion at different wavelengths.

The pH of each solution was adjusted at values ranging from pH 3-9.5 using 0.04 mol L^{-1} universal buffer. The absorbance-pH profiles reveal good response of the system at pH 9 as shown in figure 3. At pH > 9, OH^- interference takes place due to the formation of cyanohydroxocobester [HO(CN)Cbs] species. All subsequent measurements were made at pH 9.0.

Selectivity measurements

The selectivity of $[ACCbs]^+$ reagent towards HS^- ion was studied by measuring the absorbance of solutions containing fixed concentration of HS^- concentration (0.72 µg mL^{-1}), in the presence of a series of varied concentrations of different anions such as SCN^-, I^-, Br^-, Cl^-, NO_3^-, NO_2^-, HSO_3^-, SO_4^{2-}, HPO_4^{2-}, CN^-, oxalate, citrate and tartrate. The tolerance limit was taken as the amount

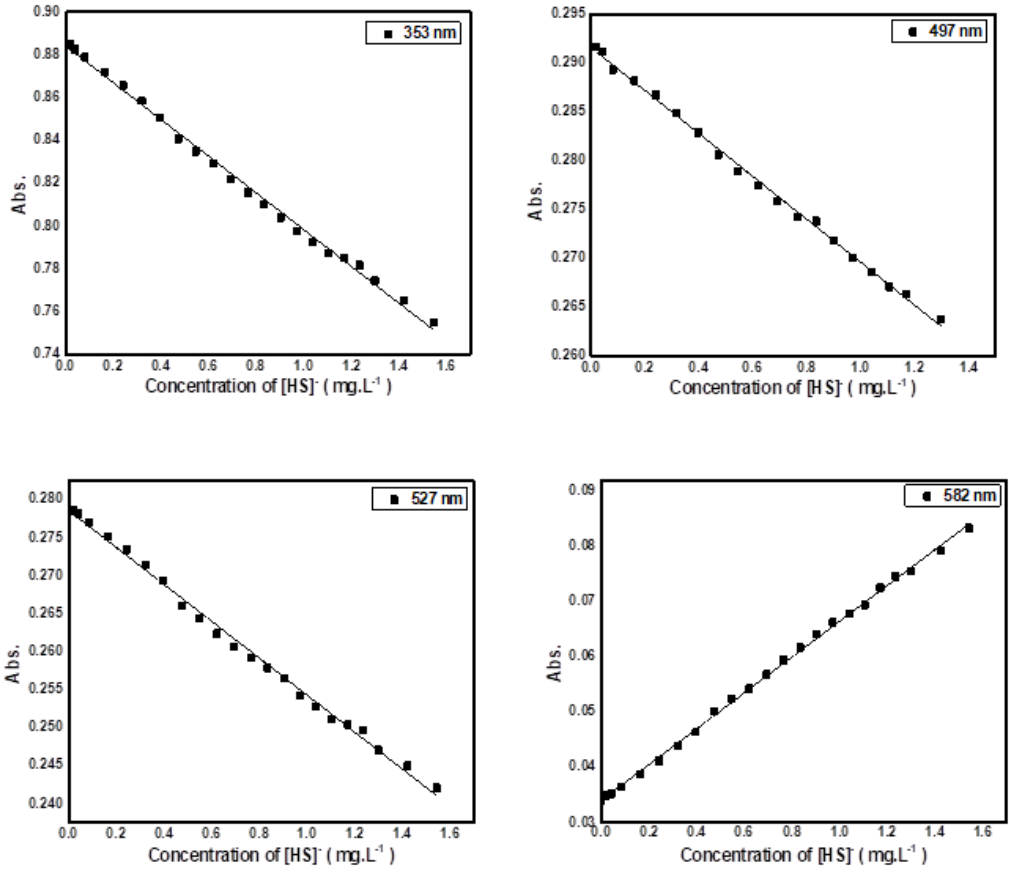

Figure 4. Calibration curves at different wavelengths of($3.5x10^{-5}$molL^{-1})[ACCbs]$^{+}$ with HS^- ion (0.02-1.55µg mL^{-1}).

that causes ±5% error in the analytical signal at 353, 497, 527 and 582 nm for the formed HS/ACCbs complex. All anions used in selectivity measurements were in the form of sodium or potassium salts. As shown in (Table 1) that summarizes the tolerance limits of the tested anions, it was found that the method displays good selectivity towards HS^- in the presence of many common anions. The method, however, suffers from slight interference by iodide ion especially at 353 nm (γ-band). High interference from CN^- and SO_3^{2-} was also observed. This can be attributed to the high affinity of both cyanide and sulfite ions for coordination with cobalt atom in the axial position of the complex. Sulfite interference was eliminated by the addition of 1 mL of 0.1 % formaldehyde to 3 mL of test solution prior to each measurement.

Batch determination of hydrosulfide ion and calibration curves

Under optimized conditions, validation of the proposed spectrophotometric method for HS^- determination was done by measuring linearity range, lower limit of detection (LOD), accuracy (recovery), precision or repeatability (within-batch variability CV_w), between-batch variability (CV_b), standard deviation and sensitivity (slope). Six batches (six determinations each) were examined at each wavelength according to the quality assurance standards[35] and the results are given in Table 2.

Table 1. Tolerance limits (change in absorbance ≤ 5 %) of some diverse ions on the reaction of aquacyanocobester with hydrogen sulfide ion (0.72 µg mL^{-1}).

Diverse ion	Tolerance ratio [DI : $[Ag(CN)_2]^-$] , w/w at λ			
	353	497	527	582
NO_2^-	180	120	280	380
NO_3^-	120	160	160	200
Cl^-	70	80	80	105
Br^-	60	90	80	80
I^-	20	22	22	22
SO_3^{2-}	0.65	0.9	0.8	1
SCN^-	75	85	85	120
SO_4^{2-}	100	110	110	110
Oxalate	160	220	180	240
Citrate	250	290	290	350
Tartarate	190	210	210	230
HPO_4^{2-}	150	160	160	160
CN^-	0.8	0.2	1.2	0.05

For HS^- determination, the absorbance change was linearly proportional to the HS^- concentration at 353, 497, 528 and 582 nm. Beer's law is obeyed over the concentration ranges of 0.04-1.543, 0.04-1.3, 0.04 -1.543 and 0.02-1.543µg mL^{-1} with a detection limit of 0.035, 0.027, 0.037 and 0.019 µg mL^{-1} at 353,497, 527 and 582 nm, respectively (Figure 4).

Table 2. Performance characteristics of the proposed colorimetric method for measuring the concentration of HS^- ion.

Parameter	**λ_{max}= 353 nm**	**λ_{max}= 497 nm**	**λ_{max}= 527 nm**	**λ_{max}= 582 nm**
Linear range (µg mL^{-1})	0.04-1.543	0.04-1.3	0.04-1.543	0.02-1.543
Detection limit (µg mL^{-1})	0.035	0.027	0.037	0.019
Sensitivity (mL μg^{-1})	0.086	0.022	0.024	0.032
Molar absorptivity ($mol^{-1}cm^{-1}L$)	9.43 x 10^4	2.41 x 10^4	2.66 x 10^4	3.55 x 10^4
Corre1ation coefficient (r^2)	0.996	0.997	0.996	0.999
Optimum pH	9	9	9	9
Standard deviation (σ %)	0.4	0.9	1.1	1.2
Between-batch variability (CVb %)	0.3	0.5	0.8	0.8
Within-batch repeatability (CVw %)	0.6	1.1	0.9	1.2
Accuracy (%)	99.5	98.7	98.4	99.1

Table 3. Spectrophotometric determination of [HS^-] test solutions at different wavelengths in the same run.

Taken µg mL^{-1}	**Recovery, %* at λ_{max} nm**			
	353	**497**	**527**	**582**
0.1	99.1±0.3	98.5±0.1	97.9±0.7	98.6±0.5
0.4	98.9±0.1	97.8±0.5	97.5±0.4	98.3±0.6
0.8	98.7±0.7	98.9±0.6	99.8±0.1	99.4±0.4
1.0	99.4±0.2	98.9±0.2	99.4±0.2	99.6±0.1

*Average of six measurements.

According to the IUPAC recommendations,[36] the lower detection limit was calculated as: LOD = $3\sigma/S$ where σ is the standard deviation of the blank measurements (n = 6), S is the slope of the calibration curve. As shown in Table 3, it presents results obtained for assessment of internal quality control HS^- test solutions (0.1-1.0 µg mL^{-1}) by absorbance measurements at four different wavelengths in the same run.

A relative standard deviation of 0.3% and a mean average recovery of 98.7% were obtained. These data obtained support the application of this proposed method for quality control assessment of HS^- in various matrices.

Table 4. Sulfide assessment in real wastewater samples.

Wastewater sample	**Sulfide content, µg mL^{-1}**		**Error (%)**
	Proposed method	**Standard method**	
Sample 1	1.1±0.08	1.05±0.05	+4.51
Sample 2	0.81±0.04	0.84±0.03	-3.57
Sample 3	0.3±0.02	0.29±0.01	+3.33
Sugarcane refinery effluent	9.3±0.6	9.81±0.3	-5.14
Power plant	191.3±2.1	195.2±2.1	-2.03
Petrochemical industry	878.4±4.5	869.6±6.3	+1.01

Analytical applications

The proposed method was tested for the determination of sulfide in some domestic sewage water samples and an effluent formed from sugarcane factory. The results obtained for the analysis by the proposed spectrophotometric and the standard method,[37] are shown in Table 4.

The calculated Student means (*t*-test) from each method at 95% confidence level do not exceed the tabulated values. An *F*-test, show no significant difference at 95 % confidence level between the means and variances of the two sets of results.

Conclusion

Novel sensitive and selective spectrophotometric method is presented for sulfide determination in domestic sewage water samples. The method is based on the substitution of axial ligands of $[ACCbs]^+$ reagent by HS^- ion for determination of HS^- ion with insignificant interference with most common ions. The reaction of HS^- with $[ACCbs]^+$ is reversible reaction with stoichiometric ratio (2:1) at pH 9. Changes of the absorbances at 353, 497, 528 and 582 nm are linearly related to HS^- concentrations over the range of 0.04-1.543, 0.04-1.3, 0.04 -1.543 and 0.02-1.543 µg mL^{-1} with a detection limit of 0.035, 0.027, 0.037 and 0.019 µg mL^{-1} for the previously shown wavelengths, respectively.

This recommended technique is distinguished by obtaining satisfactory results with simple and available reagents and it is simple, cheap, selective and highly sensitive technique for determination of traces of HS^- ion in aqueous solutions.

Advantages offered by the proposed method, compared with those previously suggested (Table 5) are the lower detection limit,[23-25,27,28] the wider working range of measurements,[20-24,27,28] the faster reaction time[20-25,27,38]and less color reagent used.[20-38]

Table 5 Comparison of the recommended colorimetric method for determination of $[HS]^-$ ion with other spectrophotometric methods

Reagents	λ_{max}, nm	Linear range, µg mL^{-1}	Detection limit (µg mL^{-1})	Major interferents	Working pH	Reac-tion time	Ref.
Peroxidase/pyrogallol and H_2O_2	420	0.02 – 0.23	0.013	CN-, I-, Fe3+, Cd2+, Co2+	6.5	4 min.	[20]
Fe^{2+} /HS^-/ catechol/ p,toluidine	510	0.035 – 1.4	Not mentioned		0.1 M HCl		[21]
Fe3+/ HS-/1,10-phen-anthroline complex	510	0.035 – 1.4		NO2-, NO3-, SO2,Fe3+, V5+		Few minutes	
Mn^{3+}/HS^-/diphenylamine	570	0.14–1.40			5 M H2SO4		
Mn^{3+}/HS^-/ barium diphenylamine sulfonate	540	0.14–1.40					
2,6-dichlorophenolindo-phenol (DCPI)	520	0.01- 1.0	0.01	10% EtOH, used in halitosis treat-ments (Halita and Perio-Aid solutions)	12	2 min	[22]
N,N-dimethyl-p-phenyl-enediamine/Fe3+	745	0.4 - 2.0	0.4	Not mentioned	Not mentioned	3 min	[23]
	745	0.17 - 1.0	0.04	Not mentioned	0.1 mol L-1HCl	95 s	[24]
Production of phenothiazine dyes	520 664 677 590	0.25–3.0 0.05–1.5 0.04–0.75 0.05–1.0	0.033 0.024 0.018 0.051	I-, F-	0.1 mol L-1 H2SO4		[25]
Sodium nitroprusside	558	5000 - 15000	Not mentioned	Not mentioned	Not mentioned	30 s	[26]
Sodium1,2-naphthaquinone-4-sulfonate (NQS)	320	0.5 - 20	0.16	CN-, SO32-, S2O32-, HCO3-, IO3-, PO43-, C2O42-, CH3COO-	0.1 M HCl	60 min	[27]
Phenylselenonitrobenzo-xadiazole derivative	551	0.33 – 3.30	0.069	-	4.8	-	[28]
Magenta	540	0.025 – 2.50	0.015	IO3-,SO32-, Hg2+, Hg+, Pb2+, Cu2+, Ag+	7	2.5 min	[38]
[ACCbs]+		0.02 – 1.543	0.019	CN-, SO32-	9	1 min	This work

References

[1]Lawrence, N. S., Davis, J. and Compton, R. G., Analytical strategies for the detection of sulfide: a review,*Talanta*, **2000**, *52(5)*, 771-784. https://doi.org/10.1016/S0039-9140(00)00421-5

[2]Oprime, M. E., Garcia, J. r. O. and Cardoso, A. A., Oxidation of H2S in acid solution by Thiobacillus ferrooxidans and Thiobacillus thiooxidans. *Process Biochem.*, **2001**, *37(2)*, 111-114. https://doi.org/10.1016/S0032-9592(01)00179-0

[3]Clesceri, L., Greenberg, A. and Eaton, A., *Standard methods for the examination of water and wastewater*, American Public Health Association (APHA), American Water Works Association, Water Environment Federation, Washington, DC. **1998.**

[4]Marczin, N. and Yacoub, M., *Disease Markers in Exhaled Breath: Basic Mechanisms and Clinical Applications* (NATO Science Series 346). Amsterdam: IOS Press, **2002.**

[5]Guidotti, T. L., Hydrogen sulfide: advances in understanding human toxicity. *Int. J. Toxicol.*, **2010**, *29(6)*, 569-581. Online ISSN: 1092-874X

[6]Pawlak, Z. and Pawlak, A. S., Modification of iodometric determination of total and reactive sulfide in environmental samples. *Talanta* **1999**, *48(2)*, 347-353. https://doi.org/10.1016/S0039-9140(98)00253-7

[7]Balasubramanian, S. and Pugalenthi, V., A comparative study of the determination of sulphide in tannery waste water by ion selective electrode (ISE) and iodimetry. *Water Res.*, **2000**, *34(17)*, 4201-4206. https://doi.org/10.1016/S0043-1354(00)00190-1

[8]Tsai, D. M., Kumar, A. S. and Zen, J. M., A highly stable and sensitive chemically modified screen-printed electrode for sulfide analysis. *Anal. Chim. Acta*, **2006**, *556(1)*, 145-150. https://doi.org/10.1016/j.aca.2005.05.038

[9]Lawrence, N. S., Jiang, L., Jones, T. G. and Compton, R. G.,Voltammetric Characterization of a N,N'-Diphenyl-p-phenylenediamine-Loaded Screen-Printed Electrode: A Disposable Sensor for Hydrogen Sulfide, *Anal. Chem.*, **2003**, *75(9)*, 2054-2059. **DOI:** 10.1021/ac020728t

[10]Cao, X., Xu, H., Ding, S., Ye, Y., Ge, X. and Yu, L.,Electrochemical determination of sulfide in fruits using alizarin–reduced graphene oxide nanosheets modified electrode. *Food Chem.*, **2016**, *194*, 1224-1229. https://doi.org/10.1016/j.foodchem.2015.08.134

[11]Hissner, F., Mattusch, J. and Heinig, K., Quantitative determination of sulfur-containing anions in complex matrices with capillary electrophoresis and conductivity detection. *J. Chromatogr., A*, **1999**, *848(1-2)*, 503-513. https://doi.org/10.1016/S0021-9673(99)00458-6

[12]Miura, Y., Ion chromatography for rapid and sensitive determination of inorganic sulfur anions in their mixtures. *JPN Analyst* **2005**, *54(8)*, 651-664. https://doi.org/10.2116/bunsekikagaku.54.651

[13]Jeyakumar, S., Rastogi, R., Chaudhuri, N. and Ramakumar, K., Determination of sulphur species in the presence of common anions with indirect measurement of sulphide by ion chromatography (IC). *Anal. Lett.*, **2002**, *35(2)*, 383-395. https://doi.org/10.1081/AL-120002537

[14]Colon, M., Todoli, J., Hidalgo, M. and Iglesias, M., Development of novel and sensitive methods for the determination of sulfide in aqueous samples by hydrogen sulfide generation-inductively coupled plasma-atomic emission spectroscopy. *Anal. Chim. Acta*, **2008**, *609(2)*, 160-168. https://doi.org/10.1016/j.aca.2008.01.001

[15]Čmelík, J., Machát, J., Otruba, V. and Kanický, V.,Contribution to vapor generation-inductively coupled plasma spectrometric techniques for determination of sulfide in water samples. *Talanta* **2010**, *80(5)*, 1777-1781. https://doi.org/10.1016/j.talanta.2009.10.022

[16]Peng, H., Cheng, Y., Dai, C., King, A. L., Predmore, B. L., Lefer, D. J. and Wang, B., A fluorescent probe for fast and quantitative detection of hydrogen sulfide in blood. *Angew. Chem. Int. Ed.*, **2011**, 50(41), 9672-9675. https://doi.org/10.1002/anie.201104236

[17]da Silveira Petruci, J. F. and Cardoso, A. A., A new palladium chelate compound for determination of sulfide. *Microchem. J.*, **2013**, *106*, 368-372. https://doi.org/10.1016/j.microc.2012.09.009

[18]Segura, D. F., da Silveira Petruci, J. F., Cardoso, A. A., Frem, R. C. G., de Godoy Netto, A. V. and Champness, N. R.,A new luminescent silver-based probe for on/off sulfide determination. *Inorg. Chem. Commun.*, **2016**, *63*, 93-95. https://doi.org/10.1016/j.inoche.2015.11.019

[19]Gerbersmann, C., Lobinski, R. and Adams, F. C., Determination of volatile sulfur compounds in water samples, beer and coffee with purge and trap gas chromatography—microwave-induced plasma atomic emission spectrometry. *Anal. Chim. Acta* **1995**, *316(1)*, 93-104. https://doi.org/10.1016/0003-2670(95)00344-Y

[20]Ghadiri, M., Kariminia, H. R., Azad, R. R.,Spectrophotometric determination of sulfide based on peroxidase inhibition by detection of purpurogallin formation. *Ecotoxicol. Environ. Saf.*, **2013**, *91*, 117-121. https://doi.org/10.1016/j.ecoenv.2013.01.015

[21]Shyla, B., Nagendrappa, G., New spectrophotometric methods for the determinations of hydrogen sulfide present in the samples of lake water, industrial effluents, tender coconut, sugarcane juice and egg. *Spectrochim. Acta, Part A*, **2012**, *96*, 776-783. https://doi.org/10.1016/j.saa.2012.07.011

[22]Rodríguez-Fernández, J., Pereiro, R. and Sanz-Medel, A., Optical fibre sensor for hydrogen sulphide monitoring in mouth air. *Anal. Chim. Acta*, **2002**, *471(1)*, 13-23. https://doi.org/10.1016/S0003-2670(02)00778-X

[23]Kong, M. C. and Salin, E. D., Spectrophotometric determination of aqueous sulfide on a pneumatically enhanced centrifugal microfluidic platform. *Anal. Chem.*, **2012**, *84(22)*, 10038-10043. **DOI:** 10.1021/ac302507t

[24]Silva, M. S. P., Galhardo, C. X. and Masini, J. C., Application of sequential injection-monosegmented flow analysis (SI-MSFA) to spectrophotometric determination of sulfide in simulated waters samples. *Talanta*, **2003**, *60(1)*, 45-52. https://doi.org/10.1016/S0039-9140(03)00044-4

[25]Santos, J. C. C., Santos, E. B. G. N. and Korn, M., A comparison of flow injection methods for sulfide determination based on phenothiazine dyes produced from diverse aromatic amines. *Microchem. J.*, **2008**, *90(1)*, 1-7. https://doi.org/10.1016/j.microc.2008.02.007

[26]Kass, M. and Ivaska, A., Spectrophotometric determination of sulphur dioxide and hydrogen sulphide in gas phase by sequential injection analysis technique. *Anal. Chim. Acta* **2001**, 449(1-2), 189-197. https://doi.org/10.1016/S0003-2670(01)01364-2

[27]Shariati-Rad, M., Irandoust, M. and Jalilvand, F., Spectrophotometric determination of hydrogen sulfide in environmental samples using sodium 1, 2-naphthoquinone-4-sulfonate and response surface methodology. *Int. J. Environ. Sci. Technol.*, **2016**, *13(5)*, 1347-1356. https://doi.org/10.1007/s13762-016-0959-6

[28]Bae, J., Choi, M. G., Choi, J. and Chang, S. K., Colorimetric signaling of hydrogen sulfide by reduction of a phenylselenonitrobenzoxadiazole derivative. *Dyes Pigments*, **2013**, 99(3), 748-752. https://doi.org/10.1016/j.dyepig.2013.06.018

[29]Markwell, A. J., Pratt, J. M., Shaikjee, M. S. and Toerien, J. G., The chemistry of vitamin B 12. Part 28. Crystal structure of dicyanocobyrinic acid heptamethyl ester and its interaction with alcohols: the effects of hydrogen bonding to co-ordinated cyanide. *J. Chem. Soc., Dalton Trans.*, **1987**(6), 1349-1357. DOI: 10.1039/DT9870001349

[30]Murakami, Y., Hisaeda, Y. and Ohno, T., Hydrophobic vitamin B12. III. Incorporation of hydrophobic vitamin B12 derivatives into single-compartment vesicles and their alkylation in various molecular aggregates, *Bull. Chem. Soc. Jpn.*, **1984**, *57(8)*, 2091-2097. https://doi.org/10.1246/bcsj.57.2091

[31]Lurie, J., *Handbook of Analytical Chemistry. The stability constants for metal complexes with inorganic ligands*. Mir Publishers: Moscow, **1975.**

[32]Hassan, S. S., Hamza, M. S. and Kelany, A. E., A novel spectrophotometric method for batch and flow injection determination of cyanide in electroplating wastewater. *Talanta* **2007**, *71(3)*, 1088-1095. https://doi.org/10.1016/j.talanta.2006.06.010

[33]Pratt, J. M., *Inorganic chemistry of vitamin B12*. London, UK, Academic Press Inc.(London) Ltd., **1972.**

[34]Salnikov, D. S., Kucherenko, P. N., Dereven'kov, I. A., Makarov, S. V., van Eldik, R., Kinetics and mechanism of the reaction of hydrogen sulfide with cobalamin in aqueous solution. *Eur. J. Inorg. Chem.*, **2014**, 2014(5), 852-862. https://doi.org/10.1002/ejic.201301340

[35]Taylor, J. K., *Quality assurance of chemical measurements*. CRC Press, **1987.**

[36]Irving, H., Freiser, H. and West, T., *IUPAC compendium of analytical nomenclature, definitive rules*. Pergamon Press, Oxford, **1981.**

[37]Clesceri, L., Greenberg, A., ANDREW, D., *Standard Methods for the Examination of Water and Wastewater*, Washington, 19th Edition Publication Office American Public Health Association (APHA), **1995.**

[38]Safavi, A. and Ramezani, Z., Kinetic spectrophotometric determination of traces of sulfide. *Talanta* **1997**, *44(7)*, 1225-1230. https://doi.org/10.1016/S0039-9140(96)02163-7

Received: 15.06.2018.
Accepted: 15.09.2018.

A FACILE METHOD FOR TESTING ANTIOXIDANT CAPACITY AND TOTAL PHENOLIC CONTENT OF *NOTOBASIS SYRIACA* AND *SCOLYMUS MACULATUS* EXTRACTS AND THEIR ANTIFUNGAL ACTIVITY

Abdullatif Azab[a,b]*

Keywords: *Notobasis syriaca; Scolymus maculatus; Rhizopus stolonifera;* total phenolic content; antioxidant capacity.

In this study, three extracts of the aerial parts of *Notobasis syriaca* and *Scolymus maculatus* were prepared. Each extract was tested for antifungal activity against *Rhizopus stolonifer* (black mold), and its total phenolic content (TPC) and antioxidant activity were measured. As for these measurements, we report here a facile method that we developed. Our results show moderate antifungal activity for both plants extracts, notably high TPC and antioxidant capacities. They are also in very good agreement with the partial published data, and our new method is consistent and validated by very well known, yet complicated or expensive methods.

* Corresponding Authors
Fax: +972-(0)4-6356168
Tel.: +972-(0)4-6357011
E-Mail: eastern.plants@gmail.com
[a] Triangle Research & Development Center, Box 2167, Kfar-Qari, Israel 30075.
[b] Eastern Plants Company, Box 868, Arara, Israel 30026.

Introduction

Notobasis syriaca (Syrian thistle, NS) and *Scolymus maculatus* (Spotted golden thistle, SM) are two of the spiny, most widespread plants of the Middle eastern region, Mediterranean basin and Western Asia, yet, the habitat of SM is wider and includes most of Asia. Both plants belong to the Asteraceae family, but to different *genera*: NS to *Notobasis* (2 different subspecies)[1] and SM to *Scolymus* (7 different subspecies).[2] NS was discovered in archeological excavations, and there are evidences that humans used this plant, mainly as food, as early as 23000 years ago.[3] Interestingly enough, and despite being very sweet tasty plant (young stems), there are no published studies of archeological findings that indicate early use of SM by humans, similar to NS.

Present time traditional societies, extensively use both plants. NS is used as food in Cyprus and Italy,[4,5,6] in Jordan it is used to treat diabetes (method not described), as food and for cheese production from milk (dry immature flowrs),[7] and in Turkey, ground seeds are eaten to treat liver diseases.[8] SM is widely used as a sweet snack in the Palestinian traditional society, in Spain,[9] in Italy,[6,7] and in Arab folk medicine, stem decoction is used to treat intestine and kidney inflammation.[10]

Despite the fact that in recent years there is renewed recognition of natural products as an impotrant source for drug discovery,[11] these two plants were very limitedly studied by modern research so far. One of the earliest published studies of the medicinal activities of NS, tested the antifungal activity (*Alternaria solani*, *Hetminthosporium sativum* and *Rhizoctonia solani*) of shoot aqueous extract and found it moderate.[12] Antimicrobial activity of ethanolic extract of aerial parts of NS was tested against six types of bacteria, including *P. acnes*.[13] The results show relatively low activity.

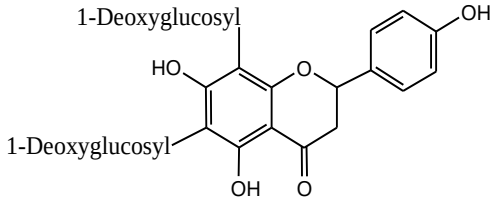

Isoschaftoside

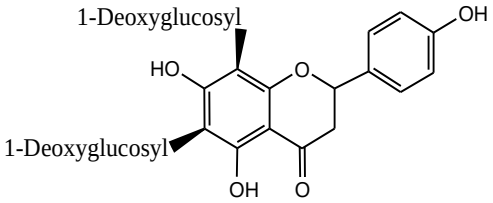

Schaftoside

Figure 1. Structures of steric isomers schaftoside and isoschaftoside found in *N. syriaca*

The complete chemical composition of NS was never published, even though some partial results were reported. Mericli and Dellamonica studied the flavonoid content of the plant and they reported the presence of nine different compounds in the aerial parts, including schaftoside and isoschaftoside (Figure 1), but none of these compounds was new.[14] An interesting study was published in 2007 and has high relevance to our research since it tested the TPC and antioxidant capacity of aqueous and methanolic extracts of NS.[15] The results are surprisingly low, compared with other reports and our current study (see results and discussion sections). El-Hela and his colleageas tested TPC and antioxidant capacity of extactly same extracts indicated in reference 15. Their findings are notably higher.[16] They also

tested them larvicidal activity of these extracts against *Aedes aegyptii*, and they were found moderately active.

Contrary to published studies about NS that did not report new compounds, a research that investigated the chemical composition of *Phomopsis* sp., an endophytic fungus of NS, reported several new compounds, including phomosine K (Figure 2) that had strong antibacterial activity.[17]

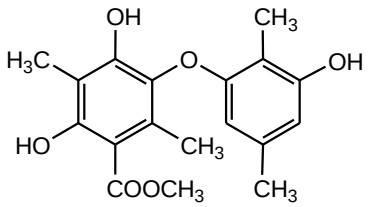

Figure 2. Phomosine K, a novel compound found on endophytic fungus of *N. syriaca*

Earlier this year, we published some results in collboration with other research group, where we studied the anti-inflammatory activity of the aqueous extract of the aerial parts of NS.[18] Based on these successful findings, we performed the current study and we are continuing the investigation of this plant.

Research findings related to SM are even much less than these of NS. In one of the only two published studies, TPC and antioxidant capacity of methanolic and aqueous extracts were tested.[15] The results are lower than ours and higher than the only second published research. This was presented as a poster by Rayan *et al*. and never published as a research article.[19] This group did not report new compounds in the three extracts that they prepared from aerial parts of SM: methanolic, ethyl acetate and hexane. Expectedly, methanolic extract has the highest antioxidant capacity. An enzyme isolated from SM, was reported by M. Benchiheub and her colleagues as successful milk-clotting agent.[20]

Black mold (*Rhizopus stolonifer*) is one of the most common fungi, and it has been a research focus since its vast damages to human health, especially to food, but also because of the potential of isolating unique biologically active compounds from it.[21] It was also reported to assist transformations of organic compounds and peptides.[22] Dozens of treatments were suggested to combat the damages of *R. stolonifer*. While some methods consisted of synthetic compounds,[23] the latest publications report the use on nanochemicals.[24] But synthetic compounds have adverse side effects, so most proposed antifungal treatments of *R. stolonifer* are plant products. Among these, essential oils,[25] extracts[26] and single natural products.[27,28,29]

Total phenolic content (TPC) and antioxidant capacity of plant materials, are among their most important properties. Several methods were developed to determine TPC, where the most commonly used is the Folin-Ciocalteu assay.[30] But variations of other methods are also used, such as in our previous work (Kumar and Jain method).[31] These methods involve many samples (or many dilutions of one sample), spectroscopic measurements and costly reagents. Testing the strongly related property of antioxidant capacity of plant materials, involves many more experimental methods, where some use costly materials and spectroscopic measurements,[31] and some use simpler methods such as potentiometic/redox titrations.[32,33,34] Some of these and other procedures are very simple, and we used their potential to develop a new, facile method to measure TPC and antioxidant capacity of plant extracts by single titration.

Experimental

Chemicals

Gallic acid and ascorbic acid were purchased from Merck KgaA (Germany). All other chemicals were purchased locally in at least analytical grade.

Plant material and extractions

Both the studied plants (*Notobasis syriaca*, NS, and *Scolymus maculatus*, SM, aerial parts) were harvested from the wild near our laboratory in Kfar-Qari (northern Israel). The green materials were washed with distilled water and air dried for 4 weeks. The dry matter of each plant was ground into a fine powder and stored at -12 °C in sealed containers.

The plant material (500 g) were stirred in 1000 mL of solvent (water, ethanol, ethyl acetate) for 24 h at 50 °C. Suspensions were allowed to cool to room temperature and filtered (Munktell quant. Grade 393) to obtain clear solutions. These were evaporated to dryness with rotary evaporator: aqueous extracts at 60 °C, ethanol and ethyl acetate extracts at 50 °C. All six extracts were solids, and they were stored in screw-capped vials at -12 °C.

Tests for Alkaloids

Presence of alkaloids in extracts was tested according to I. P. Udeozo et al., using the Wayner's reagent, with no modifications.[35] In a 100 mL volumetric flask, 2 g of iodine (I_2) and 6 g of potassium iodide (KI) were dissolved in distilled water and made up a 100 mL solution.

A sample of 0.1 g of each plant extract was placed in 20 mL test tube and dissolved in 10 mL ethanol. To the tested solution, 5 mL of Wayner's reagent were added, the tube was capped and the suspension was vigorously shaked for 30 seconds.

Antifungal activity tests

Antifungal assay was performed according to the method we reported in our previous publication, with no modifications.[31] *Rhizopus stolonifer* was grown on whole wheat bread and extracted with water. The center of each Petri dish was inoculated with 5 mm diameter disc of fungal mycelium, taken from pure culture (7 days old). Then, all inoculated dishes were incubated at 25 °C for 6 days and the radial mycelial growth was measured. The antifungal activity of each extract was calculated in terms of inhibition percentage of mycelia growth by using the following equation (1).

$$\% \text{ Inhibition} = [(dc - dt)/dc] \times 100 \quad (1)$$

where *dc* is the average increase in mycelia growth in control and *dt* is the average increase in mycelia growth in treated samples with extracts.

In all experiments, the control was the extraction solvent and we performed the antifungal tests using two concentrations for each extract, 10 % and 20 % (w/w).

Preparation of oxidative solution

Solution of sulfuric acid was prepared by diluting 0.89 mL of 96 % solution of concentrated sulfuric acid (approx. 18.11 M) with distilled water to final volume of 1000 mL. The resulting sultion was standardized by pH titration with 0.01 M of sodium hydroxide (NaOH) solution. The acid concentration was 0.016 M.

The 0.004 M solution of potassium permanganate ($KMnO_4$) was prepared by dissolving 0.633 g of the salt in 800 mL of distilled water at 60 °C. The solution was allowed to cool to room temperature, filtered and completed to 1000 mL.

The final oxidative solution was prepared by combining the acid (0.016 M) and permanganate solution (0.004 M), which was stored in 4 °C in a sealed flask.

Calibration curve of ascorbic/gallic acid

A stock solution of 600 mg of ascorbic/gallic acid in 6 mL of distilled water was prepared (100 mg mL^{-1}). By dilution with distilled water, the following concentrations of tested solutions were prepared: 10, 20, 30, 40, 50, 60, 70, 80, 90, 100 mg 10 mL^{-1}.

In a 250 mL Erlenmeyer flask that contained a magnetic stir bar, one of the ten test solutions was titrated with the oxidative solution, with pH monitoring by JK-PHM-005 pH-meter. Titration speed was 2 mL min^{-1} with continuous gentle stirring. End point was determined when ΔpH >0.1 after half way of the titration (see discussion).

Titration of plant extracts

In a 100 mL Erlenmeyer flask that contained a magnetic stir bar, 100 mg of dry plant extract were suspended with 10 mL of distilled water and stirred for 5 minutes. The solution/suspension was titrated with the oxidative solution, with pH monitoring. Totration speed was 2 mL min^{-1}, with continuous gentle stirring.

Validation of our method

TPC was also determined by the method we used in our previous work,[31] with no modifications. The sample mixture that contains 3 mg of extract (or standard gallic acid solutions) dissolved in 1 mL of solvent, was obtained by dilution of 0.3 g of extract in 10 mL stock solution 10 folds. Then it was added to 10 mL volumetric flask containing 8 mL of dd H_2O. After that, 1mL of Folin-Ciocalteu's reagent was added to the mixture. After 3 min, 1 mL of 35 % Na_2CO_3 solution was added with mixing to reach the reaction system to 10 mL. The reaction mixture was mixed thoroughly and allowed to stand for 90 min at 25 °C in the dark. Absorbance of all the sample solutions against a blank was measured at 725 nm. Calibration curve was constructed with different concentrations of gallic acid (2–12 μg mL^{-1}) as the standard and double-distilled water was used as reagent blank. The results were expressed as mg gallic acid equivalents (GAE) g^{-1} of dried extract.

Antioxidant capacity was determined according to the method we described in our previous publication, with no changes.[31] 0.1 mL of aliquot of test solution (100 mg extract) was added to 1 mL of reagent solution (0.6 M sulfuric acid, 28 mM sodium phosphate, and 4 mM ammonium molybdate). The blank was 0.1 mL of ethanol. The tubes were capped and incubated in a boiling water bath at 95 °C for 90 min, then allowed to cool to room temperature. Absorbance of the aqueous solution of each was measured at 695 nm. The antioxidant capacity was expressed as an equivalent of ascorbic acid (mg of ascorbic acid g^{-1} of dried extract).

Results

Yields of extractions

The yields of the extractions of both NS and SM with water, ethanol and ethyl acetate are shown in Table 1.

Table 1. Yields of extractions of *N. syriaca and S. maculatus* with three different solvents[a]

Plant	Water		Ethanol		Ethyl acetate	
	mass	%[a]	mass	%	mass	%
NS	42.1	8.42	42.8	8.56	23.7	4.74
SM	46.9	9.38	48.0	9.60	21.5	4.30

[a]For each extraction, 500 g of dry plant powder were extracted (aerial parts).

Alkaloid presence

All six extracts showed negative results in alkaloid presence test with Wayner's reagent.

Statistical analysis

Except for extractions (Table 1) and alkaloid presence tests, that each was done in a single experiment, all data presented below, are average values of three experiments that we peformed for each test.

Antifungal activity

Antifungal activity was measured as the of inhibition percentage of mycelia growth of *Rhizopus stolonifer*. Two concentrations of extracts were used, 10 % and 20 % (w/w) in the extraction solvent and the results are shown in Table 2 and Figure 3.

Table 2 Antifunfal activity of *N. syriaca* and *S. maculatus* extracts against *R. stolonifer*

Plant	Inhibition of extracts (%)[a]					
	Aqueous		Ethanolic		Ethyl acetate	
	10 %	20 %	10 %	20 %	10 %	20 %
NS	17.2	19.4	24.3	26.8	25.9	27.2
SM	12.3	14.4	19.2	21.8	18.8	22.3

[a]Extraction solvent in each experiment was used as control and resulted in 0 % inhibition.

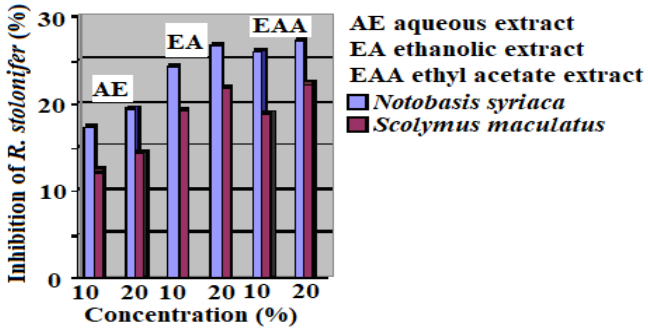

Figure 3. Inhibition (%) of *R. stolonifer* by extracts of *N. syriaca* and *S. maculatus*

Calibration curves

Concentrations of titrated ascorbic/gallic and volumes of oxidative solution needed are shown in Table 3, and calibration curves are shown in figure 4.

Total phenolic content and antioxidant capacity

Each (100 mg) extract were titrated with the oxidative solution. End point volume was multiplied by 10 in order to reach the value for 1 g of dry extract, and the final values were calculated as shown in Table 4 and Figure 5.

Validation of our method

Total phenolic content and antioxidant capacity were also measured by the known methods, described in the experimental section. The results of these measurements, as well as the results measured by our method are shown in Table 5.

Discussion

All the six qualitative tests for the presence of alkaloids in the extracts showed negative results that is no alkaloids present in *N. syriaca* or *S. maculatus*. In fact, this was expected since a closely related (and sometimes confused with) plant, *Silybum marianum* (Milk thistle), contains no alkaloids.[36,37] The cultivated Artichoke (*Cynara cardunculus* var. *scolymus*) is also closely relted to NS and SM, and it does not contain alkaloids.[38]

Antifungal activity of both plants, NS and SM, was found moderate and even weak, not only in comparison with plants with strong antifungal activity,[39] but also with other plants from other genera, such as *Carthamus tenuis* and *Cephalaria joppensis*.[31] This can be partially understood on the basis of the very limited presence of volatile, aromatic compounds, that we discovered while we tried to prepare essential oils of NS and SM, and we obtained negligible yields.

Total phenolic content and antioxidant capacity are of the most important medicinal properties of plants products, and they are strongly related.[40] Phenols and polyphenols are among the most powerful antioxidants in the plant kingdom.[41]

Based on this, we managed to develop a unified test for both properties. Our considerations included (1) use of strong oxidative solution, yet, not too strong that can cause oxidation way beyond common reagents used for this matter, (2) a facile technique that involves simple instruments and very simple and few preparations of samples and (3) Use of cheap, commercially available reagents.

We selected acidic solution of potassium permanganate. This is a strong oxidant (E^0= +1.51 V) but in low concentration, this strength is even lower, so it will not exceed the power of common oxidants that are used in other methods (see experimental section: validation of our method). The molar ratio between per manganate and acid was designed according to the stoichiometry of the reaction:

$$MnO_4^-{}_{(aq)} + 8\ H_3O^+{}_{(aq)} + 5\ e^- \rightarrow Mn^{2+}{}_{(aq)} + 12\ H_2O_{(L)} \quad (2)$$

So the ratio of MnO_4^- : H^+ is 1:8. Sulfuric acid was chosen due to its stability and strength.

Our theoretical assuptions of the stoichiometry of oxidation of ascorbic acid by this oxidant, were based on the previous studies,[42] and we designed the tests for MnO_4^- : ascorbic acid = 2:5. As for gallic acid, the stoichiometry is more complicated since there are several competing reactions, even though, one of them occur as major path of the oxidation.[43] This reaction is shown in Figure 6.

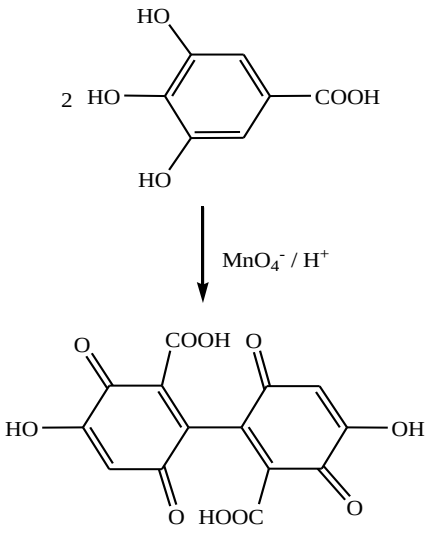

Figure 6. Major reaction of oxidation of gallic acid by acidic permanganate

Table 3. Titrated concentrations of ascorbic/gallic acid and oxidative solution volumes.

Titrated Concentration[a]		10	20	30	40	50	60	70	80	90	100
Oxidative Solution Volume[b]	AA[c]	10.2	26.6	33.1	42.8	58.4	65.2	80.6	91.4	103	109.4
	GA[d]	20.4	52.4	63.2	79.6	100	108.2	145.2	180.8	199	224.8

[a]mg 10 mL^{-1}, [b]mL, [c]Ascorbic acid, [d]Gallic acid.

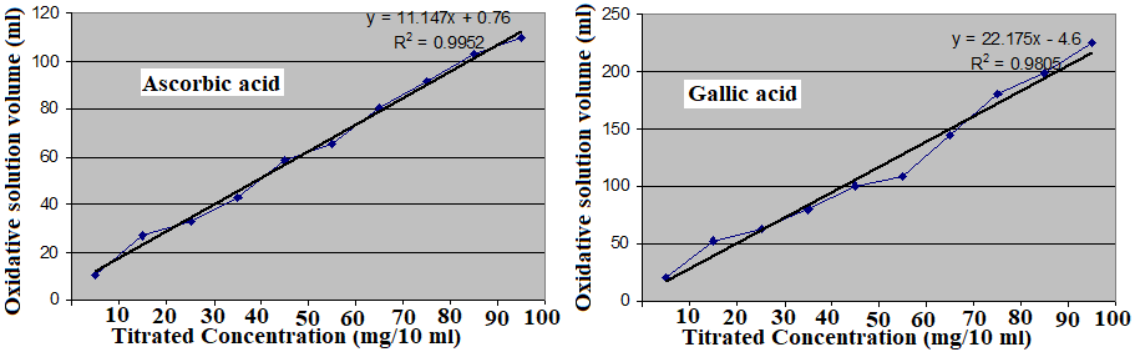

Figure 4. Calibration curves of oxidative titration of ascorbic/gallic acid with permanganate.

Table 4. Total phenolic content (TPC) and antioxidant capacity (AOC) of extracts of *N. syriaca* and *S. maculates.*

Plant	Extract	Volume of oxidizing solution	TPC[a]	AOC[b]
Notobasis syriaca	Aqueous	37.8	17.25	33.84
	Ethanolic	29.7	13.6	26.58
	Ethyl acetate	16.1	7.47	14.38
Scolymus maculatus	Aqueous	39.6	18.02	35.37
	Ethanolic	29.1	13.33	26.04
	Ethyl acetate	14.9	6.39	13.30

[a]mg of gallic acid g^{-1} of dry extract (according to 10y=22.175x-4.6); [b]mg of ascorbic acid g^{-1} of dry extract (according to 10y=11.147x+0.76)

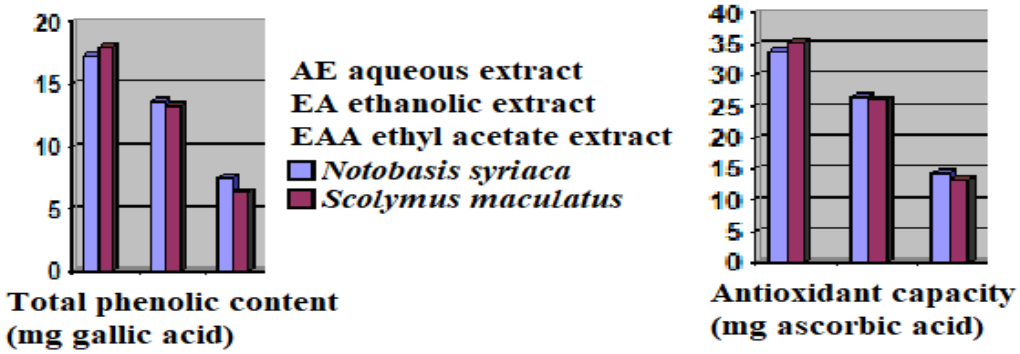

Figure 5. Total phenolic content and antioxidant capacity of *N. syriaca* and *S. maculates.*

Table 5. Total phenolic content and antioxidant capacity of *N. syriaca* and *S. maculatus*, measured by our method and known methods[a].

Plant	Extract	Total phenolic content[b]		Antioxidant capacity[c]	
		Our method	Known method	Our method	Known method
Notobasis syriaca	Aqueous	17.25	16.84	33.84	31.88
	Ethanolic	13.6	13.2	26.58	24.23
	Ethyl acetate	7.47	7.39	14.38	13.87
Scolymus maculatus	Aqueous	18.02	16.1	35.37	32.11
	Ethanolic	13.33	12.55	26.04	23.74
	Ethyl acetate	6.39	6.25	13.30	12.13

[a]See experimental section, [b]mg of gallic acid g^{-1} of dry extract, [c]mg of ascorbic acid g^{-1} of dry extract.

The formation of the bisphenyldiquinone product, involves loss of three electrons from each molecule of gallic acid. Since lower oxidations also take place but in minor amounts, we assumed that the average ratio of MnO4- : gallic acid = 1:1.2.

Titrations were monitored by pH-meter. Despite being slowly responsive, especially while titrating polyphenols,[44] this method is used for various purposes, and our work was based on a successful example.[45] To overcome the slow response, we conducted very slow titrations (2 mL min-1). Initial pH gallic acid solution was 3.64. In the beginning of the titrations, pH dropped rapidly (0.1-0.15 units drop-1), but then it was much slower (0.01 units drop^{-1}). At the end point (pH=1.39) the pH dropped by 0.2 units. As for ascorbic acid, the initial pH was 3.45 and the final, 1.21. The titration advanced in the same course as gallic acid but was slightly faster.

Our results, using this very simple method are very good. In case of antioxidant capacity, there is a high proximity between our results, the results that we obtained by other know methods (Table 5) and published results.[15,16] The results reported by Rayan et al.,[19] are lower than our results and the results reported in references 15 and 16, so we will not take them into account. All results obtained by our method, were higher that those obtained by other known methods, and the highest difference was (2.3 mg, ethanolic extract of SM) around 9.24 %.

As for TPC, differences between our method and known methods were even higher than these of antioxidant capacity, despite the fact that they are still reasonable. And again, the highest difference was SM extract, but this time, aqueous (Table 5, 11.25 %). As far as we can explain this, our understanding is that the sweet taste of SM is a result of the presence of saccharides, and these may have been oxidized and made the results obtained by our method higher, compared to other methods. We base our explanation on similar published results, where carbohydrate content affected TPC and antioxidant capacity measurements.[46,47]

Conclusions

Notobasis syriaca and *Scolymus maculatus*, are edible plants and possess high amounts of polyphenols and other antioxdants. Chemical composition of both plants is still unkown and should be investigated. Only antioxidant capacity, total phenolic content and inti-inflammatory (NS only) activities are known. Other properties must be studied. We developed a new, very simple method for measuring TPC and antioxidant capacity, that has shown good agreement with other known methods. *Notobasis syriaca* and *Scolymus maculatus*, do not contain alkaloids. The essential oil content of *Notobasis syriaca* and *Scolymus maculatus*, is negligible.

References

[1]U.S National Plant Germplasm System., *Taxon: Notobasis syriaca* (L.) Cass., https://npgsweb.ars-grin.gov/gringlobal/taxonomydetail.aspx?id=447370

[2]Vasquez, F. M., The genus *Scolymus* Tourn. EXL. (*Asteraceae*): taxonomy and distribution, *Anales Jard. Bot. Madrid*, **2000**, *58*, 83-100. DOI: https://doi.org/10.3989/ajbm.2000.v58.i1.139

[3]Snir, A., Nadel, D., Groman-Yaroslavski, I.,Melamed, Y., Sternberg, M., Bar-Yosef, O., Weiss, E., The origin of cultivation and Proto-weeds, long before Neolithic farming, *PLOS ONE*, **2015**, *10*, 12 pages. DOI: 10.1371/journal.pone.0131422

[4]Della, A., Paraskeva-Hadjichambi, D., Hadjichambis, A. C., An ethnobotanical survey of wild edible plants of Paphos and Larnaca countryside of Cyprus, *J. Ethnobiol. Ethnomed*., **2006**, *2*, 9 pages. DOI: 10.1186/1746-4269-2-34

[5]Licata, M., Tuttolomondo, T., Leto, C., Virga, G., Bonsangue, G., Cammalleri, I., Gennaro, M. C., La Bella, S., A survey of wild plant species for food use in Sicily (Italy) – results of a 3-year study in four Regional Parks, *J. Ethnobiol. Ethnomed*., **2016**, *12*, 24 pages. DOI: 10.1186/s13002-015-0074-7

[6]Biscotti, N., Bonsanto, D., Del Viscio, G., The traditional food use of wild vegetables in Apulia (Italy) in the light of Italian ethnobotanical literature, *Ital. Bot*., **2018**, *5*, 1-24. DOI: 10.3897/italianbotanist.5.22297

[7]Qasem, J. R., Prospects of wild medicinal and industrial plants of saline habitats in the Jordan Valley, *Pak. J. Bot*., **2015**, *47*, 551-570. www.researchgate.net/publication/275339308

[8]Arasan, S., Kaya, I., Some Important Plants Belonging to Asteraceae Family Used in Folkloric Medicine in Savur (Mardin/Turkey) Area and Their Application Areas *J. Food Nutr. Res*., **2015**, *3*, 337-340. DOI: 10.12691/jfnr-3-5-8

[9]Tardio, J., Pardo-de-Santayana, E., Morales, R., Ethnobotanical review of wild edible plants in Spain, *Bot. J. Linn. Soc*., **2006**, *152*, 27–71.

https://doi.org/10.1111/j.1095-8339.2006.00549.x

[10]Azaizeh, H., Saad, B., Khalil, K., Said, O., The State of the Art of Traditional Arab Herbal Medicine in the Eastern Region of the Mediterranean: A Review, *eCAM*, **2006**, *3*, 229–235. DOI: 10.1093/ecam/nel034

[11]Kayser, O., Ethnobotany and Medicinal Plant Biotechnology: From Tradition to Modern Aspects of Drug Development, *Planta Med*., **2018**, *84*, 834-839. DOI: https://doi.org/10.1055/a-0631-3876

[12]Qasem, J. R., Abu-Blan, H. A., Fungicidal Activity of Some Common Weed Extracts Against Different Plant Pathogenic Fungi, *J. Phytopathol*., **1996**, *144*, 157-161. DOI: 10.1111/j.1439-0434.1996.tb01507.x

[13]Ali-Shtayeh, M. S., Al-Assali, A. A., Jamous, R. M., Antimicrobial activity of Palestinian medicinal plants against acne-inducing bacteria, *Afr. J. Microbiol. Res*., **2013**, *7*, 2560-2573. DOI: 10.5897/AJMR12.1875

[14]Mericli, A.H., Dellamonica, G., Flavonoids of *Notobasis syriaca*, *Fitoterapia*, **1983**, *54*, 35-36. https://eurekamag.com/research/005/467/005467158.php

[15]Alali, F. Q., Tawaha, K., El-Elimat, T., Syouf, M., El-Fayad, M., Abulaila, K., Nielsen, S. J., Wheaton, W. D., Falkinham, J. O., Oberlies, N. H., Antioxidant activity and total phenolic content of aqueous and methanolic extracts of Jordanian plants: an ICBG project, *Nat. Prod. Res*., **2007**, *21*, 1121–1131. DOI: 10.1080/14786410701590285

[16]El-Hela, A. A., Abdel-Hady, N. M., Dawoud, G. T., Hamed, A. M. Morsy, T. A., Phenolic Content , Antioxidant Potential and Aedes Aegyptii Ecological Friend Larvicidal Activity of Some Selected Egyptian Plants, *J. Egypt. Soc. Parasitol*., **2013**, *43*, 215 – 234. https://www.researchgate.net/publication/236930939

[17]Hussain, H., Tchimene, M. K., Ahmed, I., Meier, K., Steinert, M., Draeger, S., Schulz, B., Krohn, K., Antimicrobial Chemical Constituents from the Endophytic Fungus Phomopsis sp from *Notobasis syriaca*, *Nat. Prod. Commun*., **2011**, *6*,1905-1906. https://www.researchgate.net/publication/221813055

[18]Azab, A., Nassar, A., Kaplanski, J., Mahajneh, R., Agam, G., Azab, A. N., Effects of aqueous extract of *Notobasis syriaca* on lipopolysaccharide-induced inflammation in rats, *Asian Pac. J. Trop. Med*., **2018**, *11*, 48-52. DOI: 10.4103/1995-7645.223533

[19]Rayan, A., Abu-Lafi, S. A., Al-Jaas, H., Abu-Farich, B., Barria, W., Phytochemical composition and antioxidant activity of wild *Scolymus maculatus* L., Poster, *3rd International Conference on Natural Products Utilization*, **2017**, www.researchgate.net/publication/320596004

[20]Benchiheub, M., Benkahoul, M., Bellil, I., Mechakra, M. A., Milk-Clotting properties and specific hydrolysis od Caseins of the acid protease extracted from *Scolymus maculatus* flowers, *Int. J. Adv. Res*., **2014**, *2*, 357-365. http://www.journalijar.com/article/1034

[21]Bullerman, L. B., "Fungi in Food – An Overview", Encyclopedia of Food Sciences and Nutrition, 2nd Ed., **2003**, 5511-5522. https://doi.org/10.1016/B0-12-227055-X/01129-9

[22]Al-Aboudi, A., Mohammad, M. Y., Musharraf, S. G., Choudhary, M. I., Atta-ur-Rahman, Microbial transformation of testosterone by *Rhizopus stolonifer* and *Fusarium lini*, *Nat. Prod. Res*., **2008**, *22*, 1498-1509. DOI: 10.1080/14786410802234528

[23]Shete, D. K., Shirote, P. J., Synthesis and Antifungal Activities of Nonsteroidal Anti-Inflammatory Carboxylic Acid Ester Derivatives of Fluconazole, *J. Pharm. Res*., **2012**, *5*, 5197-5201. https://pdfs.semanticscholar.org/db53/ac496ee7935a96151436b57e7763363a3669.pdf

[24]Decelis, S., Sadella, D., Triganza, T., Brincat, J-P., Gatt, R., Valdramidis, V. P., Assessing the anti-fungal efficiency of filters coated with zinc oxide nanoparticles, *R. Soc. Open Sci*., **2017**, *4*, 9 pages. DOI: 10.1098/rsos.161032

[25]Mohammadi, S., Aroiee, H., Aminifard, M. H., Tehranifar, A., Jahanbakhsh, V., Effect of fungicidal essential oils against *Botrytis cinerea* and *Rhizopus stolonifer* rot fungus *in vitro* conditions, *Arch. Phytopathol. Plant Protect*., **2014**, *47*, 1603-1610. DOI: 10.1080/03235408.2013.853456

[26]Sohail, M., Muhammad, A., Zafar, I., Sheena, A., Khan, S. M., Inayat, R., Khan, W., Asghar, A., Ullah, I., Numan, M., Antimicrobial activity of mycelial extracts of *Rhizopus stolonifer* against different fungal and bacterial pathogenic strains, *Int. J. Biosci*., **2014**, *4*, 276-281. https://www.researchgate.net/publication/272817630

[27]Zhou, D., Wang, Z., Li, M., Xing, M., Xian, T., Tu, K., Carvacrol and eugenol effectively inhibit *Rhizopus stolonifer* and control postharvest soft rot decay in peaches, *J. Appl. Microbiol*., **2018**, *124*, 166-178. https://doi.org/10.1111/jam.13612

[28]Muhammad, A., Rahman, Z., Ayub, M., Durrani, Y., Ali, S.A., Abroo, T., Ashbala, S., Khan, M., Khan, A., Inhibitory Effect of Ginger and Turmeric on *Rhizopus stolonifer* Growth on Bread, *J. Food Process. Technol*., **2014**, *5*, 6 pages. DOI: 10.4172/2157-7110.1000325

[29]Wang, J., Cao, S., Wang. L., Wang, X., Jin, P., Zheng, Y., Effect of β-Aminobutyric Acid on Disease Resistance Against *Rhizopus* Rot in Harvested Peaches, *Front. Microbiol*., **2018**, *9*, 10 pages. DOI: 10.3389/fmicb.2018.01505

[30]Sanchez-Rangel, J. C., Benavides, J., Basilio Heredia, J., Cisneros-Zevallos, L., Jacobo-Velazquez, D. A., The Folin–Ciocalteu assay revisited: improvement of its specificity for total phenolic content determination, *Anal. Methods*, **2013**, *5*, 5990-5999. DOI: 10.1039/c3ay41125g

[31]Azab, A., Total phenolic content, antioxidant capacity and antifungal activity of extracts of *Carthamus tenuis* and *Cephalaria Joppensis*, *Eur. Chem. Bull*., **2018**, *7*, 156-161. DOI: 10.17628/ecb.2018.7.156-161

[32]Huma, F., Jaffar, M., Masud, K., A Modified Potentiometric Method for the Estimation of Phenol in Aqueous Systems, *Turk. J. Chem*., **1999**, *23*, 415-422. https://www.researchgate.net/publication/239544616

[33]Yuris, A., Siow, L-F., A Comparative Study of the Antioxidant Properties of Three Pineapple (Ananas comosus L.) Varieties, *J. Food Stud*., **2014**, *3*, 40-56. DOI: 10.5296/jfs.v3i1.4995

[34]Zhang, M., Liu, N., Liu, H., Determination of the Total Mass of Antioxidant Substances and Antioxidant Capacity per Unit Mass in Serum Using Redox Titration, *Bioinorg. Chem. Appl*., **2014**, 6 pages. http://dx.doi.org/10.1155/2014/928595

[35]Udeozo, I. P., Akpaba Enem S., Ugwu Okechukwu, P. C., Okoye, N. H., Umedum, N. L., Qualitative alkaloidal analysis of some selected Nigerian medicinal plants used in herbal treatment of diseases, *Int. J. Life Sci. Biotechnol. Pharm. Res*., **2013**, *2*, 300-305. http://new.ijlbpr.com/jlbpradmin/upload/ijlbpr_51d44e989b00d.pdf

[36]Zahra, N., A Short Review on Ethnomedicinal Uses and Phytochemistry of *Silybum marianum*, *Nat. Prod. Chem. Res*., **2017**, *5*, 3 pages. DOI: 10.4172/2329-6836.1000292

[37]Bijak, M., Silybin, a Major Bioactive Component of Milk Thistle (*Silybum marianum* L. Gaernt.)-Chemistry, Bioavailability, and Metabolism, *Molecules*, **2017**, *22*, 11 pages. DOI: 10.3390/molecules22111942

[38]Antunes, A., Amaral, E., Belgacem, M. N., *Cynara cardunculus* L.: chemical composition and soda-anthraquinone cooking, *Ind. Crops Prod*., **2000**, *12*, 85-91. https://doi.org/10.1016/s0926-6690(00)00040-6

[39]Cerqueira Sales, M. D., Barcellos Costa, H., Bueno Fernandes, P. M., AiresVentura, J., Dummer Meira, D., Antifungal activity of plant extracts with potential to control plant pathogens in pineapple, *Asian Pac. J. Trop. Biomed*., **2016**, *6*, 26-31. https://doi.org/10.1016/j.apjtb.2015.09.026

[40]Li, X., Wu, X., Huang, L., Correlation between Antioxidant Activities and Phenolic Contents of *Radix angelicae sinensis* (Danggui), *Molecules*, **2009**, *14*, 5349-5361. DOI: 10.3390/molecules14125349

[41]Pandey, K. B., Rizivi, S. I., Plant polyphenols as dietary antioxidants in human health and disease, *Oxid. Med. Cell Longev*., **2009**, *2*, 270-278. DOI: 10.4161/oxim.2.5.9498

[42]Babatunde, O. A., A Study of the Kinetics and Mechanism of Oxidation of L Ascorbic Acid by Permanganate Ion in Acidic Medium, *World J. Chem*., **2008**, *3*, 27-31. https://www.researchgate.net/publication/238669224

[43]Caregnato, P., Gara, P. M., Bosio, G. N., Gonzalez, M. C., Russo, N., del Carmen Michelini, M., Martire, D. O., Theoretical and Experimental Investigation on the Oxidation of Gallic Acid by Sulfate Radical Anions, *J. Phys. Chem. A*, **2008,** *112*, 1188-1194. DOI: 10.1021/jp075464z

[44]Rodrigues de Almeida, V., Szpoganicz, B., Humic acid potentiometric response patterns: out-of-equilibrium properties and species distribution modeling, *Chem. Biol. Technol. Agric*., **2015**, *2*, 7 pages. DOI; 10.1186/s40538-015-0042-4

[45]Mir, S. A., Antioxidant activity of diosmin, daflon and rutin tablets and extracts of dog rose fruits by permanganate reduction titrimety, *Int. J. PharmTech Res*., **2015**, *7*, 258-265. http://sphinxsai.com/2015/ph_vol7_no2/1/(258-265)%20V7N2.pdf

[46]Babbar, N., Oberoi, H., Singh Uppal, D., Tumadu Patil, R., Total phenolic content and antioxidant capacity of extracts obtained from six important fruit residues, *Food Res. Int*., **2011**, *44*, 391-396. DOI: 10.1016/j.foodres.2010.10.001

[47]Kosmerl, T., Bertalanic, L., Maras, V., Kodzulovic, V., Sucur, S., Abramovic, H., Impact of Yield on Total Polyphenols, Anthocyanins, Reducing Sugars and Antioxidant Potential in White and Red Wines Produced from Montenegrin Autochthonous Grape Varieties, *Food Sci. Technol*., **2013**, *1*,7-15, 2013. DOI: 10.13189/fst.2013.010102

Received: 23.08.2018.

Accepted: 25.09.2018.

FORMULATION AND EVALUATION OF NANOSUSPENSIONS OF TADALAFIL USING DIFFERENT STABILIZERS

Haritha Meda,[a]* G. Devala Rao,[b] V. Harini Chowdary[c] and Mandava Bhuvan Tej[d]

Keywords: Tadalafil; oral nano suspension; sodium lauryl sulphate; Tween-20; Pluronic F127; Tween-80;

In the present study, an attempt was made to prepare oral nanosuspension of Tadalafil. Tadalafil is a PDE5 inhibitor used for treating erectile dysfunction (ED) and pulmonary arterial hypertension. Tadalafil nanosuspensions were prepared by nanoprecipitation method using different polymers (such as sodium lauryl sulphate (SLS), TWEEN-80, TWEEN-20, Pluronic F127) and acetone. Estimation of Tadalafil was carried out spectrophotometrically at 285nm. The oral nanosuspension were evaluated for various physical and biological parameters, drug content uniformity, particle size analysis, zeta potential, invitro drug release, short-term stability, drug-excipient interactions (FTIR). Out of the formulation from F1 to F12, F11 containing TWEEN-20 (0.3 %) showed 99.74 % release at the end of 30min and follows first order drug release kinetics.

* Corresponding Authors
email: medaharitha777@gmail.com
[a] Department of Pharmaceutical Sciences, Krishna University, Machilipatnam, India 521001
[b] KVSR Siddhartha College of Pharmaceutical Sciences, Vijayawada, India
[c] Department of Pharmaceutics, Acharya and B M Reddy College ofPharmacy, Bengaluru 560107, India
[d] Sri Ramachandra College of Pharmacy, Porur, Chennai, Tamilnadu, India 600 116

INTRODUCTION

Over the past few decades the major challenging task faced by the formulators is poor solubility of the drugs. Oral delivery of these drugs is problematic owing to their poor solubility which consequences in low bioavailability and lack of dose proportionality. To overcome these challenges, formulators come up with some technologies like solid dispersions, complexation, co-solvency, micellar solubilization etc.[1-3]But these technologies are lagging in terms of universal applicability. Then formulators developed novel technologies like lipid based drug delivery systems, micronization, nanonization, combination of two technologies etc.[4,5]

Tadalafil is a phosphodiesterase-5 (PDE-5) inhibitor indicated for the treatment of erectile dysfunction and was officially approved by FDA in 2003. It is the most potent PDE-5 inhibitor which exhibits 5000 times more affinity to PDE-5. Tadalafil has gained much attention and wide clinical acceptance owing to its longer duration of action and minimal ability to cause vision abnormalities. Tadalafil is a BCS class II drug with low solubility and high bioavailability which consequences in poor dissolution with variable bioavailability.

In the present research work an attempt was made to improve the solubility and dissolution rate of model drug tadalafil.

Experimental

Tadalafil was obtained as a gift sample from Dr Reddy's Laboratories. Sodium lauryl sulphate, TWEEN-80, TWEEN-20, Pluronic F127 and all other chemicals and solvents used were obtained from Rankem, Mumbai.

Preparation of Tadalafil nanosuspension

Nano suspensions were prepared by the nanoprecipitation technique. Tadalafil was dissolved in acetone at room temperature (organic phase). This was poured into water containing different polymers like TWEEN-80, SLS, TWEEN-20 or Pluronic F127, maintained at room temperature and subsequently stirred on magnetic stirrer which is stirred at rpm 800-1000 for 30 min to allow the volatile solvent to evaporate. Organic solvents were added by means of a syringe positioned with the needle directly into stabilizer/surfactant containing water. Organic solvents were left to evaporate off under a slow magnetic stirring of the nanosuspension at room temperature for 1 h followed by sonication, later the nanosuspension was collected and evaluation tests were performed.[6-9] The composition of the formulations is given in **Table 1**.

Evaluation parameters of Tadalafil nanosuspensions

Drug content uniformity

10 mL of each formulation was taken and dissolved in 10 mLof isotonic solution and kept overnight. 10 mg (similar as in formulation) of drug was taken and dilution was made to 10 μgmL^{-1}. The dilutions were filtered and analyzed using UV for their content uniformity. The absorbance of the formulations were read using one cm cell in a UV-Vis spectrophotometer. The instrument was set at 285 nm. The drug content in each formulation was calculated based on the absorbance values of known standard solutions.[10-12]

Table 1. Composition of nanosuspension of Tadalafil.

Ingredients mg/tablet	F1	F2	F3	F4	F5	F6	F7	F8	F9	F10	F11	F12
Tadalafil	10	10	10	10	10	10	10	10	10	10	10	10
SLS (mg)	10	--	--	--	20	--	--	--	30	--	--	--
Pluronic F127 (mg)	--	10	--	--	--	20	--	--	--	30	---	--
TWEEN-20(w/v)	--	--	0.1 %	--	--	--	0.2 %	--	--	--	0.3%	--
TWEEN-80(w/v)	--	--	--	0.1%	--	--	--	0.2%	--	--	--	0.3%
Acetone (mL)	5	5	5	5	5	5	5	5	5	5	5	5
Water (mL)	40	40	40	40	40	40	40	40	40	40	40	40

Entrapment efficacy

The freshly prepared nanosuspension was centrifuged at 10,000 rpm for 20 min at 5°C using cool ultracentrifuge. The amount of unincorporated drug was measured by taking the absorbance of the appropriately diluted 25 mL of supernatant solution at 285 nm using UV spectrophotometer against blank/control nanosuspensions. DEE was calculated by subtracting the amount of free drug in the supernatant from the initial amount of drug taken. The experiment was performed in triplicate for each batch and the average was calculated.[13-15]

The entrapment efficiency (EE %) could be calculated by eqn. (1)

$$EE\ \% = \text{Drug content x } 100/\text{Drug added} \quad (1)$$

Zeta potential

The zeta potential is defined as the difference in potential between the surface of the tightly bound layer (shear plane) and the electro-neutral region of the solution. The potential gradually decreases as the distance from the surface increases. The most widely-used theory for calculating zeta potential was developed by Smoluchowski in 1903. The theory is based on electrophoresis and can be expressed as eqn. (2), where (μ) is the electrophoretic mobility, (ε) is the electric permittivity of the liquid, (η) is the viscosity and (ζ) is the zeta potential. [16-18]

$$\mu = \zeta\varepsilon/\eta \quad (2)$$

Particle size and shape

Average particle size and shape of the formulated nanosuspensions was determined by using Malvern Zetasizer ZS using water as dispersions medium. The sample was scanned 100 times for determination of particle size.

***In-vitro* drug release study**

In-vitro dissolution studies were performed in USP apparatus-II (LAB INDIA DS 8000), employing paddle stirrer at rotation speed of 50 rpm and 200 mL of pH 6.8 phosphate buffer as dissolution medium. Accurately weighed bulk drug and nanosuspensions were dispersed in dissolution medium. The release study is performed at 37 ± 0.5°C. Samples of 5 mL are withdrawn at predetermined time intervals and replaced with fresh medium to maintain sink condition.[19-22] The samples were filtered through 0.22 µm membrane filter disc (Millipore Corporation) and analyzed for Tadalafil, after appropriate dilution, by measuring the absorbance at 285 nm.

RESULTS AND DISCUSSION

Tadalafil is a BCS class-II drug having low solubility and high permeability. Thus, it is challenging to enhance the solubility of tadalafil in an aqueous solution. Solvent evaporation with precipitation has been employed to produce nanosuspension of Tadalafil.

Solubility of tadalafil was carried out to determine the vehicle for evaluation. Tadalafil showed highest solubility in phosphate buffer pH 6.8 as represented in **Figure 1**. Spectral analysis was carried out and the λ-max was found to be 285 nm.

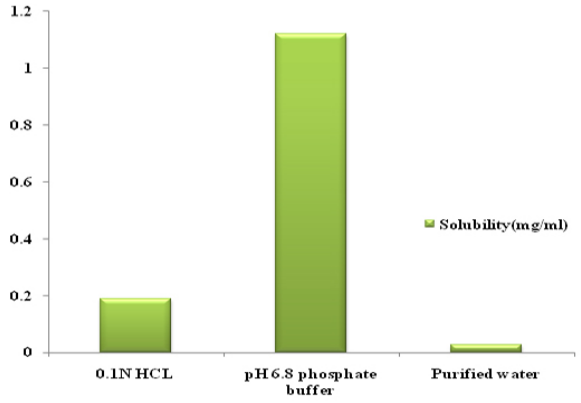

Figure 1. Solubility of Tadalafil in different solvents

Compatibility studies were performed using IR spectrophotometer. The IR spectrum of pure drug and physical mixture of drug and excipients were studied. The shift in the finger print region of tadalafil optimized formulation is within the range as that of the tadalafil pure drug as depicted in **Figure 2**.Thus it clearly indicates that there is no chemical interaction between the drug and excipients and they can be further employed for the development of nanosuspensions.

Nansuspensions of tadalafil were prepared by nanopreciptation technique using different polymerslike TWEEN-80, SLS, TWEEN-20, Pluronic F127 as stabilizers and acetone as solvent. Twelve formulations were developed and evaluated for various parameters.

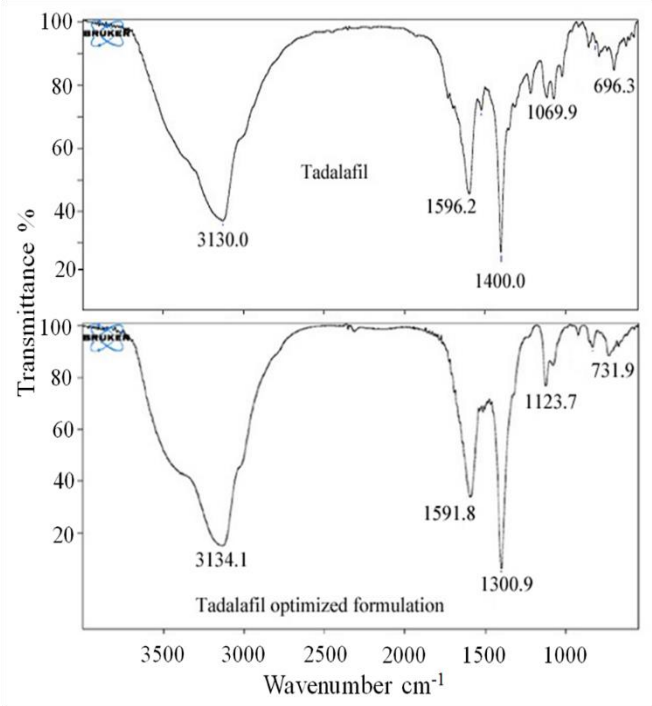

Figure 2.FTIR spectrum of Tadalafil and tadalafil optimized formulation.

The drug content of the tadalafil nanosuspension was found in the range of 76.14 %to 95.46% respectively. The entrapment efficacy of the formulated nanosuspension was found to be in the range of 87.30%-97.77%respectively. The values were reported in the Table 2**.** Based on the results it was observed that higher drug content was reported with good entrapment efficiency indicating less drug loss during formulation.

Table 2. Drug content and entrapment efficiency of tadalafil formulations.

Formulation code	Mean % drug content* ± S.D (CV)	Mean EE %* ± S.D
TF1	79.31±0.14	89.11±0.87
TF2	81.06±0.07	90.12±0.15
TF3	84.16±0.47	91.45±0.42
TF4	76.14±0.36	87.30±0.33
TF5	82.64±0.55	90.63±0.21
TF6	85.33±0.15	92.44±0.77
TF7	88.79±0.23	94.40±0.44
TF8	83.02±0.74	89.97±0.89
TF9	86.45±0.86	93.36±0.98
TF10	89.91±0.98	95.64±0.02
TF11	95.46±0.70	97.77±0.10
TF12	84.47±0.11	92.50±0.09

Further *in-vitro* drug release studies were carried out for F1 to F12formulations. Compared to all other formulations, formulation containingTWEEN-20 as stabilizer (F11) shows immediate drug release of 99.74 % drug within 30 min and it was selected as promised formulation as shown in **Figure 3**.

This formulation was selected for further analysis like SEM, zeta potential, particle size determination and stability studies were carried out.

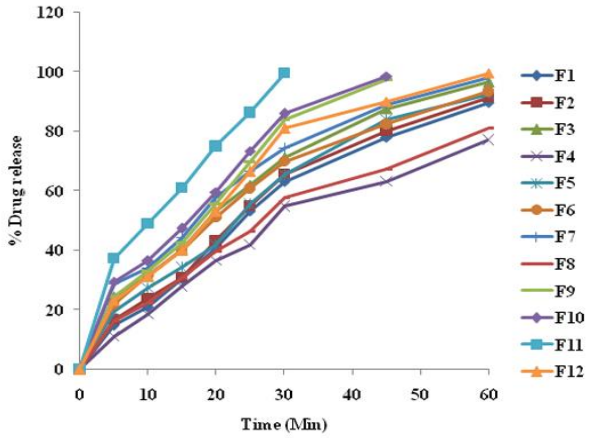

Figure 3. Percentage drug release of tadalafil from nanosuspension formulations.

From the SEM analysis it was observed that the particles were round, discrete and of nano range as shown in figure 4. The zeta potential of F11 was found to be within the acceptable limits as shown in **Figure 5.**Average particle size of nanosuspension of optimized formulations (F11)was found to be at a range of 126.6nm as depicted in **Figure 6**.

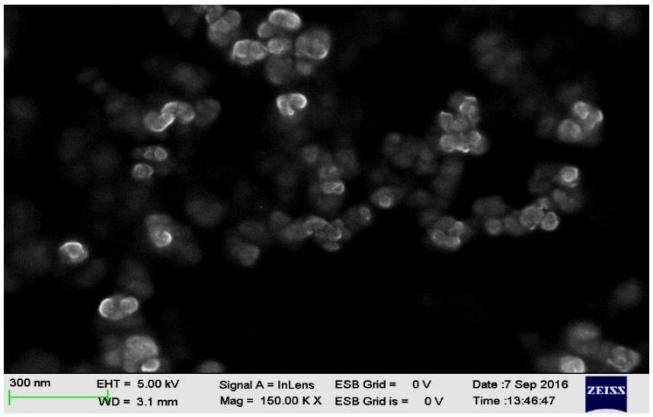

Figure 4.SEM analysis of Tadalafil optimized formulation, F11.

Table 3. In vitro drug release data of the stability formulation F11.

Time (min)	Cumulative % drug released ± S.D at 40±1°C			
	Day 1	Day 30	Day 60	Day 90
05	37.26	36.88	37.10	37.20
10	49.06	48.49	48.80	48.98
15	61.09	61.12	61.13	61.01
20	75.04	74.49	75.03	74.97
25	86.34	86.20	86.41	86.25
30	99.74	99.56	99.70	99.69

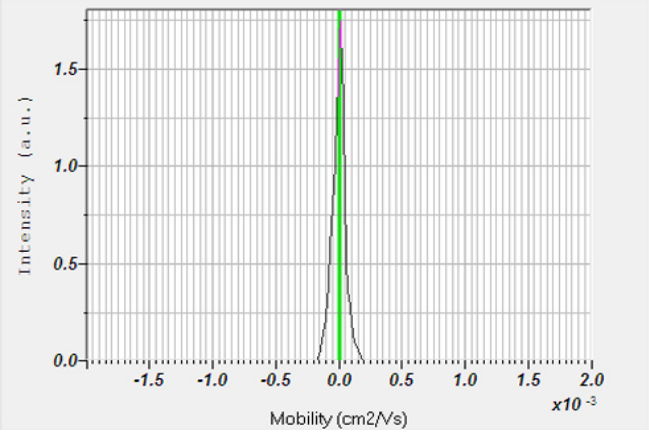

Figure 5. Zeta potential of F11 formulation.

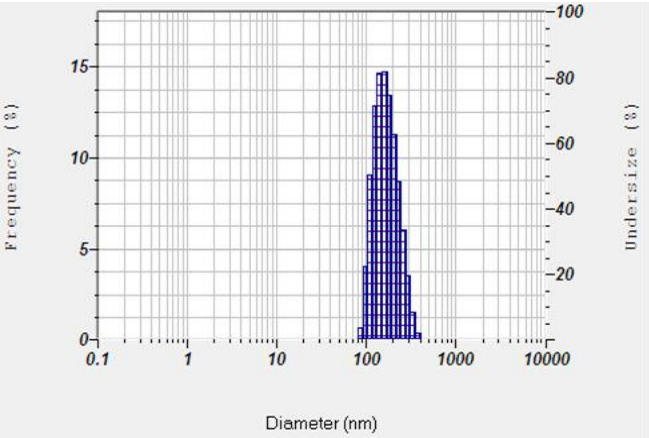

Figure 6. Particle size distribution of F11 formulation.

From the stability data obtained after 90 days study, it was inferred that there is no major difference in the drug release from the F11 formulation indicating the stability of the nanosuspension as given in Table 3.

CONCLUSION

Oral Nanosuspension of Tadalafil can be prepared by precipitation method using Tween 80, Sodium lauryl sulphate, TWEEN-20, Pluronic F127, and Acetone. When comparing all the results obtained nanosuspensions prepared using TWEEN-20 (0.3%) shows better results among all the formulations. The optimized formulation shows 99.74% of drug release by end of 30 minutes and follows first order release kinetics having R^2 value of 0.972. Finally by comparing all the formulations we can say that as the amount of polymer increases, the drug release rate increases, whereas nanosuspension strength increases.Thus nanosuspension can be a better alternative for the delivery of tadalafil.

Acknowledgements

Authors thank DST-NRDMS for the support and encouragement

References

[1]Nikhitha, I., Vani, V, CH., Rao, V.U. M., Formulation and evaluation of aripiprazole nano suspension. *Int. J. Trends. Pharm. Life Sci.*,**2015,** *1*(*3*), 317-330.

[2]Shukla, S. K., Jain, R., Pandey, A., Nanosuspension formulation to improve the dissolution rate of Clonazepam. *Int. J. Adv. Res.*,**2015,** *3*(*4*), 588-591.

[3]Devara, R. K., Mohammad, H. R., Rambabu, B., Aukunuru, J., Habibuddin, M., Optimization and Evaluation of Intravenous Curcumin Nanosuspensions Intended to Treat Liver Fibrosis. *Turk J. Pharm. Sci.*,**2015**, *12*(*2*), 207-220.

[4]Shetiya, P., Vidyadhara, S., Ramu, A., Sasidhar, R.L., Viswanadh, K., Development and characterization of a novel nanosuspension based drug delivery system of valsartan: A poorly soluble drug. *Asian J. Pharm.*,**2015**, 29-33. http://dx.doi.org/10.22377/ajp.v9i1.428

[5]Sharma, S., Issarani, R., Nagori, B.P., Effect of Solvents on Particle Size of Aceclofenac Nanosuspension Prepared by Bottom up Technique. *World J. Pharm. Pharm. Sci.*,**2015,***4*(*4*), 1022-1034.

[6]Jahagirdar, K.H., Bhise, K., Investigation of Formulation Variables Affecting the Properties of Lamotrigine Nanosuspension Prepared by Using High Pressure Homogenizer Using Factorial Design. *Int.J. Pharm. Chem. Sci.*,**2014,***3*(*3*), 732-739. PMC3232085

[7]Pattnaik, S., Stabilized Aceclofenac Nanosuspension: Development and In Vitro Characterization. *Int.J. Pharm. Bio. Chem. Sci.*,**2014,***3*(*2*), 65-68.

[8]Kamble, K.K., Preparation & Characterization of Olmesartan Medoxomil Nanosuspensions Prepared By Emulsion Diffusion Technique. *Int. J. Pharm. Res. Sch.*,**2014,***3*(*3*), 102-112.

[9]Amsa, P., Tamizharasi, S., Jagadeeswaran, M., Kumar, T.S., Preparation and Solid State Characterization of Simvastatin Nanosuspensions for Enhanced Solubility and Dissolution. *Int. J. Pharm. Pharm.Sci.*, **2014,***6*(*1*), 265-269. doi=10.1.1.517.4889&rep=rep1

[10]Papdiwal, A., Pande V, Sagar K., Design and characterization of zaltoprofen nanosuspension by precipitation method. *Der. Pharma.Chemica.*,**2014**, *6*(*3*), 161-168.

[11]Dinesh, K.B., Krishna, K.K., John, A., Paul, D., Cherian, Nanosuspension Technology in Drug Delivery System. J.,*Nanosci. Nanotech: Int. J.*,**2013,***3*(1), 1-3. http://dx.doi.org/10.22377/ajp.v3i3.261

[12]Prakash, S., Vidyadhara, S., Sasidhar, R.L.C., Abhijit, D., Akhilesh, D., Development and characterization of Ritonavir nanosuspension for oral use. *Pharm.,Lett.*, **2013**, *5*(*6*),48-55.

[13]Kotecha, R.K., Bhadra, S., Rajesh, K.S., Formulation & Process Development of Azithromycin Ophthalmic Nanosuspension. *Int J. Pharm. Pharm. Sci.*,**2013,***5*(*4*), 490-497.

[14]Amin, M.A., Osman, S.K., Aly, U.F., Preparation and Characterization of Ketoprofen Nanosuspension for Solubility and Dissolution Velocity Enhancement. *Int. J. Pharma. Bio. Sci.*,**2013,***4*(*1*), 768-780.

[15]Mohan, M., Veena, M., Narayanasamy, D., Vasanthan, M., Nelofar, S., Development & Evaluation of Aceclofenac Nanosuspension Using Eudragit RS100. *AsianJ.Biochem.Pharm. Res.*,**2012,***2*(*2*),1-10. doi.org/10.1080/10837450.2018.1486424

[16]Mohamed, J.M., Bharathidasan, P., Raffick, M.M., Preformulation and Development of Curcumin Magnetic Nanosuspension Using Magnetite (Fe3O4) and Methyl Cellulose. *Int. J. Pharma. Bio. Sci.*,**2012,***3*(*4*), 419-432.

[17]Aghajani, M., Shahverdi, A.R., Rezayat, S.M., Amini, M.A., Amani, A., Preparation and optimization of acetaminophen nanosuspension through nanoprecipitation using microfluidic devices- an artificial neural networks study. *Int. Conf.Nanostruct.*,**2012,***1*(*1*), 692-696. doi: 10.3109/10837450.2011.649854.

[18]Detroja, C., Chavhan, S., Sawant, K.,*Sci Pharm.*, Enhanced Antihypertensive Activity of Candesartan Cilexetil Nanosuspension: Formulation, Characterization and Pharmacodynamic Study. *Sci Pharm.* **2011,***79*, 635–651. doi: 10.3797/scipharm.1103-17

[19]Yonglu, W., Xueming, L.,Liyao, W., Yuanlong, X., Xiaodan, C., Ping, W., Formulation and pharmacokinetic evaluation of a paclitaxel nanosuspension for intravenous delivery. *Int. J.Nanomed.*,**2011,***72*, 1498-1506. doi: 10.2147/IJN.S21097.

[20]Raval, A.J., Patel,M.M., Preparation and Characterization of Nanoparticles for Solubility and Dissolution Rate Enhancement of Meloxicam. *Int. R. J. Pharm.*, **2011,** *1*(*2*),42-49.

[21]Chen, J., Park, H., Park, K. J., Synthesis of superporous hydrogels: hydrogels with fast swelling and superabsorbent properties. *Biomed. Mater. Res.*, **1999,** *44*(*1*), 53-62. doi.org/10.1002/(SICI)1097-4636(199901)44:1<53::AID-JBM6>3.0.CO;2-W

[22]Jun, C., William, E. B., Haesun, P.,Kinam, P., Gastric retention properties of superporous hydrogel composites. *J. Cont. Release.*,**2000,***64*, 39-51. doi.org/10.1016/S0168-3659(99)00139-X

Received: 10.09.2018.
Accepted: 05.10.2018.

2-HYDROXY-1-ARYL-2-(INDOL-3'-YL)ETHANONES: SYNTHESIS, SPECTRAL CHARACTERISTICS, STRUCTURE AND THEIR REARRANGEMENT INTO 2-HYDROXY-2-ARYL-1-(INDOL-3'-YL)ETHANONES

Vasiliy G. Shtamburg,[a]* Victor V. Shtamburg,[a] Andrey A. Anishchenko,[b] Alexander V. Mazepa,[d] Svetlana V. Kravchenko[d] and Svetlana V. Shishkina[e]

Keywords: Arylglyoxals, α- and ß-benzoins, indole, synthesis, 2-hydroxy-1-aryl-2-(indol-3-yl)ethanones, 2-hydroxy-2-aryl-1-(indol-3-yl)ethanones, spectral characteristics.

A convenient method of synthesis of 2-hydroxy-1-aryl-2-(indol-3-yl)ethanones and their isomerization to 2-hydroxy-2-aryl-1-(indol-3-yl)ethanones in the presence of triethylamine on heating or in the presence of EtONa at room temperature have been studied. The spectral tests of isomers structures are presented. The structures of 2-hydroxy-1-phenyl-2-(indol-3-yl)ethanone and 2-hydroxy-2-phenyl-1-(indol-3-yl)ethanone have been studied by XRD technique.

* Corresponding Authors
Fax: +380-97-651-61-72
E-Mail: stamburg@gmail.com
[a] Ukrainian State University of Chemical Technology, 49005 Ukraine, Dnepr, Gagarina st., 8.
[b] O. Gonchar Dnepropetrovsk National University, 49050 Ukraine, Dnepr, Nauchnaya st. 25.
[c] A.V. Bogatsky Physico-Chemical Institute of NAS of Ukraine, 65080 Odessa, Luystdorfskaya Doroga st., 86.
[d] Dnipro State Agrarian and Ecomomic University, 49600 Ukraine, Dnepr, Efremova st., 25.
[e] STC "Institute for Single Crystals", National Academy of Sciences of Ukraine, 61001 Ukraine, Kharkov, Science ave., 60 .

INTRODUCTION

Unsymmetrical arylbenzoins and aryl(heteryl)benzoins exist in two isomeric forms, α-benzoins and ß-benzoins,[1-8] for example aryl(furyl)benzoins **1a** and **1b** (Figure 1). [2,6-8] ß-Aryl(furyl)benzoin **1b** is more stable than **1a** due the possibility of the carbonyl group being in conjugation with π-donor furan ring.[2,7,8]

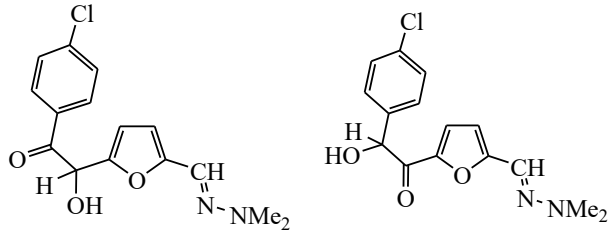

1a **1b**

Figure 1. Aryl(furyl)benzoins.

α-Aryl(furyl)benzoins can be easily obtained by arylglyoxals reaction with some furanes.[2,6-9] In many cases, they isomerize spontaneously into more stable ß-aryl(furyl)benzoins spontaneously,[7,8] however, in some cases, presence of a base and heating of reaction mixture are needed.[2,5-8]

It was first shown by Zhungietu[10,11] that phenylglyoxal hydrate and 2-thienylglyoxal hydrate react with indole in boiling benzene to give stable products α-ary(3-indolyl)benzoins **2a, b** (Scheme 1).[10,11] 4-Tolylglyoxal hydrate with indole forms α-benzoin **2c** in moderate yield.[11] Zhungietu had also reported that indole did not react with 4-methoxyphenylglyoxal in boiling benzene,[10] and with 4-chlorophenylglyoxal yields a 2:1 adduct, and not α-benzoin **2d**.[10] However, α-benzoins **2a-c** obtained by him have not been characterized by ^{1}HNMR and mass spectra. Later we have synthesized α-ary(3-indolyl)benzoins **2a,b,d,e** by interaction of indole with proper arylglyoxal hydrates or anhydrous arylglyoxals in benzene.[3,4,9,12] Their structure was confirmed by ^{1}HNMR and mass spectra data. Recently it was reported that indole reacted with arylglyoxals in 1,4-dioxane solution in the presence of $CuCl_2$ at room temperature forming α-ary(3-indolyl)benzoins **2a–h** in good yields.[13] Also recently Chinese chemists had reported that benzoic acid is an excellent catalyst of Friedel-Crafts alkylation of indole by arylglyoxals.[14] But earlier Iranian chemists had synthesized α-benzoins **2a,c-e** with excellent yields in aqueous media at room temperature in the absence of any acid catalyst,[15] this accords well with the earlier Zhungietu's reports.[10,11]

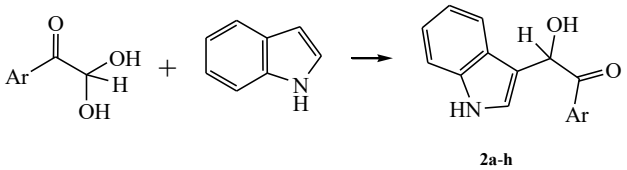

2a-h

Ar = Ph (**2a**), 2-thienyl (**2b**),4-MeC_6H_4 (**2c**), 4-ClC_6H_4 (**2d**), 4-BrC_6H_4 (**2e**), 4-FC_6H_4 (**2f**), 4-O_2NC_6H_4 (**2g**), 4-MeOC_6H_4 (**2h**)

Scheme 1. Synthesis of α-ary(3-indolyl)benzoins.

But the only reports about α→ß isomerization of α-aryl(indolyl)benzoins are our preliminary communications.[3,4] The development of efficient and general methodology for the synthesis of α-functionalized α-(indol-3-yl) ketones is highly desirable.[12] These compounds are possible precursors for the preparation of biologically

active molecules.[12] Therefore, we have investigated the synthesis of α-aryl(indolyl)benzoins and their isomerization to ß -aryl(indolyl)benzoins by the action of bases.

EXPERIMENTAL

^{1}H NMR spectra were recorded on VARIAN VXP-300, VARIAN JEMINI 400 and Bruker-Avance DRX 500 spectrometers (300, 400 and 500 MHz, respectively). ^{13}C NMR spectra were recorded on VARIAN VXP-300 spectrometer (75 MHz) and VARIAN JEMINI 400 spectrometer (100 MHz) with $(CD_3)_2SO$ as solvent and TMS as internal standard. Mass spectrum was recorded on VG 70-70EQ mass spectrometer in fast atom bombardment (FAB) mode and Kratos MS 890 mass spectrometer in electron impact (EI) mode (70 eV). Indole was sublimated under vacuum (3 Torr). The solvents were purified and dried according to standard procedures. Anhydrous arylglyoxals and 2-thienylglyoxal were obtained by rectification of proper arylglyoxal hydrates under vacuum 4 Torr.

Synthesis of α-aryl(indolyl)benzoins (2a,b)

A solution of 20 mmol anhydrous arylglyoxal and 20 mmol of indole in benzene (20 mL) was allowed to stand at 20 ºC for 72 h. The obtained precipitate was filtered off, washed by benzene (3 mL) and dried under vacuum (4 Torr.). The other α-aryl(indolyl)benzoins were synthesized in a similar manner.

2-Hydroxy-2-(indol-3'-yl)-1-phenylethanone (2a)

The compound was obtained as white crystals (66 %). m.p. 170-172°C (with decomp.) (lit. 170-172 °C,[10,11] 169-171 °C,[13] 174-177 °C[15]). ^{1}H NMR (400 MHz, $(CD_3)_2SO$) δ = 5.549 (1H, d, ^3J = 5.6, CHOH), 6.379 (1H, d, ^3J = 5.6, CHOH), 6.991 (1H, t, ^3J = 7.4, H Ind), 7.065 (1H, t, ^3J = 7.4, H Ind), 7.327 (1H, d, ^3J = 8.0, H Ind), 7.355 (1H, d, ^3J = 2.4, C(2)H Ind), 7.399 (2H, t, ^3J = 7.6, C(3,5) H Ph), 7.507 (1H, t, ^3J = 7.6, C(4)H Ph), 7.645 (1H, d, ^3J = 7.6, H Ind), 8.013 (2H,d, ^3J = 7.2, C(2,6)H Ph), 11.075 (1H, s, NH).^{13}C NMR (75 MHz, $(CD_3)_2SO$) δ = 69.5 (CHOH), 111.6, 113.3, 119.0, 119.2, 121.3, 124.9, 125.6, 128.47, 128.51, 132.9, 135.0, 136.3 (C Ph, Ind), 199.0 (C=O). MS (FAB) *m/z* 234 $[M+H-H_2O]^+$ (100), 206 $[M+H-H_2O-CO]^+$ (34), 146 (42), 118 (14), 105 Bz^+ (17). MS (FAB, KI) *m/z* 290 $[M+K]^+$ (100), 234 $[M+H-H_2O]^+$ (24), 206 $[M+H-H_2O-CO]^+$ (21), 146 (18), 105 Bz^+ (8). Anal. Calcd. for $C_{16}H_{13}NO_2$: N 5.57. Found: N 5.43.

Crystals of α-benzoin **2a** suitable for XRD study were grown from a solution in benzene at 10 ºC, monoclinic, $C_{16}H_{13}NO_2$ at 20°C ***a*** = 8.071(2), ***b*** = 8.513(3), ***c*** = 18.908(5) Å, β = 90.11(2)°, V = 1299.1(6) Å^3, M_r = 251.27, Z = 4, space group $P2_1/n$, d_{calc}= 1.285 g/cm^3, μ(MoKα) = 0.085 мм$^{-1}$, F(000) = 528. Cell parameters and intensities of 8638 reflections (2288 independent reflections, R_{int}=0.065) were measured using «Xcalibur 3» diffractometer (graphite-monochromated MoKα radiation, CCD detector, ***ω***-scan, 2 θ_{max}= 50°).

The structure was solved by direct method using SHELXTL program package.[16] Positions of hydrogen atoms were found from different synthesis of electronic density and refined using the riding model with U_{iso}=1.2U_{eqv} of non-hydrogen atom bonded with this hydrogen atom. Hydrogen atoms, taking place in hydrogen bonds formation, were refined in isotropic approximation. Full-matrix least-squares refinement against F^2 in anisotropic approximation for non-hydrogen atoms to wR_2 = 0.154 for 2288 reflections (R_1 = 0.053 for 1647 reflections with F>4σ(F), S = 1.206). The final atomic coordinates, molecular geometry parameters, and crystallographic data of compound **2a** are deposited in the Cambridge Crystallographic Data Center, 12 Union Road, Cambridge CB2, 1EZ, UK (fax:+44-1223-336033, e-mail: deposit@ccdc.cam.ac.uk) and is available on request quoting the deposition number CCDC 1864358).

2-Hydroxy-2-(indol-3'-yl)-1-(thien-2''-yl)ethanone (2b)

The compound was obtained as white crystals (75 %). m.p. 175-177 °C (with decomp.) (lit. 178-180 °C[10,11,13]). ^{1}H NMR (400 MHz, $(CD_3)_2SO$) δ = 5.800 (1H, d, ^3J = 5.2, CHOH), 6.091 (1H, d, ^3J = 5.2, CHOH), 6.976 (1H, t•d, ^3J = 7.4, ^4J = 1.2, H Ind), 7.061 (1H, , t•d, ^3J = 7.5, ^4J = 1.2, H Ind), 7.134 (1H, d•d, ^3J = 4.8,^3J = 4.0, H(4) Th), 7.330 (1H, d, ^3J = 8.0, H Ind), 7.411 (1H, d,^3J = 2.8, C(2)H Ind), 7.643 (1H, d, ^3J = 7.6, H Ind), 7.9055 (1H, d•d, ^3J = 4.8,^4J = 1.2, H Th), 8.0035 (1H, d•d, ^3J = 4.0,^4J = 1.2, H Th), 11.085 (1H, s, NH). ^{13}C NMR (75 MHz, $(CD_3)_2SO$) δ =70.8 (CHOH), 111.6, 113.6, 119.0 119.4, 121.3, 124.8, 125.6, 128.4, 134.6, 136.3, 140.83 (C Th, Ind), 192.3 (C=O). MS (EI) *m/z* 257 M^+ (1.05), 256 (0.3), 255 (3.2), 241 (15), 240 (14), 239 (78), 212 (20), 211 (49), 210 (67), 146 (23), 145 (15), 144 (100), 130 (75),128 (16), 116 (15), 111 (87), 101 (30), 89 (17). MS (FAB) *m/z* 240 $[M+H-H_2O]^+$ (100), 212 $[M+H-H_2O-CO]^+$ (33), 146 (87), 111 $ThC^+=O$ (23). MS (FAB, KI) *m/z* 296 $[M+K]^+$ (67), 240 $[M+H-H_2O]^+$ (50), 146 (100), 111 (28). Anal. Calcd. for $C_{14}H_{11}NO_2S$: N 5.44. Found: N 5.31.

Benzoins **2a**,**b** also were identified by ^{1}H NMR spectra with the samplessynthesized by known method[10,11].

2-Hydroxy-2-(indol-3'-yl)-1-(thien-2''-yl)ethanone (2b)

The mixture of 2-thienylglyoxal hydrate (199 mg, 1.257 mmol), indole (147 mg, 1.257 mmol) and AcOH (7 mL) was stirred at 20 ºC for 23 h. The obtained precipitate was filtered off, washed by cold water (10 mL) and dried under vacuum (4 Torr) giving α-benzoin **2b** as colorless crystals (191 mg, 59 %), identified by its ^{1}H NMR spectrum.

2-Hydroxy-2-(indol-3'-yl)-1-(4''-methylphenyl)ethanone (2c)

4-Methylphenylglyoxal hydrate (221 mg, 1.327 mmol) was dissolved in boiling benzene (8 mL), then a solution of indole (178 mg, 1.518 mmol) was added, the reaction solution was boiled for 30 min, kept at 15 ºC for 19 h, then it was evaporated under vacuum (25 Torr) to a volume of 4 mL. To obtained residue, it was kept at 4 ºC for 2 days. The obtained precipitate was filtered off, washed by CCl_4 (0.5 mL) and dried under vacuum (4 Torr) giving 2-hydroxy-2-(indol-3'-yl)-1-(4''-methylphenyl)ethenone (**2c,** 128 mg, 36 %), as white crystals, m.p.146-147°C (benzene) (with

decomp.), (lit. 144-146°C,[13] 154-158°C[15]). ^{1}H NMR (300 MHz, $(CD_3)_2SO$) δ = 2.270 (3H, s, Me), 5.479 (1H, d, ^3J = 5.7, CHOH), 6.332 (1H, d, ^3J = 5.7, CHOH), 6.968 (1H, td, ^3J = 7.4, ^4J = 1.2, H Ind), 7.051 (1H, td, ^3J = 7.4,^4J = 1.2, H Ind),7.192 (2H, d, ^3J = 8.1, C(3,5)H C_6H_4Me), 7.324 (1H, d, ^3J = 7.5, H Ind), 7.332 (1H, d,^3J = 2.7 C(2)H Ind),7.616 (1H, d, ^3J = 7.5, H Ind), 7.906 (2H, d, ^3J = 8.1, C(2,6)H C_6H_4Me), 11.055 (1H, s, NH). ^{13}C NMR (75 MHz, $(CD_3)_2SO$) δ =21.1 (Me), 69.3 (CHOH), 111.6, 113.5, 118.9, 119.2, 121.3, 124.9, 125.6, 129.0, 132.4, 136.3, 143.3 (C Ind, C_6H_4), 198.6 (C=O). MS (FAB) *m/z* 248 $[M+H–H_2O]^+$ (100), 220 $[M+H–H_2O\text{-}CO]^+$ (71), 146 (20), 119 $MeC_6H_4C(O)^+$ (60), 118 (14). MS (FAB, KI) *m/z* 304 $[M+K]^+$ (100),248 $[M+H–H_2O]^+$ (34), 220 $[M+H–H_2O\text{-}CO]^+$ (61), 146 (20), 119 $MeC_6H_4C(O)^+$ (83), 118 (27).

To the filtrate CCl_4 (1 mL) was added, the obtained precipitate was filtered off, additionally yielding α-benzoin **2c** (30 mg, 8 %).

The compound was prepared by another method also. The solution of 4-methylphenylglyoxal hydrate (276 mg, 1.659 mmol) and indole (204 mg, 1.741 mmol) in benzene (5 mL) was boiled at 100 ºC for 1h in sealed tube, kept at 18 ºC for 23 h, then it was evaporated under vacuum (25 Torr) to 3 mL. To obtained residue, it was kept at 4 ºC for 2 days, the obtained precipitate was filtered off, washed with CCl_4 (1 mL) and dried under vacuum (4 Torr), giving 2-hydroxy-2-(indol-3'-yl)-1-(4''-methylphenyl)ethanone **2c** (276 mg, 63 %), as white crystals, m.p.146-148°C (benzene) (with decomp.)

2-Hydroxy-2-(indol-3'-yl)-1-(4''-chlorophenyl)ethanone (2d)

The solution of 4-chlorophenylglyoxal hydrate (2.426 g, 13 mmol) and indole (1.524 g, 13 mmol) in benzene (17 mL) was boiled for 2 h under nitrogen, then it was kept at 20 ºC for 2 day. The obtained precipitate was filtered off, washed by CH_2Cl_2 (6 mL), dried under vacuum (2 Torr) to give **2d** as colorless crystals (2.226 g, 60 %), m.p. 145-146 ºC (benzene) (with. decomp.), (lit. 134-138 °C,[13] 144-146 °C).[15] ^{1}H NMR (500 MHz, $(CD_3)_2SO$) δ = 5.619 (1H, d, ^3J = 5.5, CHOH), 6.314 (1H, d, ^3J = 5.5, CHOH), 6.972 (1H, t, ^3J = 8.0, H Ind), 7.052 (1H, t, ^3J = 8.0, H Ind), 7.312 (1H, d, ^3J = 8.0, H Ind), 7.334 (1H, d,^3J = 2.0, C(2)H Ind), 7.464 (2H, d, ^3J = 9.0, H(3,5) C_6H_4Cl), 7.592 (1H, d, ^3J = 8.0 H Ind), 8.007 (2H,d, ^3J = 9.0, H(2,6) C_6H_4Cl), 11.077 (1H, s, NH). ^{13}C NMR (100 MHz $(CD_3)_2SO$) δ = 69.69 (CHOH); 111.53, 112.88 (C(2), C(3) Ind), 118.89, 119.07, 121.25 (C(5), C(6), C(4) Ind), 124.81 (C(7) Ind), 125.43 (C(1) C_6H_4Cl), 128.46 (C(3,5) C_6H_4Cl), 130.26 (C(2,6) C_6H_4Cl), 133.49, 136.19 (C(8), C(9) Ind), 137.68 (C(4) C_6H_4Cl), 197.83 (C=O). MS (FAB) *m/z* 270 $[M+H–H_2O]^+$ (34), 268 $[M+H–H_2O]^+$ (82), 242 $[M+H–H_2O\text{-}CO]^+$ (17), 240 $[M+H–H_2O\text{-}CO]^+$ (54), 145 (100). MS (FAB, KI) *m/z* 326 $[M+K]^+$ (15),324 $[M+K]^+$ (38), 270 $[M+H–H_2O]^+$ (17),268 $[M+H–H_2O]^+$ (47), 242 $[M+H–H_2O\text{-}CO]^+$ (6), 240 $[M+H–H_2O\text{-}CO]^+$ (17), 146 (100). Anal. Calcd. for $C_{16}H_{12}ClNO_2$: C 67.26, H 4.23, N 4.90. Found: C 67.42, H 4.27, N 4.72.

2-Hydroxy-2-(indol-3'-yl)-1-(4''-chlorophenyl)ethanone (2d)

The solution of 4-chlorophenylglyoxal hydrate (147 mg, 0.786 mmol) and indole (93 mg, 0.790 mmol) in AcOH (5 mL) was kept at 19 ºC for 1 h, then the solvent was evaporated under vacuum (4 Torr). The residue was extracted with water (10 mL) at 4 ºC. the obtained precipitate was filtered off, washed by water (5 mL), dried under vacuum (4 Torr), giving α-benzoin **2d** as white crystals (217 mg, 96 %), identified by its ^{1}H NMR spectrum.

2-Hydroxy-2-(indol-3'-yl)-1-(4''-bromophenyl)ethanone (2e)

The solution of 4-bromophenylglyoxal hydrate (808 mg, 3.5 mmol) and indole (410 mg, 3.5 mmol) in benzene (40 mL) was boiled for 2 h, then it was kept at 30 ºC for 3 day. The obtained reaction solution was evaporated to 80 % under vacuum, the obtained precipitate was filtered off, washed by cold benzene, giving 2-hydroxy-2-(indol-3'-yl)-1-(4''-bromophenyl)ethanone **2e** (673 mg, 58 %), as white crystals, m.p. 159-160ºC (with. decomp., benzene) (lit. 159-161°C[15]). ^{1}H NMR(400 MHz, $(CD_3)_2SO$) δ = 5.614 (1H, d, ^3J = 5.2, CHOH), 6.3055 (1H, d, ^3J = 5.2 CHOH), 6.971 (1H, t, ^3J = 7.2, H Ind), 7.054 (1H, t, ^3J = 7.2, H Ind), 7.314 (1H, d, ^3J = 8.8, H Ind), 7.3285(2H, d,^3J = 2.8, C(2)H), 7.589 (1H, d, ^3J = 8.0, H Ind), 7.6085 (2H, d, ^3J = 8.4, C(3,5)H C_6H_4Br), 7.9265 (2H, d, ^3J = 8.4, C(2,6)H C_6H_4Br), 11.073 (1H, s, NH). ^{13}C NMR (75 MHz, $(CD_3)_2SO$) δ = 69.7 (CHOH), 111.6, 113.0, 119.0, 119.2, 121.3, 124.9, 125.5, 127.0, 128.3, 130.5, 130.6, 131.5, 134.0 (C Ar, Ind), 136.3 (C-Br), 198.2 (C=O). MS (FAB) *m/z* 314 $[M+H–H_2O]^+$ (35), 312 $[M+H–H_2O]^+$ (31), 146 (100). MS (FAB, KI) *m/z* 370 $[M+K]^+$ (18),368 $[M+K]^+$ (20), 314 $[M+H–H_2O]^+$ (33),312 $[M+H–H_2O]^+$ (34), 146 (100). Anal. Calcd. for $C_{16}H_{12}BrNO_2$: C 58.20, H 3.66, N 4.24. Found: C 58.41, H 3.72, N 4.32.

2-Hydroxy-2-(indol-3'-yl)-1-(4''-bromophenyl)ethanone (2e)

The mixture of 4-bromophenylglyoxal hydrate (336 mg, 1.452 mmol), indole (172 mg, 1.471 mmol) and AcOH (9 mL) was stirred at 17 ºC for 50 min, the obtained solution was evaporated under vacuum (4 Torr) and the residue was extracted by water (10 mL) at 4 ºC. The obtained precipitate was filtered off, washed by water (8 mL) and dried under vacuum (4 Torr) to yield α-benzoin **2e** as white crystals (412 mg, 86 %), identified by its ^{1}H NMR spectrum.

2-Hydroxy-2-(indol-3'-yl)-1-(4''-fluorophenyl)ethanone (2f)

4-Fluorophenylglyoxal hydrate (110 mg, 0.648 mmol) was converted in anhydrous fluorophenylglyoxal by heating to 130 ºC under vacuum (10 Torr), then it was dissolved in benzene (5 mL) and indole (76 mg, 0.648 mmol) was added. The reaction solution was kept at 20 ºC for 88 h and then the solvent was evaporated under vacuum (25 Torr). The obtained residue was dissolved in CCl_4 (4 mL), the solution was filtered, and hexane (5 mL) was added. The obtained precipitate was filtered off, washed with hexane (5 mL) and dried under vacuum (4 Torr) to give 2-hydroxy-2-(indol-3'-yl)-1-(4''-fluorophenyl)ethanone **2f** (89 mg, 51 %), as white crystals, m.p.**2f•**PhH 116-117ºC (with. decomp., benzene). ^{1}H NMR (300 MHz, $(CD_3)_2SO$) δ = 5.618 (1H, d, ^3J = 5.4, CHOH), 6.345 (1H, d, ^3J = 5.4, CHOH), 6.987 (1H, t, ^3J = 7.0, H Ind), 7.066 (1H, t, ^3J = 7.0, H Ind), 7.227 (2H, dd, ^3J = 8.7, $^{H\text{-}F}J$ = 9.0, C(3,5)H C_6H_4F), 7.334 (1H, d, ^3J = 8.1, H Ind),), 7.3635 (1H, d,^3J = 2.1, C(2)H Ind),7.6305(1H, d, ^3J = 8.1, H Ind), 8.104 (2H, dd, ^3J = 8.7,$^{H\text{-}F}J$ = 5.7, C(2,6)H C_6H_4F), 11.090 (1H, s, NH). ^{13}C NMR (75 MHz$(CD_3)_2SO$)

δ = 66.7 (CHOH), 111.6, 113.2, 115.4, 119.0, 119.2, 121.3, `124.9, 125.6 (C Ind, C_6H_4F),131.5 (d, *J* = 9.0, C(3,5)C_6H_4F), 136.3 (C(1) C_6H_4F), 164.7 5 (d, *J* = 249.0, C(4)C_6H_4F), 197.6 (C=O). MS (FAB) *m/z* 252 $[M+H–H_2O]^+$ (93), 224 $[M+H–H_2O\text{-}CO]^+$ (100), 146 (59), 123 $FC_6H_4C(O)^+$ (51), 118 (46). MS (FAB, KI) *m/z* 308 $[M+K]^+$ (100),252 $[M+H–H_2O]^+$ (53), 224 $[M+H–H_2O\text{-}CO]^+$ (69), 146 (51), 123 $FC_6H_4C(O)^+$ (61), 118 (45).

2-Hydroxy-2-(indol-3'-yl)-1-(4''-nitrophenyl)ethanone (2g)

The solution of 4-nitrophenylglyoxal hydrate (146 mg, 0.740 mmol) and indole (87.3 mg, 0.745 mmol) in AcOH (5 mL) was kept at 19ºC for 1 h, then AcOH was evaporated under vacuum (4 Torr) at 19 ºC. The obtained residue was washed by water (10 mL) at 5ºC for 1 h. The obtained precipitate was filtered off, washed by water (5 mL) and dried under vacuum (4 Torr) to yield 2-hydroxy-2-(indol-3'-yl)-1-(4''-nitrophenyl)ethanone **2g** (215 mg, 98 %), as yellow crystals, **2g**•benzene, m.p. 126-127°C (benzene).^{1}H NMR (400 MHz, $(CD_3)_2SO$) δ = 5.798 (1H, d, ^3J = 5.2, CHOH), 6.394 (1H, d, ^3J = 5.2, CHOH), 6.992 (1H, t, ^3J = 7.4, H Ind), 7.064 (1H, t, ^3J = 7.4, H Ind),7.320 (1H, d, ^3J = 8.0, H Ind), 7.369 (1H, d,^3J = 2.4 C(2)H Ind),7.604 (1H, d, ^3J = 8.0, H Ind), 8.193 – 8.228 (4H, m as 8.21 s, H(2,3,5,6) $C_6H_4NO_2$), 11.116 (1H, s, NH). ^{13}C NMR (75 MHz$(CD_3)_2SO$) δ = 70.3(CHOH), 111.7, 112.3, 119.1, 121.5, 123.6, 125.2, 125.5, 128.4, 129.8, 136.4, 140.1, 149.6 (C Ar, Ind), 198.2 (C=O). MS (FAB) *m/z* 279 $[M+H–H_2O]^+$ (100), 146 (75).

The compound was prepared by another process also. Mixture of 4-nitrophenylglyoxal hydrate (127 mg, 0.645 mmol) and water (15 mL) was stirred at 30 ºC for 1 h, then indole (72 mg, 0.614 mmol) was added. The reaction mixture was stirred at 30 ºC for 3 h, the aqueous phase was separated from resin, was kept at 30 ºC for 20 h, at 10 ºC for 2 h, then the yellow precipitate was filtered off, washed by cold water (2 mL) and dried under vacuum (2 Torr) to yield **2g** (56 mg, 31 %).

2-Hydroxy-2-(indol-3'-yl)-1-(4''-methoxyphenyl)ethanone (2h)

The solution of 4-methoxyphenylglyoxal hydrate (198 mg, 1.086 mmol) and indole (141 mg, 1.196 mmol) in toluene (6 mL) was boiled for 1h, was then kept at 15 ºC for 19 h. It was then it was evaporated under vacuum (25 Torr) to 2 mL and CCl_4 (5 mL) was added. The obtained mixture was kept at 4 ºC for 24 h, the formed precipitate was filtered off, washed by cold CCl_4 (3 mL), dried under vacuum (4 Torr) to give **2h** (160 mg, 52 %), as white-pink crystals (unstable at storing). ^{1}H NMR (300 MHz, $(CD_3)_2SO$) δ = 3.754 (3H, s, Me), 5.437 (1H, d, ^3J = 5.7, CHOH), 6.292 (1H, d, ^3J = 5.7, CHOH), 6.915 (2H, d, ^3J = 8.7, C(3,5)H C_6H_4OMe), 6.966 (1H, td, ^3J = 7.5, ^4J = 1.2, H Ind), 7.050 (1H, td, ^3J = 7.4,^4J = 1.5, H Ind),7.312 (1H, d, ^3J = 7.8, H Ind), 7.333 (1H, d,^3J = 2.7 C(2)H Ind),7.612 (1H, d, ^3J = 7.8, H Ind), 7.997 (2H, d, ^3J = 8.7, C(2,6)H C_6H_4OMe), 11.049 (1H, d,^3J = 2.1, NH). ^{13}C NMR (75 MHz$(CD_3)_2SO$) δ = 55.4 (MeO), 69.2(CHOH), 111.6 (C Ind), 113.7 (C(3,5) C_6H_4), 113.8, 118.9, 119.3, 121.3, 124.7, 125.6, 127.5 (C Ind), 130.9 (C(2,6) C_6H_4), 136.3 (C(1) C_6H_4), 162.9 (C(4) C_6H_4), 197.5 (C=O). MS (FAB) *m/z* 264 $[M+H–H_2O]^+$ (100), 236 $[M+H–H_2O\text{-}CO]^+$ (72), 146 (58), 135 $MeOC_6H_4C(O)^+$ (58), 118 (7). MS (FAB, KI) *m/z* 320 $[M+K]^+$ (100),264 $[M+H–H_2O]^+$ (15), 236 $[M+H–H_2O\text{-}CO]^+$ (35), 146 (17), 135 $MeOC_6H_4C(O)^+$ (37), 118 (13).

2-Hydroxy-1-(indol-3'-yl)-2-phenylethanone (3a)

The solution of compound **2a** (554 mg, 2.205 mmol) and Et_3N (363 mg, 3.585 mmol) in EtOH (5 mL) was boiled for 5 h under nitrogen, kept at 20ºC during 20 h and then it was evaporated under vacuum (15 Torr). The residue was washed by Et_2O (7 mL), recrystallized from i-PrOH (5 mL), the obtained crystal were filtered off and dried under vacuum (3 Torr), to give **3a** (310 mg, 56 %), colorless crystals, m.p. 167-168ºC (benzene). ^{1}H NMR (500 MHz, $(CD_3)_2SO$) δ = 5.791 (1H, d, ^3J = 5.5, CHOH), 5.909 (1H, d, ^3J = 5.5, CHOH), 7.152–7.221 (3H, C(4)H Ph and C(5,6)H Ind), 7.296 (2H, t, ^3J = 7.5, C(3,5)H Ph), 7.451 (1H, d, ^3J = 8.0, H Ind), 7.528 (2H, d, ^3J = 7.5, C(2,6)H Ph), 8.179 (1H, d, ^3J = 8.0, H Ind), 8.544 (1H, s, C(2)H Ind), 11.984 (1H, s, NH).^{13}C NMR (100 MHz, $(CD_3)_2SO$) δ = 76.24 (CHOH); 112.10, 113.06 (C(2), C(3) Ind), 121.27, 121.86, 122.91 (C(5), C(6), C(4) Ind), 125.88 (C(7) Ind), 126.74 (C(3,5) Ph),127.18 (C(4) Ph), 128.08 (C(2,6) Ph), 134.70, 136.18 (C(8), C(9) Ind), 141.45 (C(1) Ph), 194.34 (C=O). MS (FAB) *m/z* 252 $[M+H]^+$ (63), 236 (6), 206 $[M+H–H_2O\text{-}CO]^+$ (100), 145 (48), 91 (29). Anal. Calcd. for $C_{16}H_{13}NO_2$: N 5.57. Found: N 5.64.

Crystals of ß-benzoin **3a** suitable for XRD study were grown from a solution in benzene at 10 ºC, monoclinic, $C_{16}H_{13}NO_2$, at 20°C ***a*** = 8.144(1), ***b*** = 7.5178(7(3), ***c*** = 21.738(3) Å, β = 99.17(1)°, V = 1313.8(3) Å^3, M_r = 251.27, Z = 4, space group $P2_1/n$, d_{calc}= 1.270 g/cm^3, μ(MoKα) = 0.084 мм$^{-1}$, F(000) = 528. Cell parameters and intensities of 13188 reflections (3835 independent reflections, R_{int}=0.081) were measured using «Xcalibur 3» diffractometer» (graphite-monochromated MoKα radiation, CCD detector, ***ω***-scan,$2\theta_{max}$= 60°). The structure was solved by direct method using SHELXTL program package.[16] Positions of hydrogen atoms were found from different synthesis of electronic density and refined using the riding model with U_{iso}=1.2U_{eqv} of non-hydrogen atom bonded with this hydrogen atom. Hydrogen atoms, taking place in hydrogen bonds formation, were refined in isotropic approximation. Full-matrix least-squares refinement against F^2 in anisotropic approximation for non-hydrogen atoms to wR_2 = 0.135 for 3745 reflections (R_1 = 0.052 for 1882 reflectionswith F>4σ(F), S = 0.884). The final atomic coordinates, molecular geometry parameters, and crystallographic data of compound **3a** were deposited in the Cambridge Crystallographic Data Center, 12 Union Road, CB2, 1EZ, UK (fax:+44-1223-336033, e-mail: deposit@ccdc.cam.ac.uk and is available on request quoting the deposition number CCDC 1864359).

2-Hydroxy-1-(indol-3'-yl)-2-(thien-2''-yl)ethanone (3b)

The solution of compound **2b** (611 mg, 2.375 mmol) and Et_3N (363 mg, 3.585 mmol) in i-PrOH (8 mL) in sealed tube was heated at 100ºC for 5 h, then it was concentrated under vacuum (20 Torr) to a volume of 5 mL. The obtained precipitated was filtered off, washed by CH_2Cl_2 (4 mL) and dried under vacuum (4 Torr), giving 2-hydroxy-1-(indol-3'-yl)-2-(thien-2''-yl)ethanone **3b** (318 mg, 52 %), colorless

crystals, m.p. 162–163ºC (with. decomp.).^{1}H NMR (500 MHz, $(CD_3)_2SO$) δ = 6.058 (1H, d, ^3J = 5.5, CHOH), 6.128 (1H, d, ^3J = 5.5, CHOH), 6.928 (1H, t, ^3J = 4.0, C(4)H Th), 7.110 (1H, d, ^3J = 3.0, H Th), 7.189 (1H, t, ^3J = 7.0, H Ind), 7.219 (1H, t, ^3J = 7.0, H Ind), 7.391 (1H, d, ^3J = 5.0, H Th), 7.475 (1H, d, ^3J = 7.0, H Ind),8.193 (1H, d, ^3J = 7.0, H Ind), 8.563 (1H, s, C(2)H Ind), 12.042 (1H, s, NH).^{13}C NMR (75 MHz, $(CD_3)_2SO$) δ = 72.4 (CHOH), 112.3, 112.8, 121.4, 122.1, 123.1, 125.2, 125.5, 126.0, 126.6, 134.9, 136.4, 145.2 (C Ar, Ind), 193.1 (C=O). MS (EI) *m/z* 257 M^+ (0.76), 256 (2.43), 255 (9.82), 239 (22.7), 210 (26.3), 145 (49.6), 144 (100), 116 (53.3). MS (FAB) *m/z* 258 $[M+H]^+$ (34), 240 $[M+H–H_2O]^+$ (19), 212 $[M+H–H_2O\text{-}CO]^+$ (55), 144 (100). Anal. Calcd. for $C_{14}H_{11}NO_2S$: N 5.44, S 12.46. Found: N 5.25, S 12.53.

2-Hydroxy-1-(indol-3'-yl)-2-(4''-chlorophenyl)ethanone (3d)

The solution of compound **2d** (576 mg, 2.226 mmol) and Et_3N (363 mg, 3.585 mmol) in i-PrOH (7 mL) in a sealed tube was heated at 82 ºC for 4 h, then it was evaporated under vacuum (12 Torr), the residue was recrystallized from i-PrOH (4 mL), the obtained crystals were filtered off, washed by cold i-PrOH (2 mL) and dried under vacuum (2 Torr), giving **3d** (414 mg, 72 %), colorless crystals, m.p. 165- 167ºC (with decomp., benzene**)**. ^{1}H NMR (300 MHz, $(CD_3)_2SO$) δ = 5.8315 (1H, d, ^3J = 5.1, CHOH), 6.0655 (1H, d, ^3J = 5.1, CHOH), 7.151–7.234 (2H, m,H Ind), 7.3675 (2H, d,^3J = 7.5, C(2,6)H C_6H_4Cl), 7.472 (1H, d,^3J = 7.2, H Ind), 7.5625 (2H, d,^3J = 7.5, C(3,5)H C_6H_4Cl), 8.194 (1H, d,^3J = 7.2, H Ind), 8.586 (1H, s, C(2)H Ind), 12.044 (1H, s, NH).^{13}C NMR (75 MHz $(CD_3)_2SO$) δ = 75.5 (CHOH), 112.2, 113.1, 121.3, 122.0, 123.1, 126.0 (C Ind), 128.2, 128.6 (C(2,3,5,6) C_6H_4Cl), 131.9, 134.9 (C Ind), 136.3 (C(1) C_6H_4Cl), 140.5 (C(4) C_6H_4Cl), 194.1 (C=O). MS (EI) *m/z*) 287 M^+ (1.64), 285M^+ (3.49), 283 (1.70), 271 (0.63), 269 (2.11), 144 (100), 116 (29.2). MS (FAB) *m/z* 288 $[M+H]^+$ (9), 286 $[M+H]^+$ (34), 242 $[M+H–H_2O\text{-}CO]^+$ (23), 244 $[M+H–H_2O\text{-}CO]^+$ (75), 145 (100). Anal. Calcd. for $C_{16}H_{12}ClNO_2$: N 4.90. Found: N 4.94.

This compound **3d** was prepared by another method also. α-Benzoin **2d** (113 mg, 0.395 mmol) was dissolved in freshly obtained solution of Na (20 mg, 0.870 g-atom) in EtOH (5 mL), the reaction mixture was kept at 16 ºC for 20 min, then AcOH (57 mg, 0.957 mmol) was added, the reaction mixture was evaporated under vacuum (10 Torr). The solid residue (**C**) was extracted by CH_2Cl_2 (12 mL), CH_2Cl_2-extract was evaporated under vacuum(10 Torr), the residue was washed by water (10 mL) and the solid residue was dried under vacuum (2 Torr), giving ß-benzoin **3d** (49 mg, 43 %), which was identified by ^{1}H NMR spectrum.

Solid residue of CH_2Cl_2-extraction (**C**) was washed by water (10 mL), the unsolved white precipitate was dried under vacuum (2 Torr), additionally giving ß-benzoin **3d** (16 mg, 14 %).

2-Hydroxy-1-(indol-3'-yl)-2-(4''-bromophenyl)ethanone (3e)

The solution of compound **2e** (270 mg, 0.817 mmol) and Et_3N (132 mg, 1.307 mmol) in i-PrOH (5 mL) in sealed tube was heated at 82 ºC for 4 h, kept at 20 ºC for 24 h and then it was evaporated under vacuum (12 Torr). The residue was extracted with boiling CH_2Cl_2 (3 mL), cooled, the obtained precipitate was filtered off, then it was extracted with boiling CH_2Cl_2 (2 mL), cooled, the obtained precipitate was washed by CH_2Cl_2 (1 mL) and dried under vacuum, giving **3e** (69 mg, 26 %), white crystals, m.p. 175-177ºC (with decomp.). ^{1}H NMR (400 MHz, $(CD_3)_2SO$) δ = 5.789 (1H, d, ^3J = 5.6, CHOH), 6.038 (1H, d, ^3J = 5.6, CHOH), 7.186 (2H, quint•d, ^3J = 7.4, ^4J = 1.6, C(5,6)H Ind), 7.439–7.473 (1H, m, H Ind), 7.475–7.520 (4H, m, C_6H_4Br), 8.1595 (1H, d•d, ^3J = 6.8, ^4J = 1.6, H Ind), 8.564 (1H, d,^3J = 6.8, C(2)H Ind), 12.025 (1H, s, NH).^{13}C NMR (75 MHz $(CD_3)_2SO$) δ = 75.5 (CHOH), 112.1, 113.1, 120.5, 121.2, 121.9, 123.0, 125.9, 128.9, 131.0, 134.8, 136.2 (C Ar,Ind), 140.9 (C-Br), 194.0 (C=O). MS (FAB) *m/z* 332 $[M+H]^+$ (22), 330 $[M+H]^+$ (22), 286 $[M+H–H_2O\text{-}CO]^+$ (31), 284 $[M+H–H_2O\text{-}CO]^+$ (30), 144 (100). Anal. Calcd. for $C_{16}H_{12}BrNO_2$: N 4.24. Found: N 4.14.

This compound **3e** was prepared by another method also. Compound **2e** (105 mg, 0.371 mmol) was dissolved in the freshly obtained solution of EtONa [obtained by sodium (25.8 mg, 1.122 mmol) dissolved in EtOH (4 mL)], the reaction mixture kept at 8 ºC for 2 h and then a solution of AcOH (80 mg, 1.333 mmol) in EtOH (1 mL) was added. The solvent was evaporated under vacuum (5 Torr). The residue was extracted CH_2Cl_2 (16 mL), the CH_2Cl_2 extract was concentrated under vacuum to 6 mL, the obtained white precipitate was filtered off and dried under vacuum, giving **3e** (33 mg, 32 %), white crystals, which was identified by its ^{1}H NMR spectrum.

RESULTS AND DISCUSSION

We had synthesized known[10,11] α-phenyl(indol-3-yl)benzoin **2a** and α-(thien-2-yl)l(indol-3'-yl)benzoin **2b** with moderate yields (Scheme 1) by reaction of indole and appropriate arylglyoxals in benzene at room temperature or in acetic acid solution at room temperatures. α-Aryl(indolyl)benzoin **2c** has been synthesized with moderate yield in boiling benzene accordingly Zhungietu's methodic.[10,11] But, if this reaction was carried out at 100ºC in sealed tube, the yield of α-benzoin **2c** was higher. α-Aryl(indolyl)benzoins **2d**,**e** had been synthesized as by known method,[4,9] in acetic acid solution at room temperature by keeping the reagents for 1 h.

α-(4-Fluorophenyl)(indolyl)benzoin **2f** was obtained by an interaction of 4-fluorophenylglyoxal with indole in benzene at room temperature. α-(4-Nitrophenyl)(indolyl)benzoin **2g** was obtained by an interaction of 4-nitrophenylglyoxal hydrate with indole in acetic acid at 19 ºC for not more than 1 h. Increasing the interaction with acetic solution increases yields of by products. α-Benzoin **2g** also was synthesized in aqueous media, as reported earlier.[15]

α-(4-Methoxyphenyl)(indolyl)benzoin **2h** was synthesized with moderate yield by an interaction of 4-methoxyphenylglyoxal hydrate with indole in boiling toluene. In all cases, presence of copper(II) chloride[13] or benzoic acid[14] were not necessary. This reaction occurs with good yields in absence of any catalyst in organic solvent and with excellent yield in aqueous media.[15]

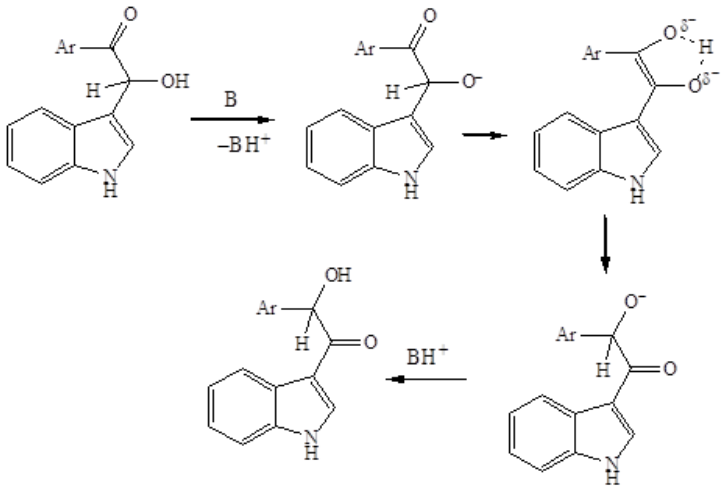

Scheme 2. Isomerization of 2-hydroxy-1-aryl-2-(indol-3'-yl)ethanones) into ß-aryl(indolyl)benzoins.

Structure of α-aryl(indolyl)benzoins **2a**–**h** was consistent with by data of ^{1}H and ^{13}C NMR spectra, and mass spectra (see further).

We have found that all α-aryl(indolyl)benzoins **2a**,**b**,**d**,**e** (2-hydroxy-1-aryl-2-(indol-3'-yl)ethanones) readily isomerize into ß-aryl(indolyl)benzoins **3a**,**b**,**d**,**e** (2-hydroxy-2-aryl-1-(indol-3'-yl)ethanones) in presence of triethylamine in alcohol solution by heating (Scheme 2). The reaction must be protected from air oxygen, in a sealed tube or else under nitrogen.

Evidently α→ß isomerization α-aryl(indolyl)benzoins **2a**,**b**,**d**,**e** occurs as transformation of anion of α-benzoin **A** via mutual anion **B** to anion **C** of ß-benzoin (Scheme 2). The similar route to ß-aryl(indolyl)benzoins **3d**,**e** is isomerization of α-aryl(indolyl)benzoins **2d**,**e** in the presence of EtONa in ethanol solution at room temperature during short time. But in other cases this method did not gave positive results (e.g. for **2g**).

Structure of isomeric 2-hydroxy-2-aryl-1-(indol-3'-yl)ethanones(ß-aryl(indolyl)benzoins) **3a**,**b**,**d**,**e** was confirmed by ^{1}H and ^{13}C NMR spectra and MS.

The substantial difference was observed in NMR MS of α-aryl(indol-3-yl)benzoin **2** and ß-aryl(indolyl)benzoins **3**. In ^{1}H NMR spectra 2-hydroxy-2-aryl-1-(indol-3'-yl)ethanones **3a**,**b**,**d**,**e** the chemical shifts of C(2)H indolyl proton and NH proton lie in lower field than the chemical shifts of proper protons of 2-hydroxy-1-aryl-2-(indol-3'-yl)ethanones **2a**–**h** (Table 1). Probably, this phenomenon is caused by conjugation of indol-3-yl moiety with carbonyl group in ß-aryl(indolyl)benzoins **3a**,**b**,**d**,**e**.

In ^{13}C NMR spectra of α-aryl(indolyl)benzoins **2** and ß-aryl(indolyl)benzoins **3** shifts of **C**HOH carbon and **C**=O carbon atoms can be regard as the characteristic carbon shifts (Table 2). In ß-aryl(indolyl)benzoins **3** shift of C=O carbon lies in some upper field than of C=O carbon of α-aryl(indolyl)benzoins **2** due to more conjugation of carbonyl group with 3-indolyl moiety. Shift of CHOH carbon forß-aryl(indolyl)benzoins **3** is observed yo some lower field than that of α-aryl(indolyl)benzoins **2**.

Table 1. The characteristic ^{1}H NMR chemical shifts of α-aryl(indolyl)benzoins and ß-aryl(indolyl)benzoins.

Resonance, σ, ppm					
α-Benzoins			ß-Benzoins		
Ar	**C(2)$_{ind}$H**	**NH**	**Ar**	**C(2)$_{ind}$H**	**NH**
2a	7.355	11.075	**3a**	8.544	11.984
2b	7.411	11.085	**3b**	8.563	12.042
2d	7.334	11.077	**3d**	8.586	12.044
2e	7.3285	11.073	**3e**	8.564	12.025
2f	7.3635	11.090			
2c	7.332	11.055			
2g	7.369	11.116			
2h	7.333	11.049			

Table 2. The characteristic ^{13}C NMR chemical shifts of α-aryl(indolyl)benzoins and ß-aryl(indolyl)benzoins.

Resonance, ^{13}C chemical shift, ppm					
α-Benzoins			ß-Benzoins		
Ar	**CHOH**	**C=O**	**Ar**	**CHOH**	**C=O**
2a	69.5	199.0	**3a**	76.2	194.3
2b	70.8	192.3	**3b**	72.4	193.1
2c	69.3	198.6			
2d	69.7	197.8	**3d**	75.5	194.1
2e	69.7	198.2	**3e**	75.5	194.0
2f	66.7	197.6			
2g	70.3	198.2			
2h	69.2	197.5			

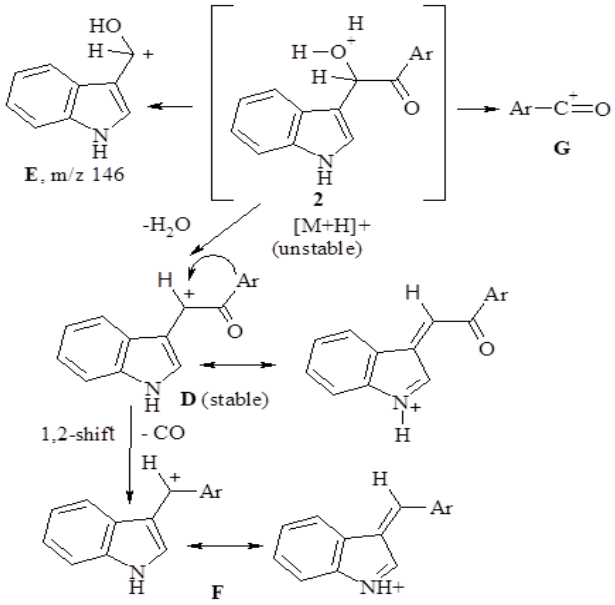

Scheme 3. Fragmentation pattern of α-aryl(3-indolyl)benzoins **2** under MS (FAB).

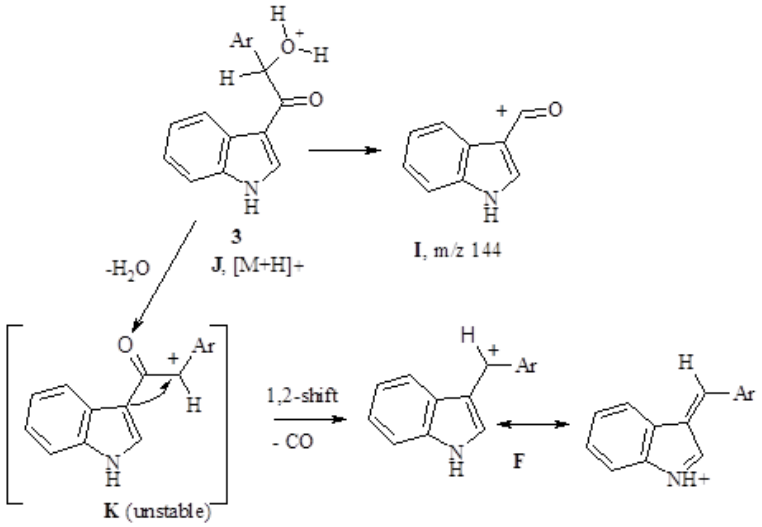

Scheme 4. Fragmentation pattern of ß-aryl(3-indolyl)benzoins **3** under MS (FAB).

Probably, it is caused by more electronegativity of the aryl groups compare to indol-3-yl moiety.

Earlier MS spectra α- and ß-aryl(3-indolyl)benzoins[3,4,17] and α- and ß-aryl(2-furyl)benzoins[7,18] were obtained in EI regime, and peaks of M^+ ions were recorded in all cases. It was found that main direction of molecular ion fragmentation was breaking of C–C bond between CHOH group and C=O group yielding stable acyl and benzyl cations. In EI regime relative intensity of peaks depends of temperature of their generation.

As FAB regime of ionization is not connected with heating, it was used for the compounds **2** and **3** characterization.

Protonation of aryl(3-indolyl)benzoins molecules in FAB-MS conditions causes substantial difference of their FAB–MS spectra relatively to their EI–MS spectra. In FAB–MS spectra of α-aryl(indolyl)benzoins **2** peaks of $[M+H]^+$ ions are absent **(**Scheme 3), but KI addition to the samples yields peaks of $[M+K]^+$ions, whereas in FAB-MS spectra of ß-aryl(indolyl)benzoins **3** $[M+H]^+$ peaks of cations **J** are observed (Scheme 4).

The analysis of linked scanning (B/E linked scanning and B^2/E linked scanning) gave main directions of fragmentation of protonated molecular ions of α- and ß-aryl(3-indolyl)benzoins **2** and **3** (Scheme 3 and 4).

In MS spectra (FAB regime) of α-aryl(indolyl)benzoins **2,** peaks of stable indolylions **D** $[M+H-H_2O]^+$ and "benzylic" ion **E** with m/z 146 are dominating (Scheme 3).

In this case of α-aryl(indolyl)benzoins **2** the cations $[M+H-H_2O-CO]^+$ **F** are observed, presumably obtaining from cations **D** by synchronous 1,2-shieft of aryl moiety to caution center and CO elimination. Acyl cations **G** are also observed. However, in MS spectra of ß-aryl(indolyl)benzoins **3** peaks of ions $[M+H]^+$ **J,** $[M+H-H_2O-CO]^+$ **F** and acyl cation **I** with *m/z* 144 are dominating (Scheme 4). In this case aryl(indolyl) cations **F** are observed too, presumably obtaining from cations **J** by H_2O elimination and unstable cations **K** formation. Peaks ions $[M+H-H_2O]^+$ **K** have low intensity. Further cations **K** convert into stable cations **F** probably by route of synchronous 1,2-shieft of indolyl moiety to cation center and CO elimination (Scheme 4).

As shown by Scheme 3 and 4, the water molecule elimination from protonated molecules benzoins **2** and **3** leads to the formation of ions having cation center in α-position to the indol-3-yl moiety in the case of α-aryl(indolyl)benzoins **2** and in α-position to the aryl moiety in the case of ß-aryl(indolyl)benzoins **3**. Seemingly, the indolyl moiety much effectively stabilized the positive charge than the aryl moiety. This phenomenon causes the high stability of ions **D** and low stability of ions **K**. Probably, the first causes the absence of $[M+H]^+$ ions in FAB-MS spectra of α-aryl(indolyl)benzoins **2**.

With an aim of understanding α→ß aryl(indol-3-yl)benzoins isomerization, XRD study of α-phenyl(indol-3-yl)benzoin **2a** and ß-phenyl(indol-3-yl)benzoin **3a** were made.

It was found that in α-phenyl(indol-3-yl)benzoin **2a** (**Figure 2**) 3-indolylmethyl moiety was situated in the plane which orthogonaly oriented to the benzoyl group plane.

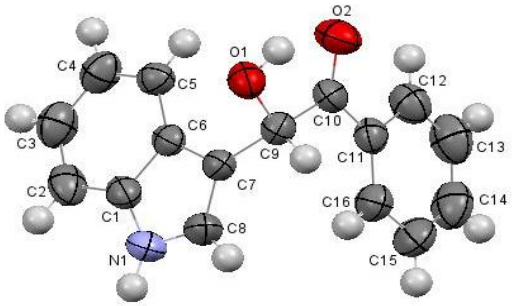

Figure 2. The molecular structure of 2-hydroxy-2-(indol-3'-yl)-1-phenylethanone **2a**

The angle between these fragments planes is 89º. The weak steric repulsion occurs between phenyl group and C(9) atom (the H16…C9 length is 2.69 Å whereas the vander Waals radii sum is 2.87 Å.[19] This steric repulsion causes some weak carbonyl group rolling toward phenyl moiety plane (the O2–C10–C11–C12 torsion angle is -9.7(3)º). HO-Group is coplanar oriented to C=O carbonyl due to intramolecular hydrogen bonding O1–H…O2 (H…O 2.24 Å, OH…O 104º). The length of C=O bond (C10=O2 bond) is 1.218(2) Å (the average length of C=O is 1.210 Å[20]). That means the negligible C=O bond deformation is due to its conjugation with benzene ring. The length of C10–C11 bond is 1.480(3) Å.

In the crystal molecules of compound **2a** form centrosymmetric dimmer due to O1-H…O2' (2-x, 2-y, 1-z) (H…O 2.12 Å, O-H…O 157º) intermolecular hydrogen bond. The dimmers are bonded in the links due to intermolecular bond N1-H…O1' (1.5-x, -0.5+y, 1.5-z) (H…O 2.10 Å, N-H…O 165º) (Figure 3).

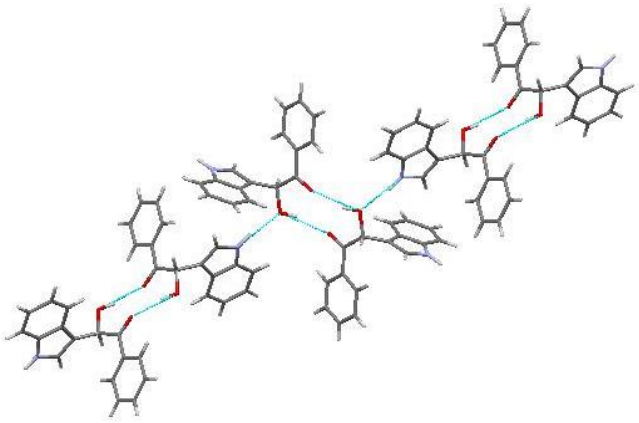

Figure 3. The packing of molecules of α-benzoin **2a** in the crystal

In ß-phenyl(indol-3-yl)benzoin **3a** (Figure 4) 3-indolyl substituent and carbonyl group C(9)=O(1) are coplanar (the C6–C7–C9–O1 torsion angle is 6.9(2)º). The phenyl substituent is orthogonally oriented to the mutual plane of indolyl moiety and carbonyl C(9)=O(1) group (the O1–C9–C10–C11 torsion angle is -97.0(2)º).

The C7–C9 bond $(C(3)^{Ind}–C(=O))$ is some shortened (1.439(2) Å) compare to average this bond length 1.455 Å[20] and C(9)=O(1) bond is substantially elongated to 1.242(2) Å compare to average length of C=O (1.210 Å[20]).

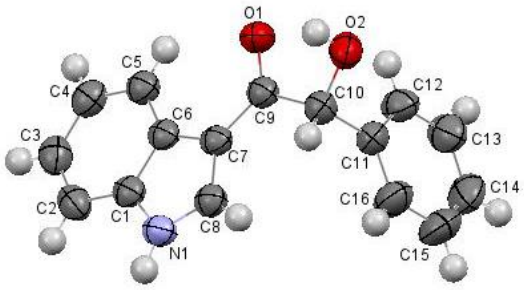

Figure 4. The molecular structure of 2-hydroxy-1-(indol-3'-yl)-2-phenylethanone **3a**.

This phenomena is caused by strong degree of conjugation of the carbonyl group with the indolyl moiety compare to degree of conjugation of the carbonyl group with phenyl substituent inα-phenyl(indol-3-yl)benzoin **2a**.

In indolyl substituent of ß-benzoin **3a** C7–C8 bond ($C(3)^{Ind}$–$C(2)^{Ind}$ bond) is elongated to 1.389(2) Å compare to that bond in α-benzoin **2a** (1.355(3) Å). And vice versa, in ß-benzoin **3a** N1–C8 bond (($N(1)^{Ind}$–$C(2)^{Ind}$ bond) is shortened to 1.349(2)Å compared to the same bond of α-benzoin **2a** (1.422(2) Å).

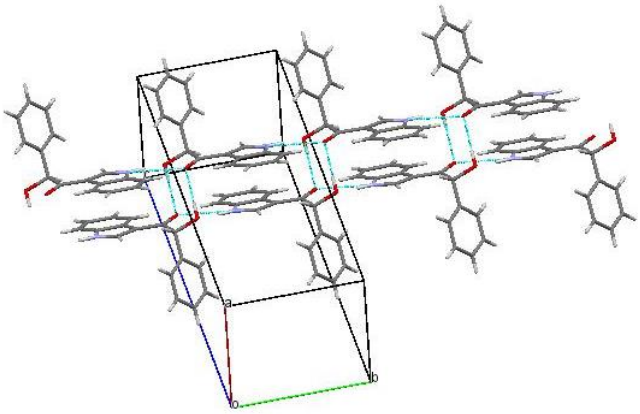

Figure 5. The packing of molecules of ß –benzoin **3a** in the crystal.

Earlier the same elongation of carbonyl group (1.236(5)Å) and shortening of $C(2)^{Fur}$–C(=O) (1.433(5)Å) has been established for ß-aryl(fur-2-yl)benzoin **1b**.[8] In compound **1b** the furan ring, carbonyl group and N,N-dimethylhydrazonyl moiety are situated in the same plane too. This data show on stronger conjugation of C=O group with hetaryl moiety in ß-benzoins **1b**, **3a** relatively to conjugation of C=O group with aryl substituent in α-benzoins **1a**, **2a**. Evidently, that realization of strong conjugation is moving force of α→ß benzoin rearrangement.

In the crystal lmolecules of compound **3a** form twice links (Figure 5) due to intermolecular hydrogen bond O2-H…O1' (2-x, 2-y, 1-z) H…O 2.07 Å O-H…O 167º and bifurcate hydrogen bonds with participating NH-group as proton donor (N1-H…O1' (x, y-1, z) H…O 2.26 Å N-H…O 141º; N1-H…O2' (x, y-1, z) H…O 2.29 Å N-H…O 147º).

The isomerization ofα-aryl(indolyl)benzoins can be regarded as convenient method of synthesis of ß-aryl(indolyl)benzoins which can not obtained from proper aldehydes by usual benzoin condensation.[1]

Conclusion

A convenient method of synthesis of 2-hydroxy-1-aryl-2-(indol-3-yl)ethanones, their isomerization in 2-hydroxy-2-aryl-1-(indol-3-yl)ethanones in presence of triethylamine on heating or in presence of EtONa at room temperature and spectral data of both isomers were discussed. The spectral tests of isomers structure were found. The structure of α- and ß-benzoins has been studied.

This work was supported by Department of Education and Science of Ukraine (grant no 0116U001722).

References

[1]Ide, W. S., Buck, J. S., The synthesis of benzoins, in: *Organic Reactions*, R. Adams (Ed.), Wiley, New York, **1948**, *4*, 269−304.

[2]Shtamburg, V. G., Anishchenko, A. A., Ivonin, S. P., 3-Aryl-2-furylqinoxalines, *Chemistry of Nitrogen Containing Heterocycles−2000*, Thesis, Kharkiv, **2000**, 117.

[3]Shtamburg, V. G., Anishchenko, A. A., Shtamburg, V. V., Pleshkova, A. P., Lapandin, A. V., Dimitrova, I. S., Ivonin, S. P., 2-Thienylglioxal based synthesis of unsymmertic acyloins and its heteroanaloges, *Vestnik Dnepropetrovsk. University, Khimia*, **2002**, *8*, 49−56.

[4]Shtamburg, V. G., Anishchenko, A. A., Klots, E. A., Pleshkova, A. P., 2-(3'-Indolyl)-1-arylacyloins, its obtaining and isomerization into 2-aryl-1-(3'-indolyl)acyloins, *Vestnik Dnepropetrovsk. University, Khimia*, **2003**, *9*, 71−76.

[5]Ivonin, S. P., Lapandin, A. V., Shtamburg, V. G., Isomerization of (Het)arylbenzoins in Basic Media, *Chem. Heterocycl. Comp.*, **2004**, *40(2)*, 154−160. https://doi.org/10.1023/B:COHC.0000027885.61368.a7

[6]Ivonin, S. P, Lapandin, A. V., Anishchenko, A. A., Shtamburg, V. G., Mutual Influence of (Dimethylhydrazono)methyl Groups and α - Hydroxy Ketone Moieties in Hetaryl Analogues of Unsymmetric Benzoins, *Eur. J. Org. Chem.*, **2004**, 4688−4693. https://doi.org./10.1002.ejoc200400293.

[7]Anishchenko, A. A.,Shtamburg, V. G., Shtamburg, V. V., Mazepa, A. V., Unusual Spontaneous $\alpha \rightarrow \beta$ Isomerization of Unsymmetrical Benzoins, *Eur. Chem. Bull.*, **2013**, *2*, 361−366. https://doi.org./10.17628.ecb2013.2.361-366.

[8]Anishchenko, A. A., Shtamburg, V. G., Shishkin O. V., Zubatyuk R. I., Shtamburg, V. V., Kostyanovsky, R. G., The Structure of Mixed β-Aryl(furyl)benzoin, 2-Hydroxy-2-(4''-chlorophenyl)-1-(5'-N,N-dimethylhydrazonylfuryl-2')-ethanone-1, *Eur. Chem. Bull.*, **2014**, *3*, 472−473. https://doi.org./10.17628/ECB2014.3.472-473.

[9]Ivonin, S. P, Lapandin, A. V., Anishchenko, A. A., Shtamburg, V. G., Reaction of Arylglyoxals with Electron-Rich Benzenes and π - Excessive Heterocycles. Facile Synthesis of Heteroaryl α-Acyloins, *Synth. Commun.*, **2004**, *34*, 451−461. https://doi.org./10.1081/SCC-120027284.

[10]Zhungietu, G. I., Chukhrii, F. N., Reaction of indole with phenylglyoxal, *Chem. Heterocycl. Comp.*, **1969,** *5(5)*, 711. https://doi.org/10.1007/BF00957402

[11]Zhungietu, G. I., Chukhrii, F. N., Reaction of indole with α-ketoaldehydes *Zh. Mendeleev Vses. Khim. Obshchest.*, **1970**, *15*, 353−354. Chem. Abstr., **1970**, *73*, 55918t

[12]Suarez, A., Martinez, F., Sanz, R., Synthesis of α-functionalized α-indol-3-yl carbonyls through direct S_N reactions of indol-3-yl α-acyloins, *Org. Biomol. Chem.*, **2016**, *14*, 11212−11219.https://doi.org./10.1039/c6ob02125e

[13]Zhan, Z., Zhang G., Cheng, X., Lu, G., Zheng, Y., Hai, L., Wu, Y., $CuCl_2$-Promoted Friedel-Crafts Hydroxyalkylations of Indoles, *Chin. J. Org. Chem.*, **2015**, *35*, 2559−2567. DOI:10.6023/cjoc201507005

[14]Lu, G., Cheng, X., Zheng, Y., Li, W., Hai, L., Wu, Y., Benzoic acid: am efficient and rapid catalyst for the synthesis of α-hydroxyl(indolyl)ethanones from indoles, *Chem. Res. Chin. Univ.*, **2016**, *32(2)*, 212–218. https://doi.org./10.1007/s40242-016-5301-9

[15]Mohammad, A.-A., Mahndieh, T., Reaction of arylglyoxals with pyrrole or indole in aqueous media: facile synthesis of heteroaryl α-acyloins, *J. Iran. Chem. Soc.*, **2014**, *11*, N 4, 963–968. https://doi.org./10.1007/s13738-013-0362-x

[16]Sheldrick, G. M., A short history of SHELX, *Acta Cryst., Sect. A.*, **2008**, *A64*, 112-122.

[17]Ivonin, S. P., Mazepa, A. V., Lapandin, A. V., Mass-spectral behavior and thermal stability of hetaryl analogs of

unsymmetrical benzoins, *Chem. Heterocycl. Comp.*, **2006**, *42*, 451−457.

[18]Ivonin, S. P., Anishchenko, A. A., Samukha, A. V., Lapandin, A. V., Serdiuk, V. N., Pleshkova, A. P., Shtamburg, V. G., Aryl(furyl)acyloins, *Vestnik Dnepropetrovsk. University, Khimia*, **2000**, *5*, 27−32.

[19]Zefirov, Yu. V., Reduced intermolecular contacts and specific interactions in molecular crystals, *Crystallogr. Reports*, **1997**, *42(5)*, 865–886.

[20]Burgi, H.-B., Dunitz, J. D., *Structure correlation*. Vol. 2, VCH, Weinheim, **1994**, 741−784.
https://doi.org./10.1107/S0108768195009931

Received: 18.09.2018
Accepted: 13.10.2018.